Dissertation

submitted to the
Combined Faculties of Natural Sciences and Mathematics
at the Ruperto-Carola University of Heidelberg, Germany
for the degree of
Doctor of Natural Sciences

Put forward by

M.Sc. Marios Tsatsos

born in Larisa, Greece

Oral examination: 02. 02. 2012

The impact of angular momentum on the stability and fragmentation of two- and three- dimensional attractive Bose-Einstein condensates

Referees: **Prof. Dr. Lorenz S. Cederbaum**
Prof. Dr. Dirk Dubbers

Der Einfluss des Drehimpulses auf die Stabilität und die Fragmentierung zwei- und drei-dimensionaler attraktiver Bose-Einstein Kondensaten – In dieser Dissertation wird die Physik von gefangenen, attraktiven Bose-Einstein Kondensaten in zwei und drei Raumdimensionen untersucht. Das Hauptaugenmerk liegt unter anderem auf dem Kollaps des Gases, wenn die Stärke der Wechselwirkung einen kritischen Wert übersteigt. Die Zustände des Systems mit guten Drehimpulsquantenzahlen werden untersucht und Verbindungen zwischen dem Drehimpuls und der Fragmentierung der Zustände gezeigt. Im zweidimensionalen Fall können mean-field Zustände benutzt werden um Zustände mit guter Drehimpulsquantenzahl zu beschreiben. Analytische Resultate für die Energie, die Besetzungszahlen und die Stabilität des Grundzustandes mit L als Drehimpulsquantenzahl werden mithilfe eines mean-field Ansatzes hergeleitet. Im dreidimensionalen Fall hingegen ist die mean-field Theorie nicht ausreichend für die korrekte Beschreibung von Zuständen mit guter Drehimpulsquantenzahl. Die Eigenzustände beider Drehimpulsoperatoren ($\hat{L}^2$ und $\hat{L}_z$) werden berechnet und es wird gezeigt, dass diese im Allgemeinen Vielteilchenzustände sind. Es wird gezeigt, dass Drehimpuls einen allgemein stabilisierenden Einfluss auf das Gas hat und dieser Einfluss wird quantifiziert. Zum Abschluß, wird der Grundzustand des Systems Untersucht, wenn das externe Potential in Rotation versetzt wird. Hier zeigt es sich, dass durch die Attraktion die Symmetrie des Grundzustandes erhalten bleibt und kein Drehimpuls von der Rotation auf das Gas übertragen wird und dieser damit auch keine Auswirkungen auf die Stabilität hat.

The impact of angular momentum on the stability and fragmentation of two- and three- dimensional attractive Bose-Einstein condensates – In this Dissertation the physics of trapped, attractive Bose-Einstein condensates in two and three spatial dimensions are examined. Particular emphasis is put on the collapse of the gas, when the attractive interparticle interaction is raised above a critical value. The states of the system that possess good angular momentum quantum numbers are scrutinized and connections between the angular momentum and the fragmentation of the states are investigated. In two spatial dimensions mean-field states can describe states of good angular momentum. Using a mean-field ansatz, analytical results for the energy, the occupation numbers and the stability of the ground state carrying L quanta of angular momentum are obtained. In three dimensions, however, a mean-field theory does not suffice for the proper description of angular momentum states. The eigenstates of both total angular momentum operators ($\hat{L}^2$ and $\hat{L}_z$) are derived and it is shown that they are generally many-body states. It is shown, moreover, that angular momentum has a general stabilizing effect on the gas and this connection is expressed quantitatively. Finally, the ground state of the gas is examined, when its container is set into external rotation. It is found that due to the attraction the symmetry of the ground state does not change, angular momentum is not transfered from the rotation to the gas and thus no significant impact in the stability is seen.

Foreword

> " ... *scheint es geratener, zunächst einen großen Reichtum von Begriffen in eine physikalische Theorie einzuführen, ohne Rücksicht auf die strenge Rechtfertigung durch die Erfahrung, und der Natur im Einzelfall jeder Theorie die Entscheidung darüber zu überlassen, ob und an welchen Punkten eine Revision der Grundbegriffe erforderlich sei.*"
> W. Heisenberg[1]

The present doctoral Thesis is the product of my research on ultracold attractive bosonic gases conducted within the Theoretical Chemistry Group of Heidelberg University, during the years 2007-2011. Herein, I have put an effort into building up a picture of the physics of ultracold gases that is not only self-explanatory but also as consistent as possible. All the necessary relevant notions are introduced and explained, so that the reader can acquire the minimal required knowledge in order to follow the analysis of the various physical problems on which I have carried out research. However, a good knowledge of quantum mechanics is required, together with the basic ideas of some relevant mathematical techniques and algebra.

In the presentation line I follow the plural 'we', rather than the singular 'I' form, for two reasons. Mainly, to actively include the reader in the process of obtaining the results and, secondly, to tacitly acknowledge the contribution of other people (i.e., supervisors and colleagues) to the present work. Certainly, a Thesis is an individual pursuit but, altogether, science has primarily been evolving as a collective endeavor.

[1] *Die physikalischen Prinzipien der Quantentheorie*, Bibliographisches Institut AG, Mannheim, 1958.

Acknowledgements

I feel the need to thank my supervisor Prof. Lorenz S. Cederbaum for initiating and consistently promoting research on "ultracold bosons with multi-orbital methods"; the field where the present work falls in. I was honoured to have my Thesis read and evaluated by Prof. Dirk Dubbers, whose exceptional interest on the Thesis I would like to acknowledge. Prof. Ofir E. Alon has been always providing invaluable guidance to me, not only in the physics part but also in obtaining, arranging and presenting scientific results. A big part of my work would not have been carried out without his support. My collaboration with Dr. Alexej Streltsov has been beneficial and has helped me several times grasp a different, yet interesting physical point of view over specific problems. Colleagues Dr. Kaspar Sakmann and Axel Lode have made my whole experience far more interesting since the very first days of it. I am indebted to Axel Lode, Dr. Daniel Pelaez-Ruiz and Dr. Julian Grond for providing essential remarks on the manuscript. Very special thanks to Christian, Axel, Daniel, Matthis, Yannis, Panos, Alexandros and the entire Theoretical Chemistry group for making bad times less bad and good times unforgettable. To all friend, mates and co-explorers in Heidelberg, and emphatically to the 'pareaki' in Greece. By all means, thanks to my family, mother and brothers; to tolerant and supportive Zalorén. Last but not least, to my father Akis and daughter Eleni: the late and the oncoming generation.

Contents

List of abbreviations and symbols

Abbreviation	**Meaning**
BEC	Bose-Einstein condensate
AM	Angular momentum
OAM	Orbital angular momentum
GS	Ground state
GP	Gross-Pitaevskii
MF	Mean-field
BMF	Best-mean-field
MB	Many-body
CI	Configuration Interaction
MCHB	Multi-Configurational Hartree for Bosons
MCTDHB	Multi-Configurational Time Dependent Hartree for Bosons
RDM	Reduced density matrix
LLL	Lowest Landau level

Symbol	Meaning
Ψ, Φ	Many-body states
ψ, ϕ, χ	single-particle states (orbitals)
$\|\vec{n}\rangle$	Fock state (permanent)
N	Particle number
N_c	Critical particle number for collapse
N_c^{GP}	Critical particle number for collapse as given from the GP theory
n_i, ρ_i	Occupation numbers
α_i	Relative occupation numbers
$\mathcal{H}$	Matrix representation of the Hamilton operator H
E	Total energy
ϵ	Energy per particle
L, M_L	Total AM quantum numbers
$\mathcal{L}$	Total angular momentum per particle L/N
$\mathfrak{L}$	Matrix representation of the total AM operator $\hat{L}^2$
$\mathfrak{l}$	Matrix representation of the OAM operator $\hat{L}_z$
$\tilde{L}_{MF}$	MF angular momentum pseudo-quantum number
λ_0	Interaction strength
$\lambda_{0,c}$	Critical interaction strength for collapse
λ	$\|\lambda_0\|(N-1)$
$\overline{\lambda}$	$\|\lambda_0\|N$
λ_c	Critical λ for collapse
σ, σ_i	Scaling parameter of the Gaussians
C_i ($\mathcal{C}$ or $\mathbf{C}$)	Expansion coefficients (on vector forms)
d_i	$1 - \rho_i/N$, i.e., depletion from the i-th orbital
$\tau_i^2, \|\tau\|$	Variance of the MB state
ω, ω_i	Frequencies of the trap
ε	Anisotropy of the trap on the x-y plane
ζ	Anisotropy of the trap on the z-direction
Ω	Frequency of external rotation of the trap
Ω_r	Resonant frequency of external rotation of the trap
D, d	Number of spatial dimensions

Chapter 1

Introduction

In this first chapter the very basic notions are introduced and the framework is laid out, over which the ideas of the present Thesis are unwrapped. The reader is introduced to the novel idea of Bose-Einstein condensation at zero absolute temperatures and the importance of studying such ultracold gases is emphasized. Nonetheless, this chapter should not be read as a stand-alone introduction to this very rich and deep field of physics, but rather as the necessary 'glossary' of terms and notions with which the reader can follow the subsequent analysis without significant hardship.

1.1 A historical overview: 1920's to present day

Bose-Einstein condensation is one of the 'weirdest' consequences that quantum mechanics has brought up since the very first days of its existence. Quantum mechanics is the theory that has given a wave substance to particles and Bose-Einstein condensation must be perceived as a wave phenomenon. Such a condensation of particles of a gas is sometimes characterized as an 'atom-laser' [1], compared thus to a laser which has its photons replaced by atoms. A Bose-Einstein condensate (BEC) is the state of matter in which all – or practically all – atoms of a bosonic gas occupy the same quantum state, making thus a macroscopic coherent state that behaves as a single particle. Such a gas, typically consisting of $\sim 10^2 - 10^6$ particles, can be described with the quantum state of a single particle and hence exhibits quantum mechanical properties on a large scale [2].

But how did we get to this point? In 1924, Indian scientist S. Bose [3] introduced a new statistical law that photons, i.e., quanta of light, obeyed and from this he was able to derive Planck's law. This set of statistics was, a year later, generalized to atoms by A. Einstein [4]. Later on, it became clear that this type of statistics – named Bose-Einstein statistics – is of fundamental importance, along with the Fermi-Dirac distribution (a different statistical law) because these two distributions divide all known particles[1] into two categories: the *bosons*, that obey the Bose-Einstein statistics and the *fermions*, that obey the Fermi-Dirac statistics. Additionally, it has been found [5–7] that a fundamental

[1]With the exception of *anyons*, quasi-particles that live in two spatial dimensions only.

connection between the statistics of the particles and their spin exists: fermions are particles with half-integer spin while bosons have integer spin and as such do not obey the Pauli exclusion principle. Most importantly, in Bose and Einstein's works it was proposed that a new type of condensation can occur to bosons when the temperature is sufficiently lowered. Condensation in this case is not to be understood as spatial condensation or vapor condensation, but rather as a condensation in the 'configuration-state space', a purely quantum mechanical phenomenon of bosonic particles. This unique behavior originates from the statistics that an ensemble of bosons follow. The Bose-Einstein statistical distribution yields a mean occupation number n^0 of the single-particle state u as a function of the energy ϵ_u associated with this state and the temperature T given by [8]:

$$\langle n^0(T)\rangle = \frac{1}{e^{(\epsilon_u-\mu)/k_BT}-1}, \tag{1.1}$$

where μ is the chemical potential, i.e., the energy difference resulting when a particle is removed from the system at constant volume and entropy, and k_B is the Boltzmann constant. From this distribution, Bose and Einstein noted that when the temperature of an atomic gas is lowered below a critical value T_c a macroscopic fraction of particles N_0, i.e., of order N, occupies the lowest-in-energy microscopic state with a very small negative value for μ. This is the manifestation of Bose-Einstein condensation. The critical temperature T_c, at which the ideal gas is expected to condense is [8]:

$$T_c = \left[\frac{n}{\zeta(3/2)}\right]^{2/3} \frac{2\pi\hbar^2}{mk_B} \approx 3.31\frac{\hbar^2 n^{2/3}}{mk_B}, \tag{1.2}$$

for a three-dimensional gas in free space or

$$T_c = \left[\frac{N}{\zeta(3)}\right]^{1/3} \hbar\omega \approx 0.94N^{1/3}\hbar\omega, \tag{1.3}$$

for a three-dimensional gas confined by an external harmonic potential of frequency ω. Here n is the particle density, m the mass of the boson, $\hbar$ the reduced Planck constant and ζ is the Riemann zeta function. One can also estimate (qualitatively only) the transition temperature in the following heuristic way[2]. As said, condensation is a purely quantum phenomenon. We know that, quantum effects in a ensemble of particles arise when the de Broglie wavelength λ_{dB} becomes comparable to the mean interparticle distance d. Thus, $\lambda_{dB} \sim d$ or

$$\lambda_{dB} \sim n^{-1/3}. \tag{1.4}$$

We know that the kinetic energy of the particle moving with an average velocity v equals the thermal energy of the gas, i.e., $mv^2 = k_BT$ and hence

$$v = \sqrt{k_BT/m}. \tag{1.5}$$

[2]See the talk of W. Ketterle in Ref. [1] for an intuitive treatment.

Now λ_{dB} becomes:

$$\lambda_{dB} = \frac{h}{mv} = \frac{h}{\sqrt{k_B T m}}, \tag{1.6}$$

where h is the Plank constant. Namely, the de Broglie wavelength increases inversely to the square root of the temperature. This suggests the existence of the critical temperature at which Eq. (1.4) will be fulfilled:

$$\frac{h}{\sqrt{k_B T m}} \sim n^{-1/3} \qquad \Leftrightarrow \tag{1.7}$$

$$T_c \sim \frac{h^2 n^{2/3}}{m k_B}\,, \tag{1.8}$$

which – qualitatively – agrees with the expression given in Eq. (1.2).

The first experimental production of a BEC came seven decades after its initial theoretical prediction as a result of the seminal work of three independent research groups, at JILA-Boulder, Rice and MIT [9–11]. Their accomplishments were so enthusiastically celebrated that the three scientists (W. Ketterle, E. Cornell and C. Wieman) received the 2001 Nobel prize in Physics just six years after their discovery. The BECs produced were dilute gases of rubidium, lithium and sodium atoms respectively, at temperatures as low as 170 nanokelvin (nK). Today even colder temperatures are experimentally feasible, as, e.g., the few-hundred picokelvins temperature achieved in Ref. [12]. Currently, research is undertaken in the search of a new femtokelvin regime [13]. It should be noted that the above discussion pertains to an ideal, i.e., non-interacting, and dilute bosonic gas. The diluteness of the gas is critical for the achievement of the condensation, since molecule formation and atomic collisions have to be carefully avoided in the laboratory. In the present Thesis we consider systems at absolute zero temperature; we examine the microscopic configurations of the Bose gases and do not consider thermal effects, which constitutes a different research subject on its own.

1.2 Bose-Einstein condensation in interacting systems

How can the above definition of a BEC be extended to a gas of interacting bosons? The answer came in 1956 by Onsager and Penrose [14], whose approach we follow herein. It should be noted that several alternative definitions were proposed later on (see Ch. 2 of Ref. [8] for an overview), but we find Onsager and Penrose's argument most useful and transparent.

A finite system of N interacting bosons is quantum mechanically described by the $(N+1)$-variable wave function $\Psi_N = \Psi(\mathbf{r}_1, \mathbf{r}_2, \ldots, \mathbf{r}_N; t)$, assumed normalized. In the following we will consider time-independent states only, i.e., $\Psi_N = \Psi(\mathbf{r}_1, \mathbf{r}_2, \ldots, \mathbf{r}_N)$, but the results of this paragraph can be easily generalized to time-dependent states. One

defines the single-particle reduced density matrix (RDM) $\rho_1(\mathbf{r}, \mathbf{r}')$ as [8, 15]:

$$\rho_1(\mathbf{r}|\mathbf{r}') = N \int \Psi^*(\mathbf{r}', \mathbf{r}_2 \dots \mathbf{r}_N)\Psi(\mathbf{r}, \mathbf{r}_2 \dots \mathbf{r}_N) d\mathbf{r}_2 d\mathbf{r}_3 \dots d\mathbf{r}_N. \tag{1.9}$$

This is a matrix with respect to the variables $\mathbf{r}, \mathbf{r}'$ and is furthermore a Hermitian matrix. Loosely speaking, it gives the probability amplitude that a particular particle is found at position $\mathbf{r}$ multiplied by the probability amplitude to find it at $\mathbf{r}'$, while the rest of the variables of the N-body system are integrated out. This matrix can be written in the form:

$$\rho_1(\mathbf{r}|\mathbf{r}') = \sum_{i,j} \rho_{ij} \phi_i^*(\mathbf{r}')\phi_j(\mathbf{r}), \tag{1.10}$$

with the help of the functions ϕ_i. Of special interest is the diagonal (with respect to the indices i, j) representation of Eq. (1.9) over a special finite set of functions χ_i:

$$\rho_1(\mathbf{r}|\mathbf{r}') = \sum_i n_i \chi_i^*(\mathbf{r}')\chi_i(\mathbf{r}). \tag{1.11}$$

The functions χ_i are known as *natural orbitals* and the eigenvalues n_i are called the *natural occupations*. So, let us suppose that one has come up with the solution, i.e., the wave function Ψ that exactly describes the configuration of the N-particle system at some time t. Then, one can calculate the single-particle reduced density matrix given in Eq. (1.9), write it on the diagonal form of Eq. (1.11) and finally interpret the eigenvalues n_i as the population of bosons sitting in the natural orbital χ_i.

According to Nozières [16] a system of N ultracold bosons is said to be: i) Bose-Einstein condensed if only one eigenvalue n_K is of order N, while all others are of order unity, ii) a fragmented condensate if two or more eigenvalues n_i are of order N and the rest of order unity and iii) non-condensed or normal if all of the eigenvalues are of order unity.

It should be noted that, the above definition of a single-particle RDM can be extended to higher order matrices, i.e. n-particle RDMs (see Ch. 3). In the following chapters we make extensive use of the natural orbitals analysis and also apply the Onsager-Penrose-Nozières criterion whenever we examine the states of the bosonic systems.

1.3 The peculiarity of the attractive Bose gas

The overwhelming majority of BECs today consists of interacting gases. The interparticle interaction can have different forms, i.e., it can vary in time or space, it could be attractive, repulsive or even both, as, for example, in the case of a long-range interaction with a sign that changes in space. Furthermore, one can prepare a gas of bosons possessing two types of interaction: a short- and a long-range one (usually a dipole-dipole) that can have opposite signs. In the present Thesis gases interacting purely attractively are considered, and this section suggests why such attractive bosonic systems are particularly interesting.

Among the many exceptionalities of a Bose-Einstein condensate is the amount of control one can exert on a system of ultracold bosonic atoms in the laboratory. Its properties, in sharp contrast to other systems (optical or solid state systems), can be externally managed and accurately changed. For instance, the interaction between two atoms of such a dilute gas can be modified or even have its sign changed. This means that a gas initially prepared to be repulsive can be switched to an attractive one by applying the appropriate external magnetic fields and utilizing the so-called *Feshbach resonance* techniques [17–22].

Interestingly, attractive BECs were already created in the laboratory in 1995, that is, during the very first days of the experimental existence of the BECs [10, 23]. Perhaps the most peculiar feature of the attractive BEC is that it suffers from collapse. A trapped attractive BEC can collapse due to its self-energy in a very similar fashion as an astronomical massive star collapses through a supernova [24]. This happens when either the interaction strength or the particle number exceeds some critical value. Then the interaction energy grows so large that the gas shrinks unstoppably towards the center of the trap and eventually implodes. Below the critical value, the interacting energy is compensated by the kinetic energy and the system can exist in a stable or metastable configuration, for at least some finite time t. In Sec. 3.8 we use an example to illustrate the collapse of the ground state of systems of different dimensionalities. In Chs. 4, 5 and 6 we scrutinize the stability of the gas as a function of its angular momentum and fragmentation.

The collapse of the attractive gas has been experimentally demonstrated in a gas of rubidium-85 atoms [25] and given the amusing name 'Bosenova experiment' by the JILA group. In this experiment, a stable repulsive BEC is initially produced inside a trap. Then the interaction strength is switched from repulsive to attractive, resulting in a violent explosion where more than half of the particles of the system burst out and leave the trap. Later on, several ways and situations in which the collapse can be postponed or even cancelled have been proposed, mostly from the theoretical point of view. Vorticity of the gas [26], fragmentation of the states [27] and definite angular momentum states [28] have been suggested to stabilize the gas against collapse.

The attractive nature of the interaction does not only imply collapse of the gas. Even in the metastable regime of the gas, its ground state looks quite different than its repulsive 'counterpart'. Since 1998 it has been suggested that an attractive BEC with some non-zero angular momentum does not condense but rather fragments among a finite number of single-particle states [29]. This general behavior of the attractive gas determines the ways an attractive BEC can carry angular momentum and distinguishes it even more from the repulsive systems (for a pedagogical presentation see Ch. 9 of Ref. [30] and also Ch. 2 herein).

The research work of this Thesis is devoted to the study of the ground states of attractive gases, their collapse and the connection of the angular momentum to them.

1.4 Overview of the Thesis

The first part of the present Thesis consists of Chs. 1-3. There we give the important definitions, describe the basic theory and survey known results related to the succeeding research, so that the reader can follow the analysis of the second part (Chs. 4 - 6). It should be, however, noted that attention has been given to preserving the completeness of each one of the different chapters of the Thesis, so that each one of Chs. 4 - 6 can be read as an independent piece of research.

A discussion on angular momentum comes in the second chapter to underline the significance of angular symmetries for the present work. Specifically, Ch. 2 defines the basic notions of angular momentum in quantum mechanical many-body systems. A brief overview of known results that pertain to finding the ground or excited state of an interacting many-body system with some given angular momentum is given. In Ch. 3 we introduce all the different theoretical tools and methods that we need in order to deal with atomic gases of ultracold interacting bosons and that we use extensively throughout the present analysis. The line of presentation therein goes from the simplest and more basic theory to the most advanced and general theoretical approach.

In the second part, i.e., chapters 4 - 6, we present our research results, i.e., the new findings that this Thesis has to offer. They all deal with trapped ultracold attractive bosons. More precisely, we describe the stationary, i.e., time-independent, state of the gas under specific constraints with the theoretical tools described in Ch. 3. Chapter 4 analyzes the quantum gas confined in two spatial dimensions, Ch. 5 the three-dimensional case and Ch. 6 the three-dimensional gas that is externally set into rotation. The ground and excited states are found variationally either within the multi-orbital mean-field approximation (Ch. 4) or with a many-body approach (Chs. 5 and 6). Comparisons and discussion of the different predictions of the mean-field and many-body approaches are also given (Chs. 5 and 6). This main part of the Thesis closes with Ch. 7, where the most important conclusions are drawn and an outlook on the present research is given. The Appendices provide all relevant derivations, proofs and relations that are used in or are relevant to the analysis, but for brevity are omitted from the bulk of the Thesis.

Chapter 2

The role of the angular momentum in the Bose gas

This chapter surveys the main known results on the angular momentum of many-body interacting systems and lays the ground upon which our research results rest. To this end, it starts with a brief description of the standard angular momentum algebra of a single-particle and then moves on to many-particle systems. Subsequently, the main behavior that is theoretically predicted or experimentally reported on ultracold interacting gases with finite angular momentum is codified. Due to the generality and range of the topic only the most important and relevant results, that will be later on useful for reference and comparison to the results of Chs. 4,5 and 6, are presented.

2.1 General

Angular momentum (AM) is an omnipresent property, characterizing all physical systems in two or three dimensions, classical or quantum, from the simplest to the most complex one at all energy and length scales. Indeed, it is of great importance and has proven highly helpful in the analysis of the motion of particles, atoms, molecules and other quantum and classical systems. In the quantum theory it has helped clarifying and explaining many phenomena, such as the Zeeman effect or the Stern-Gerlach experiment. In the present Thesis, angular symmetries occupy a central part in the analysis. For this reason, we give in this section the necessary definitions and in short discuss their meaning. In-depth and detailed derivations can be found in numerous standard textbooks, as, for instance, in Ref. [31].

Single-particle symmetries. Let us make the following distinction. In the classical world, AM is a physical quantity that a particle of mass m has when moving with velocity $\mathbf{v}$ and linear momentum $\mathbf{p} = m\mathbf{v}$ on a general curvilinear orbit. Quantitatively,

$$L = \mathbf{r} \times \mathbf{p}, \tag{2.1}$$

where $\mathbf{r}$ is the particle's position from the origin. So, AM in classical physics is the amount of 'curved' or rotational motion that a particle has.

In quantum mechanics, axiomatically, all physical quantities are expressed as linear operators acting on states ψ of a Hilbert space $\mathcal{E}$. To quantize the AM one has to promote it to an operator as:

$$L \to \hat{L} = -i\hbar\hat{\mathbf{r}} \times \hat{\nabla}. \tag{2.2}$$

For the sake of brevity in the following we will drop the hats from all operators and only use them again in Chs. 5 and 6 so that confusion is avoided between the operators and their eigenvalues. The qualitative – bulk – difference that results from quantizing the AM is that the original meaning of the AM is gone. Or better, hidden. AM is now not a real number attached to any particle executing a motion in space, but rather a linear operator L that acting on the state ψ will transform it to another vector state ψ'. Immediately one recognizes that there is a special class of vectors (wave functions) χ_i that will *not* transform[1] under the action of L. These are, of course, the eigenvectors of the operator L. The eigenstates constitute an orthocomplete basis and are states with the specific symmetry that the operator L encodes. So, a spatial symmetry, here angular, is associated with a linear operator acting on $\mathcal{E}$.

The operator L associated with the AM is a vector operator. That is, in three-dimensional space it consists of three (Cartesian) components L_x, L_y, L_z. Each one of these is the generator of rotations in space, around the axes x, y, z respectively (for details see Refs. [31, 32]). However, the knowledge of the eigenvalues of two or all three of the components at the same time is not possible and this flows from the commutation relation:

$$[L_i, L_j] = i\hbar\varepsilon_{ijk}L_k,$$

that the operators L_x, L_y, L_z obey. Here i, j, k denote one of the three components x, y, z and ε_{ijk} is the Levi-Civita permutation symbol. On the other hand the operator L^2 commutes with any of the three components L_i:

$$L^2 = L_x^2 + L_y^2 + L_z^2 = \frac{1}{2}(L_+L_- + L_-L_+) + L_z^2, \tag{2.3}$$

where $L_\pm = L_x \pm iL_y$. The two operators L_z, L^2 are of physical and computational importance. The relation $[L^2, L_z] = 0$ suggests that there is a common set of eigenfunctions of the two operators. These are the famous spherical harmonic functions $Y_{l,m_l} = Y_{l,m_l}(\theta, \phi)$ and are extensively used in the analysis of the present Thesis. It should be noted that in the case of a two-dimensional system, i.e., a system confined on a plane, there exists only one operator – conventionally L_z. This reflects the fact that one can, of course, perform a rotation around only one axis: the axis perpendicular to the plane. In that case $L^2 \equiv L_z^2$ and the spherical harmonics become $Y_{l,m_l} \to Y'_m = e^{im\phi}$.

[1] Or better, will transform without changing their direction.

Many-body symmetries. The AM operators defined above can easily be extended to the case of an N-particle system:

$$L_{z,\text{total}} = \sum_{i=1}^{N} L_z^i$$

and

$$L^2_{\text{total}} = \left(\sum_{i=1}^{N} L^i \right)^2 ,$$

where $L_{z,\text{total}},\ L^2_{\text{total}}$ are the operators acting on the total many-body wave function of the system Φ and $L^i \equiv L^i(\mathbf{r}_i),\ L_z^i \equiv L_z^i(\mathbf{r}_i)$ the operators that act on the single-particle wave functions $\phi(\mathbf{r}_i)$. The working forms, in second quantization language and their evaluations are given in Ch. 5. We are interested in finding the eigenvalues and eigenfunctions of the total AM operators. This is done also in Ch 5, where the found states are utilized to describe the interacting problem. In the special case that the Hamiltonian operator describing a physical one- or many-body problem commutes with the operators L^2, L_z one can find the eigenfunctions of the three operators. That is, solutions of the problem that will also respect the angular symmetry. The commutation or not of the Hamiltonian and AM operators depends on the form of the trapping potential $V(\mathbf{r}_i)$ as well as on the form of the interacting potential $w(\mathbf{r}_{i_1}, \mathbf{r}_{i_2}, \ldots \mathbf{r}_{i_N})$, i.e., the function that models the interparticle interaction. Since, a big part of the present Thesis is concerned with isotropic (or central) trapping and interacting potentials the angular symmetries are preserved.

An essential remark on the relation of the one- and many-body symmetries. A total symmetry of the system does not necessarily imply the existence (or conservation) of the same symmetry on each of the particles of the system. A self-adjoint operator $\mathcal{A}$ that acts on the Hilbert space of the N-body wave functions Ψ is associated with a measurable physical quantity of this N-body system. The expression of the state Ψ of the system as an eigenfunction of the operator $\mathcal{A}$ allows one to speak of a 'symmetric' state $\Psi_{\mathcal{A}}$. In order to provide a proper description of the system the state $\Psi_{\mathcal{A}}$ has to be also an eigenfunction of the Hamiltonian operator of this system H. This implies the vanishing commutator of the two operators $[H, \mathcal{A}] = 0$. At the N-particle level, the quantities $H, \mathcal{A}$ and Ψ are functions of N variables. We assume that $\mathcal{A}$ is a linear operator that can be expressed as a sum of single-particle operators $\mathcal{A}_i$. Which symmetry does the commutator $[H, \mathcal{A}] = 0$ imply now? In fact, it only suggests that there is one constraint – conserved quantity; the eigenvalue of $\mathcal{A}$ or, alternatively, the total quantum number A. What do we know about the 'microscopic' symmetries, i.e., the commutators $[H, \mathcal{A}_i] = 0$? In fact nothing. It could well be that the symmetries at the single particle level are not conserved, while they are at the many-particle level. That is, the sum $\sum_i \mathcal{A}_i$ commutes with H while its components do not. Consider, for instance, the example of angular momenta (see Ref. [31], vol. 2, Ch. 10). In that case, a spherically symmetric potential $V(\mathbf{r}) = V(r)$ and an interaction potential that depends only on the distance between two particles, for

instance, a two-body interaction of the form $u(\mathbf{r}_i, \mathbf{r}_j) = u(|\mathbf{r}_i - \mathbf{r}_j|)$, would preserve the *total* angular momentum $L = \sum_i L_i$ but not necessarily each one the of single-particle operators L_i, $i = 1, \dots N$. In other words, exchange of angular momenta between the particles is possible, even when the relation $[H, L] = 0$ is satisfied.

What does this mean in the case of a Bose gas? Interestingly, in a Gross-Pitaevskii description (see Sec. 3.3), where only $M = 1$ orbital participates, such an exchange cannot occur. In fact, within this theory, the many-body and the single-particle wave functions are identified – one writes $\Phi(\mathbf{r}_1, \dots, \mathbf{r}_N) = \phi(\mathbf{r})^{\otimes N}$. So, if the symmetry is preserved at the single-particle level it is necessarily so at the many-body level and vice versa. In the multi-orbital mean-field theory (see Ch. 3 for details) we have found also no such an exchange. Only at the many-body level, where the total wave function is expanded over a finite set of mean-field states (see Ch. 3) one can – in principle – speak of $[H, L] = 0$ and simultaneously $[H, L_i] \neq 0$ for all or some i. In our present research, however, we have found no such states; the 'exact diagonalization' procedure (Ch. 5) yields symmetry-preserving states at all levels. Hence in this work $[H, L] = 0 \Leftrightarrow [H, L_i] = 0$ for all i. It is an open question if such states (i.e., symmetry-broken at the single-particle level but symmetry-preserving at the many-body level) exist at all, and whether they have the bosonic symmetry.

2.2 Yrast states

Long before the advent of the ultracold many-body physics, another field involving the study of quantum systems of N-particles had been developed: that of nuclear physics[2]. And as a result, several of the problems of ultracold bosons, researchers in nuclear physics have faced long ago. In the context of studying heavy nuclei and their properties, the concept of yrast[3] states has been suggested already since the late 1960's [33]. This is simply the state of the many-body system lowest in energy for some given total AM. In 1999 Mottelson [34] introduced the term 'yrast state' for the description of states of a BEC with non-zero AM. The idea behind that is to determine the ground state energy of a system of trapped bosons, for some given AM and investigate the dependence of the structure of the yrast states on the nature, sign and strength of the interaction.

Various groups and researchers have examined the structure of the yrast states of BECs mostly in the repulsive [35–38] and less often in the attractive [29, 34] case. Principally, one is interested in the dependence of the interaction energy ϵ_{int} on the total AM L and this connection is highly relevant for the present Thesis. One common result for two-dimensional gases, is that the absolute value of the interaction energy $|\epsilon_{\rm int}(L)|$ is a non-increasing function of the total AM L (see, for instance, Ref. [35]). Specifically, it has been found that the interaction energy of the gas in a ground (yrast) state with some

[2]We refer here, as well as in the bulk of the Thesis, to non-relativistic quantum theories and hence do not include relativistic quantum field theories developed mainly in the context of high-energy and particle physics.

[3]Yrast is the superlative of the swedish word *yr* which translates to whirling or dizzy.

given AM will depend linearly on the AM L if the interaction is repulsive [35, 39] and not depend at all on L if the interaction is attractive [29, 40]. Precisely:

$$\epsilon_{\text{int}} = \begin{cases} \lambda_0(N-1-L/2) & \text{if } \lambda_0 > 0, \\ \frac{\lambda_0}{4\pi}(N-1) & \text{if } \lambda_0 < 0, \end{cases} \tag{2.4}$$

where λ_0 measures the strength of the interaction, L the total AM and N the particle number. We stress the fact that the above results are obtained from a 2D analysis, where $L = L_z$ holds. It should be noted, also, that most of the known works consider bosons that interact weakly. In Chs. 4 and 5 we investigate, among others, the yrast states and their structure in two- and three-dimensional condensates, respectively, for both weak and stronger attractive interaction.

2.3 Quantized Vortices

Generally, a vortex is the way a fluid – classical or quantum – can rotate. And this is to be contrasted to the rigid-body rotation. While the (norms of the) velocities of a rotating rigid body obey the familiar relation

$$v = \omega r,$$

the vortex rotation implies a velocity inversely proportional to the distance from the center of rotation

$$v \sim 1/r.$$

Hence, unlike a rotating rigid body, the further away from the centre of rotation the particle is, the slower it rotates. This means that at $r_0 = 0$ the velocity tends to infinity. In order to avoid this infinity, nature forbids the center of the fluid to be occupied by particles, and hence the 'eye of the hurricane' remains empty. Tornadoes and cyclones are illustrious examples of vortices seen in nature. Vortices are very important for the study of various fluid phenomena, as for example classical or quantum turbulence.

A quantum fluid can also rotate, incorporating this type of rotation, i.e., the vortex motion. The possibility of such a configuration has been theoretically noted already since the 1950's by Feynman, Onsager and Abrikosov independently [2, 41, 42], for bosonic quantum fluids, such as liquid helium-4. A quantum fluid – or more correctly its condensed fraction – that occupies the quantum state $\psi(\mathbf{r}) = \rho(r)e^{iS(\theta)}$, with ρ and S real functions of the coordinates r and θ respectively, yields the velocity field $\mathbf{v} = \frac{\hbar}{m}\nabla S$. Provided that the geometry is simply connected, i.e., there are no vortex lines, the velocity field $\mathbf{v}$ is irrotational, i.e., $\nabla \times \mathbf{v} = 0$. The single-valuedness of the wave function, i.e., that the wave function can at most acquire a phase $2k\pi$ with k integer around a closed loop c, provides the quantization condition for the circulation of the vortex state:

$$\Gamma = \oint_c \mathbf{v} \cdot d\mathbf{l} = \frac{2\pi\hbar}{m}k = \frac{h}{m}k. \tag{2.5}$$

The vorticity in a quantum gas is considered to be a hallmark property of the fluid, whose presence alone is enough to characterize it as a superfluid [30, 43, 44]. The first experiments showing the signatures of vortices in liquid helium-4 date back to 1950's [45, 46]. These and later experiments are the well-known rotating bucket experiments. Therein it has been observed that when the container of the fluid rotates with a frequency less than a critical one the fluid remains still without following the rotation of its container. As the rotating frequency is increased, a vortex is suddenly created in the fluid and the symmetry of the system is spontaneously broken. For faster rotations more and more vortices are being created, leading to a lattice of vortices in a triangular spatial distribution, the so-called Abrikosov lattice [47–49].

Are quantized vortices present in bosonic atomic gases? The answer is affirmative. Experiments since 1999 have shown that indeed vortices can be nucleated in clouds of ultracold atomic gases. The first of those were performed by the Paris [50–52] and MIT [53] groups, that followed two independent methods of transferring angular momentum to the atomic gas. In the first of the two experiments the vortex was created by a rotating anisotropy on top of the trapping potential, thus mimicking the rotating-bucket experiment of helium. In the second, a 2π phase was imprinted on the wave function by exciting internal states of the gas, that consisted of two types of bosons. Due to this phase the gas acquired a velocity field and the wave function a node in the centre of the trap. Later on, additional experiments have been performed revealing the existence of vortex lattices [54], giant vortices [55], vortex dipoles [56], vortex clusters [57], strongly correlated rotating lattices [58] and more (see also the Reviews of Refs. [59–62]).

However, all of the experiments performed with rotating condensates are done with repulsive condensates, i.e., gases whose particles repel each other. To the best of our knowledge there has been, to present day, no experimental report on vortices or any other rotational collective motion in attractive gases. Ch. 6 of this Thesis is devoted to the behavior of attractive gases under external rotation of harmonically trapped gases and explains the absence of symmetry breaking/changing of the wave function. It should be noted that it has been shown theoretically that vortices can be nucleated in a rotating anharmonic (quadratic+quartic) trap [63].

Does the AM affect the collapse, as described in Ch. 1, of an attractive gas? It has been shown already in Ref. [26] within the Gross-Pitaevskii theory (see Sec. 3.3) that a vortex state in a 3D attractive gas can support a greater particle number than the ground state with no vortex. In Chs. 4 and 5 we examine the problem of the stability of the gas as the AM of it is increased and we connect this problem to the fragmentation of the state [27, 28].

We note that a quantized vortex, as a rotating state of the gas, is a coherent object by definition, where each boson carries the same angular momentum $l = \hbar = L/N$. In other words, a vortex implies angular momentum, all equally distributed to each boson of the system. But angular momentum does not necessarily imply a vortex! For instance, the AM L of an attractive BEC is distributed among different single-particle states, and is not absorbed into a single orbital with orbital angular momentum (OAM) l [29]. A coherent vortex in this case is an excited state and would be energetically costly.

2.4 State of the art and known results

Rotating states of quantum fluids, vortex lines and angular momentum state have been the subject of scientific research already since the 1960's in the context of mean-field theories [64, 65]. In fact, the celebrated Gross-Pitaevskii equation was derived in order to describe vortex lines in the Bose gas, a landmark superfluid property. More recent advances, also within mean-field theories, attempted to explain collective motions of the gas [66], spontaneous symmetry breaking and vortex nucleation [44], externally rotated gases [67] and other situations [24, 26, 68–72]. On the other hand, there has been also significant contribution from work that utilizes methods that go beyond the mean-field theory (see next chapter for a discussion of the different theoretical approaches). Specifically, light has been shed on the different configurations of the gases that bear AM in the repulsive [34, 35] and attractive [29, 34] cases, on the yrast states [43], on gases in harmonic and quartic trapping potentials [63, 73] and many other cases [28, 36, 39, 74–84].

We close this chapter with a concise exposition of the three different ways a gas can bear AM. In most, but not all, of the cases the question on how can one distribute or add angular momentum in the Bose gas is answered in the context of a mean-field analysis. Following the exposition of Ref. [30], Chs. 7 and 9, one can identify three different phases of the gas that possesses AM: i) the vortex state, ii) the surface modes [85, 86], and iii) the center-of-mass rotation [29]. The vortex state, that has been discussed in Sec. 2.3, is a rotating – coherent – state with a wave function $\psi \sim re^{-r^2/2}e^{im\theta}$. It carries m quanta of angular momentum and a node is imprinted in the center $r_0 = 0$ of the rotation. The surface modes are found in strongly repulsive gases. They are perturbations on the density n that vanish in the centre of the gas and take a maximum value on the surface of the cloud and can, additionally, possess AM [30]. Rotating *nodeless* density perturbations $\delta n \sim Y_{l,m_l}(\theta, \phi)$ have been experimentally created – for instance, for $l = m = 2$, as reported in Ref. [85]. While the cases i) and ii) describe rotating states of the repulsive gas, the third one pertains to attractive ones. It is the phase where the center of mass carries all the angular momentum (collective motion of the center of mass). It is expressed as $\psi \sim r_c^L e^{\sum_i^N -r_i^2/2}$, where r_c is the center of mass and L the AM. In that case it has been found (in the two-dimensional analysis of Ref. [29]) that it is energetically more favorable if the centre of mass absorbs all existing AM. Thus, the interaction part of the energy $\epsilon_{\rm int}$ will remain the same as that of the non-rotating ground state. Given the fact that $|\epsilon_{\rm int}(L = 0)| > |\epsilon_{\rm int}(L > 0)|$, for any L, this special center-of-mass rotation indeed minimizes the energy. In accordance to that, the authors of Ref [80] identify only two possibilities for the ground state with some non-zero AM: either the vortex state for repulsive gases or a collective rotation for attractive ones. It is interesting that these results are obtained for any functional form of the interaction and not only the common delta-function representation.

In Ch. 4 we scrutinize, using new mean-field theoretical methods, the ground state of the attractive gas with some AM. We arrive at results that deviate, at some point, from those of Ref. [29] and identify the found ground state as a fourth 'phase' or possibility for

the gas to bear AM.

Chapter 3

Ultracold bosonic gases in a trap: tools and methods

In this chapter the known theoretical methods that are relevant for the description of the ultracold bosonic gases are introduced. The basic notions are given and derivations of the governing equations (Schrödinger-like equations) are briefly but concisely discussed. The different *ansätze* that are used in order to approximate the stationary solution of the many-body Schrödinger equation are presented, from the many- to the single-particle level. The general methods presented in this chapter are used throughout the whole Thesis.

3.1 Introduction

Modern physics is concerned with problems that involve many interacting quantum-mechanical particles, at many different levels. Nuclear physics, the study of molecular cluster and physics of ultracold atoms are such examples. Solving, however, the Schrödinger equation with dN degrees of freedom, for a system of N particles in d spatial dimensions, is in the majority of the situations impossible. A mean-field (MF) theory is an approximate way to tackle such complex N-particle problems. MF theories have been developed for and applied to various physical problems that involve many interacting, particles. In the context of nuclear physics MF theories are known and used since the 1950's [87], the best known of them being the Hartree-Fock approximation. A MF theory is, roughly speaking, a way of mapping the MB problem to a one-body problem with a chosen effective potential [87, 88]. This effective field replaces the result of the interaction of all the other particles of the system to an arbitrary particle with a single function (interacting potential). One, in order to reduce the complexity of the problem, describes the state of the many-body system in terms of single-particle states. This means, approximating the many-body state with an *ansatz* which is built explicitly on one single-particle state. MF theory by construction, disregards any quantum fluctuations of the system, and can be also thought of as a zeroth-order expansion of the Hamiltonian in fluctuations.

The celebrated Gross-Pitaevskii (GP) theory is the best example of such a MF theory derived for and applied to gases of bosonic atoms at zero temperature. Within the GP theory the system is described by a MF *Hartree* product over a single orbital, symbolically $\Psi_{MB} = \psi^{\otimes N}$.

There have been, however, several efforts to exactly solve the MB Schrödinger equation for bosons and circumvent the assumptions that MF theories introduce. For example, the quantum Monte Carlo computational techniques have been developed to simulate many-body quantum systems and also applied to bosonic systems [89]. More recently, a successful and rigorously defined theory was formulated; the Multi-Configurational Hartree for Bosons (MCHB), that we very briefly describe in Sec 3.5.2.

In this Thesis we describe the stationary (time-independent) state of various attractive bosonic gases in two and three spatial dimensions. We follow different methods – as described further in this section – and compare the findings. Starting from rather physical questions on the ground state of the system we conclude that GP theory is not enough to describe configurations of the gas under specific requirements. Specifically, we ask how the quantum states of definite angular momentum eigenvalues look like and what the (low-lying) excitations of the ground-state of Bose gas in two or three dimensions are and we find that these states do not fit in a GP description.

3.2 A system of N ultracold bosons

We consider a system of N identical spinless and structureless bosons of mass m at zero temperature, confined by an external time-independent potential $V(\mathbf{r})$. The bosons can interact with each other, pairwise. The nature of the interaction and its functional expression depend on the nature of the particles, on the magneto-optical fields applied externally to the gas and other parameters. This interaction enters the total Hamiltonian of the system as a general two-body interaction potential $w(\mathbf{r}_i - \mathbf{r}_j)$, where $\mathbf{r}_i$ are the space coordinates of the i-th boson.

The Hamiltonian of the system is hence:

$$H = H_0 + \lambda_0 W, \tag{3.1}$$

with

$$H_0 = \sum_i^N h(\mathbf{r}_i) = -\frac{\hbar^2}{2m} \sum_i^N \nabla^2_{\mathbf{r}_i} + \sum_i^N V(\mathbf{r}_i) \tag{3.2}$$

and

$$W = \sum_{i<j}^N w(\mathbf{r}_i - \mathbf{r}_j), \tag{3.3}$$

where the parameter λ_0 measures the strength of the interparticle interaction. This parameter is proportional to the s-wave scattering length α_s and takes on negative values for

attractive interaction. Precisely, in the three-dimensional case[1] $\lambda_0 = 4\pi\alpha_s\sqrt{\frac{\hbar}{m\omega}}$, where ω is the frequency of the (here isotropic) trapping potential. Throughout the Thesis we choose $V(\mathbf{r}_i) = V(r_i)$, i.e., the trap potential has spherical symmetry, except in the last chapter on rotating condensates, where slightly asymmetric traps are examined as well. Furthermore, we consider only contact (or zero-range) interaction. This means that the bosons will 'feel' each other's presence – they will exchange energy – only when they occupy the same point in space. Hence we use for the interaction operator the common delta-function representation, $w(\mathbf{r} - \mathbf{r}') = \delta(\mathbf{r} - \mathbf{r}')$. This approximation makes a physical sense in gases at very low densities and zero temperatures and captures the effects of the s-wave scattering. The system of N particles is fundamentally described by the time-independent MB Schrödinger equation, This reads:

$$H\Psi = E\Psi, \tag{3.4}$$

where $\Psi = \Psi(\mathbf{r}_1, \mathbf{r}_2, \ldots \mathbf{r}_N)$ is the MB wave function of the system of N interacting bosons and E the eigenvalue of the operator H, corresponding to the state Ψ. The question is now how to find or estimate this wave function Ψ. Even in the simplest case, where the confining potential $V(\mathbf{r})$ is isotropic, no analytic solutions[2] for the MB Schrödinger equation of $3N$ variables are known. Moreover, an exact numerical solution of the problem would require – already for small N – a tremendous amount of computational power. In order to come up with physically meaningful solutions one has to admit specific approximations, whose generality will determine the range of validity and applicability of the approach. We discuss in the following sections three different approaches in the description of the solution, starting with the less general one.

3.3 The Gross-Pitaevskii approach

We assume a specific distribution of the bosons of the gas over the single-particle wave functions – also called *orbitals*: all N particles occupy one and the same single-particle state (orbital). Then, the total wave function of the system simply becomes a product of N times the prototypal orbital ϕ_0 in question:

$$\Phi_{GP}(\mathbf{r}_1, \mathbf{r}_2, \ldots, \mathbf{r}_N) = \prod_i^N \phi_0(\mathbf{r}_i) = \phi_0(\mathbf{r}_1)\phi_0(\mathbf{r}_2)\ldots\phi_0(\mathbf{r}_N). \tag{3.5}$$

Now the quantum state of the BEC is uniquely described by this orbital ϕ_0 which generally depends on time, $\phi_0 = \phi_0(\mathbf{r}, t)$. The orbital is normalized to unity

$$\int d\mathbf{r}|\phi_0(\mathbf{r})|^2 = 1,$$

[1]The relation of the coupling parameter λ_0 of the Hamiltonian to the s-wave scattering length in two dimensions is somewhat more complicated. See, for instance, Refs. [90, 91].

[2]Except in the case of two interacting bosons, where there is an analytic known solution [92].

although the normalization $\int d\mathbf{r}|\phi_0(\mathbf{r})|^2 = N$ is widely used as well. We follow hereafter the normalization to unity. So, by construction, all atoms of the gas occupy the orbital ϕ_0 and hence the state of the system is the condensed state Φ_{GP}. Its energy E is given by:

$$\langle\Phi_{GP}|H|\Phi_{GP}\rangle = N\int d\mathbf{r}\left[\frac{\hbar^2}{2m}|\nabla\phi_0(\mathbf{r})|^2 + V(\mathbf{r})|\phi_0(\mathbf{r})|^2 + \lambda_0\frac{N-1}{2}|\phi_0(\mathbf{r})|^4\right]. \tag{3.6}$$

Minimizing this energy with respect to infinitesimal variations in $\phi_0^*(\mathbf{r})$ while holding the number of atoms constant leads to the time-dependent Gross-Pitaevski equation:

$$i\hbar\frac{\partial\phi_0}{\partial t} = \left[-\hbar^2\frac{\nabla^2}{2m} + V(\mathbf{r}) + \lambda_0(N-1)|\phi_0(\mathbf{r})|^2\right]\phi_0\ . \tag{3.7}$$

For a solution of the type $\phi_t(\mathbf{r},t) = e^{-i\mu t/\hbar}\phi_0(\mathbf{r})$ one arrives at the time-independent Gross-Pitaevskii equation:

$$\left[-\hbar^2\frac{\nabla^2}{2m} + V(\mathbf{r}) + \lambda_0(N-1)|\phi_0(\mathbf{r})|^2\right]\phi_0 = \mu\phi_0, \tag{3.8}$$

where μ is the chemical potential of the system. For an overview and derivation of the GP Equation see Refs. [30, 93]. The GP equations is an effective, nonlinear Schrödinger-like equation, whose solution ϕ_0 carries *all* the information about the system. It should be valid at very low densities [8, 30]:

$$\sqrt{n\alpha_s^3} \ll 1, \tag{3.9}$$

where n is a typical value of the density and α_s the s-wave scattering length. GP theory constitutes nowadays the most standard and widely accepted MF theory to describe ultracold Bose gases and has been indeed applied successfully in various cases (for instance, in the studies of sound waves, collective excitations, quantized vortices and others [93]). Nevertheless, the reader should not forget that the GP equation is only, as said, an effective equation, based on the restrictive assumption that all the bosons of the system reside in one orbital ϕ_0 and hence the system remains condensed throughout the time-evolution of the system. It should be noted that, as a matter of fact, no direct physical conditions – perhaps other than the resemblance to superfluid systems – enforce such a restricted one-orbital approach, as the GP theory. For a discussion and critique on the definitive assumptions of the GP equations see Sec. 4.3 of Ref. [8] and Ref. [94]. Historically, the GP equation was developed in the context of quantum field theory in order to describe vortex lines in superfluid systems [64, 95]. In any case, it is today a widely accepted theory for the bosonic gases in all aspects. We shall see in the following how the GP description can be generalized.

3.4 Multi-orbital Best-Mean-Field Theory: extending the GP case

We saw in the previous section how a specific assumption about the distribution of the population of the system – the simplest one – leads to a specific equation and description

of the quantum state of the gas. Let us now relax the above assumption. We allow the gas to populate more than one orbitals $\phi_i,\ i = 1, \dots M$. The total wave function of the system then becomes:

$$\Phi(\mathbf{r}_1, \mathbf{r}_2, \dots, \mathbf{r}_N) = \mathcal{S} \prod_i^N \phi_1(\mathbf{r}_1) \dots \phi_1(\mathbf{r}_{n_1}) \phi_2(\mathbf{r}_{n_1+1}) \dots \phi_2(\mathbf{r}_{n_2}) \dots \phi_M(r_N). \tag{3.10}$$

Here, the operator $\mathcal{S}$ is applied in order to ensure the appropriate bosonic symmetry (positive sign under exchange of any two coordinates i, j) of the wave function Φ. The above *ansatz* describes a system where n_i particles reside in the orbital ϕ_i. The RDM of such a state yields M eigenfunctions ϕ_i with eigenvalues n_i. Hence, it is a *fragmented* state (see also Sec. 1.2) and the orbitals ϕ_i are called *fragments*. The state of Eq. (3.10) can be regarded as the permanent of the matrix with elements $\phi_i(\mathbf{r}_j)$, i.e., the symmetric analogue of a Slater determinant. In the present Thesis we shall use the term *permanent* to refer to an ansatz of the type of Eq. (3.10). Another possibility to express a fragmented state is by a Fock space representation:

$$\Phi = |\vec{n}\rangle = |n_1, n_2, \dots, n_M\rangle. \tag{3.11}$$

Here it is meant that n_i particles occupy the i-th single particle state.

Fock states are particularly convenient in the second-quantization framework. The creation and annihilation operators acting on a Fock state are defined as:

$$b_k^\dagger |n_1, \dots, n_k, \dots, n_M\rangle = \sqrt{n_k + 1}\ |n_1, \dots n_k + 1, \dots, n_M\rangle \tag{3.12}$$

and

$$b_k |n_1, \dots, n_k, \dots, n_M\rangle = \sqrt{n_k}\ |n_1, \dots n_k - 1, \dots, n_M\rangle. \tag{3.13}$$

The operators satisfy $b_i b_j^\dagger - b_j^\dagger b_i = \delta_{ij}$. Now, Eq. (3.11) can be rewritten as:

$$\Phi = \frac{1}{\sqrt{n_1! n_2! \dots n_M!}} (b^\dagger)^{n_1} (b^\dagger)^{n_2} \dots (b^\dagger)^{n_M} |\text{vac}\rangle, \tag{3.14}$$

where $|\text{vac}\rangle$ is the Fock state of no particles. The resulting energy, i.e., the expectation value of the Hamiltonian operator over the state of Eq. (3.10) is:

$$E_{\text{BMF}} = \sum_i^M n_i h_i + \frac{\lambda_0}{2} \sum_i^M (n_i - 1) n_i w_{ii} + \lambda_0 n_i n_j \sum_{i \neq j}^M w_{ij}, \tag{3.15}$$

where we used the shorthand notation $h_i = \int d\mathbf{r} [\frac{\hbar^2}{2m} |\nabla \phi_i(\mathbf{r})|^2 + V(\mathbf{r}) |\phi_i(\mathbf{r})|^2]$ and $w_{ij} = \int d\mathbf{r} d\mathbf{r}' \phi_i^*(\mathbf{r}) \phi_j^*(\mathbf{r}') w(\mathbf{r}, \mathbf{r}') \phi_i(\mathbf{r}) \phi_j(\mathbf{r}')$. After substituting the two-body interaction operator $w(\mathbf{r}, \mathbf{r}')$ with the commonly used Dirac δ function, we get:

$$E_{\text{BMF}} = \sum_i^M n_i h_i + \frac{\lambda_0}{2} \sum_i^M (n_i - 1) n_i |\phi_i|^4 + \lambda_0 \sum_{i \neq j}^M n_i n_j |\phi_i|^2 |\phi_j|^2. \tag{3.16}$$

How will the equations of motion for this new MF ansatz look like? A standard Lagrange multipliers minimization of the energy E_{BMF} with respect to the function ϕ_k^* yields M self-consistent (here time-independent) equations for the M different, orthonormal orbitals ϕ_k:

$$\left[h_k + \lambda_0(n_k - 1)|\phi_k|^2 + 2\lambda_0 \sum_{j\neq k}^{M} n_j|\phi_j|^2\right]\phi_k = \sum_{j}^{M} \mu_{kj}\phi_j, \quad k = 1, \ldots M, \tag{3.17}$$

where μ_{ij} are the Lagrange multipliers. This is a set of M coupled partial differential equations[3]. This can be regarded a generalization of the GP equation to the case where $M > 1$ orbitals are macroscopically occupied and explicitly taken into account in the construction of the many-body state of the system. Of course, if $M = 1$ Eqs. (3.17) boil down to the GP equation, with μ_{11} being the usual chemical potential. Generally, with this mean-field theoretical method, the energy of the system is variationally optimized and M orbitals and their respective occupations are found by solving Eqs. (3.17). This method was given the name *Best Mean Field* (BMF) because it allows to determine the lowest-in-energy mean-field, and hence the name 'best'. Similar to Eqs. (3.17), time-dependent equations of motions have been also derived. The details on the derivations can be found in Ref. [96] for the time-independent and in Ref. [97] for time-dependent cases.

3.5 Beyond mean-field theories

In this section we present two methods which enable us to describe the Bose gas beyond a MF theory. Generally, an ansatz, i.e., a trial wave function that serves as (the approximation to the) solution of the system, is called a MF ansatz when it can be written as a single permanent [Eq. (3.11)], and a MB ansatz otherwise. A good way to unlock ourselves from the MF restriction is the so-called *Configuration Interaction* (CI) method. This method was developed already in the first days of quantum mechanics (see the seminal work of Hylleraas [98], where he applies CI to compute excitation spectra of a helium atom) and later on extensively used to the study of molecular and chemical many-body systems [99]. Also known as *exact diagonalization*, it is based on representing the many-body Hamiltonian as a matrix, over a pre-chosen orbital basis, and then diagonalizing it on this basis. This method has been fruitfully applied to ultracold bosonic systems, as a tool to go beyond a MF description (see, for instance, [35, 100]).

A more advanced and accurate approach to the solution of the many-body Schrödinger equation, is the Multi-Configurational Hartree for Bosons (MCHB) [101]. The advantage and generality of this method, besides that it utilizes by construction the CI expansion, relies on the fact that it provides equations of motion for all M independent orthonormal orbitals that can in principle be exactly calculated.

[3]It should be noted that, without the choice $w \to \delta$ the present best-mean-field equations are a set of coupled integro-differential equations.

3.5.1 Configuration Interaction

To start with, one needs to express the MB ansatz Ψ of the system not as a single permanent (i.e., a MF state $|\Phi\rangle$) but rather as an expansion over a finite set of them $\{\Phi_i\}$

$$|\Psi\rangle = \sum_{i}^{N_p} C_i |\Phi_i\rangle, \tag{3.18}$$

where N_p is the total number of permanents used in the expansion and $C_i,\ i = 1 \dots N_p$ the corresponding coefficients. The question that arises is what the set of MB basis functions $\{\Phi_i\}$ consists of. Generally, this includes, as already mentioned, all the permanents that result from distributing N bosons over M orbitals. Readily, these states are those of Eq. (3.10) or Eq. (3.11), where n_j denotes the respective occupation number of the single-particle functions (orbitals) ϕ_j.

Mathematically seen, the permanents $|\Phi\rangle$ are the vectors that span the Fock space $\mathcal{F}$ of all N-body wave functions. Consider for the time being conserved spatial symmetries, that is, eigenfunctions Φ^L of the angular momentum L and parity Π operators. It is then possible to reduce the size of the 'working' Fock spaces, by partitioning the initial space into Π- and L-subspaces, i.e., spaces of permanents with definite parity and angular momentum. The purpose to do so is twofold; firstly the resulting solution $|\Psi\rangle$ will possess the rotational symmetries of the system and secondly the working $\{\Phi_i^L\}$ spaces are each time much smaller in size than the initial $\{\Phi_i\}$ one. It should be noted that, while this partitioning of the configuration space with respect to angular momentum L is trivial in a two-dimensional system, it is not straightforward in the full 3D case. This side-remark is important for the analysis of Ch. 5.

Then, the MB Hamiltonian H in the $\{\Phi_i\}$-basis is represented as a *secular* matrix $\mathcal{H}$, with elements:

$$\mathcal{H}_{i,j} = \langle \Phi_i | H | \Phi_j \rangle. \tag{3.19}$$

By diagonalizing the above equation one can obtain the energies (eigenvalues) and coefficients C_i (eigenvectors) for the ground and the excited states of the system. It can be shown [99] that, equivalent to diagonalizing the matrix of Eq. (3.19) is solving the equation

$$\mathcal{H}\mathbf{C} = \mathcal{E}\mathbf{C}, \tag{3.20}$$

where $\mathbf{C}$ is the column vector of the expansion coefficient $\mathbf{C} = \{C_1, C_2 \dots, C_{N_p}\}^T$ and $\mathcal{E}$ the corresponding eigenvalue.

It should be noted that, in order to evaluate the expression of Eq. (3.19) and, of course, determine the solution of Eq. (3.18) one needs to specify the single-particle states ϕ_i, over which the permanents Φ are built. On one hand, the number M of these single-particle states will result in a larger or smaller size for the matrix $\mathcal{H}$. On the other hand, the symmetries of the system will generally reduce the size of the configuration space. Hence, the complexity of a CI problem is determined from both the number M and the symmetries. Since a *complete* configuration space would be infinite-dimensional, the space

of the orbitals (and hence that of the permanents) has to be truncated and limited down to a relatively small number M, so that real calculations can be performed.

There are many 'guesses' for the single-particle states one could make and they strongly depend on the nature of the physical system under consideration. A general method is to use, as such guesses, the set of functions that solve the non-interacting problem, that have been somehow modified, i.e., extended to the case of interacting particles. In other words, we imply a constraint to the single-particle wave functions ϕ_j; we suppose that the single-particle states can be well approximated by wave functions – *ansätze* – that are completely known, upon some real parameters σ_i. Hence, we fix *a priori* the solutions of the system of M coupled nonlinear differential equations to M mono-parametric families of complex wave functions and we then look for the values of σ_i that 'optimize' the solution, i.e., values that assign an extremal value to the energy functional. Such ansätze have also been applied in other works [102–104] and since they are taken in our case after the (exact) solution of the corresponding non-interacting system they inherit the symmetries of the original system. The orbital bases that we use are discussed in Sec. 3.6 and in more detail within each chapter separately, in close connection to the problem that we attack each time.

3.5.2 Multiconfigurational Hartree for Bosons (MCHB)

Even though the CI expansion has proven to be an efficient way to solve quantum N-body problems beyond MF approximations, it suffers from few drawbacks. Most importantly, the results depend strongly on the chosen basis set. To resolve this, a general Multi-Configurational Time-Dependent Hartree (MCTDH) method has been proposed two decades ago [105]. MCTDH was developed in the context of multi-dimensional molecular systems and its advantage is that the single-particle states are time-adaptive and determined fully variationally. That is, instead of a fixed initial guess for the orbitals, the MCTDH algorithm fully determines the M orbitals that – within given constraints – minimize the energy. More recently, a version of MCTDH has been derived for indistinguishable bosons. Namely, the time-independent *Multi-Configurational Hartree for Bosons* [101] and the *Multi-Configurational Time-Dependent Hartree for Bosons (MCTDHB)* [106]. A detailed presentation and discussion of these theories and their implications goes beyond the scopes of the present Thesis. Since they are not the main tool of our analysis we only give a brief account of them. Nonetheless, MCHB is relevant to the methods used herein and is, furthermore, used for the GS energy calculation in Ch. 4, in the special case where $L = 0$. The starting point of MCHB, is to write the MB wave function Ψ as a CI expansion, evaluate the action S over this state Ψ and then minimize S with respect to the orbitals $\phi_j,\ j = 1, \ldots, M$ and coefficients C_i. The crucial difference between the MCHB and all other exact diagonalization methods is that the orbitals are now determined completely variationally. The resulting coupled equation of motions are somewhat more complicated than the BMF ones and the solutions of them are obtained numerically. For details in the method see [101, 106, 107], while applications of MCTDHB include Refs. [108–112].

3.6 Single-particle states

To perform explicit calculations and utilize the above methods, as said, one needs to determine a specific set of orbitals. Of course, these must be cleverly chosen, to allow both computational efficiency and also encompass the very fundamental properties that the solution of the system is expected to possess, at the single-particle level. The orbitals that we use in the analysis of the following chapters are 'modeled' after the single-particle states that solve exactly the non-interacting problem. This allows us to preserve all the symmetries of the non-interacting case to the interacting one. This is, of course, desired, since the two-body interaction operator $w(|\mathbf{r}_i - \mathbf{r}_j|)$ respects the many-body (total) symmetries. The states that solve the harmonic oscillator problem are the well known Gaussian-times-Hermitian functions. However, in order to use and extend these solutions in the presence of interaction, one needs to take a crucial correction into account. Once the interaction (here attraction) is switched on the shape of the orbitals will not remain unaffected. So, we give an extra degree of freedom to the orbitals and allow the width of them to vary as a function of the interaction strength. To this end, we employ scaled Gaussians[4] as our orbital-basis, i.e.,

$$\phi(\mathbf{r},\sigma) \sim H_{n_x}\left(\frac{\omega_x}{\sigma_x},x\right) H_{n_y}\left(\frac{\omega_y}{\sigma_y},y\right) H_{n_z}\left(\frac{\omega_z}{\sigma_z},z\right),$$

where H_k is the Hermite polynomial of degree k. In terms of spherical harmonics Y_{lm} the orbitals read:

$$\phi(\mathbf{r},\sigma) \sim \sigma^{-3/2}\exp[-r^2/(2\sigma^2)]Y_{lm_l}(\theta,\phi),$$

for integer values of n_x, n_y, n_z and $|m_l| \leq l$. The total energy E of the system is in principle a functional $E = E[\Phi]$ that has to be evaluated over the many-body wave function Φ (or generally $\Psi = \sum C_i\Phi_i$). With a specific choice of an orbital basis the quantity E becomes a function of the scaling parameters σ_i, i.e., $E = E(\{\sigma_i\})$. Such a basis can consist of the above orbitals ϕ, truncated to some maximum values of n_x, n_y, n_z or l, m_l. The values of σ_i that will minimize the total energy E of the system are the optimal widths. It should be noted that the inclusion and optimization of σ_i is not only a quantitative improvement of the results, but also a qualitative advance: it can capture the collapse of the gas. If the strength of the interaction exceeds a critical value (see Secs. 1.3 and 3.8) the atomic cloud will shrink and implode. By modifying the width of the orbitals, the shrink and collapse can be seen and quantified in this scaled-Gaussians approximation. This will be clear in the following chapters.

In this work much of the analysis of the quantities of the system (energy, occupation numbers, variances of expansion coefficients) is done with respect to the scaling parameter(s). So for example, we expect to see a (local) minimum in the plot of the total energy $E(\sigma_i)$ as a function of σ_i if the system is metastable, while the absence of minimum will signal a collapsing condensate. Moreover, the analysis of the properties of the

[4]Here normalization is not taken into account. In each one of the subsequent chapters the orbital basis is discussed in more details and the normalized expressions are given.

found many-body states (e.g. depletion, angular momentum) is always performed at the optimal values of the parameter(s) σ_i.

3.7 Natural orbital analysis

The n-th order reduced density matrix (RDM) is a very useful quantity for the analysis of the system. Generally, it maps the total wave function $\Psi(\mathbf{r}_1, \mathbf{r}_2, \dots \mathbf{r}_N)$ to a function $\rho_K(\mathbf{r}_1, \mathbf{r}_2 \dots \mathbf{r}_K | \mathbf{r}'_1, \mathbf{r}'_2 \dots \mathbf{r}'_K)$, $K \leq N$ of $2K$ variables, while integrating out $N-K$ of them. In Sec. 1.2 the RDM of first order has been introduced as:

$$\rho_1(\mathbf{r}|\mathbf{r}') = N \int \Psi^*(\mathbf{r}', \mathbf{r}_2 \dots \mathbf{r}_N)\Psi(\mathbf{r}, \mathbf{r}_2 \dots \mathbf{r}_N) d\mathbf{r}_2 d\mathbf{r}_3 \dots d\mathbf{r}_N = \sum_{i,j} \rho_{ij} \phi_i^*(\mathbf{r}')\phi_j(\mathbf{r}) \quad (3.21)$$

The second order RDM is given by:

$$\begin{aligned} \rho_2(\mathbf{r}_1, \mathbf{r}_2 | \mathbf{r}'_1, \mathbf{r}'_2) &= N(N-1) \int \Psi^*(\mathbf{r}'_1, \mathbf{r}'_2, \mathbf{r}_3 \dots \mathbf{r}_N)\Psi(\mathbf{r}_1, \mathbf{r}_2, \mathbf{r}_3 \dots \mathbf{r}_N) d\mathbf{r}_3 \dots d\mathbf{r}_N = \\ &= \sum_{i,j,k,l} \rho_{ijkl} \phi_i^*(\mathbf{r}'_1)\phi_j^*(\mathbf{r}'_2)\phi_k(\mathbf{r}_1)\phi_l(\mathbf{r}_2), \end{aligned} \quad (3.22)$$

with $\rho_{ij} = \langle \Psi | b_i^\dagger b_j | \Psi \rangle$, $\rho_{ijkl} = \langle \Psi | b_i^\dagger b_j^\dagger b_k b_l | \Psi \rangle$ and $b_i^\dagger$ (b_i) the creation (annihilation) operators of Eq. (3.12) [Eq. (3.13)]. As introduced in Sec. 1.2, the single-particle functions ϕ_i^{NO} that diagonalize the right hand side of Eq. (3.21) are the the natural orbitals and the eigenvalues ρ_i are the natural occupations. It should be noted that, the natural orbitals need not be eigenfunctions of the Hamiltonian operator H, associated with the particular physical system. The eigenfunctions of $\rho_2(\mathbf{r}_1, \mathbf{r}_2 | \mathbf{r}'_1, \mathbf{r}'_2)$ are called *natural geminals* [15]. The diagonal elements

$$\rho_{ii} \equiv \rho_i = \sum_{\vec{n}} C_{\vec{n}}^* C_{\vec{n}} n_i = \langle n_i \rangle, \quad (3.23)$$

$i = 1, \dots, M$, are the expectation values of the number operators associated with the natural orbitals ϕ_i and are, as explained, the natural occupations ρ_i of the respective natural orbitals. The above summation is performed over all possible different permanents $|\vec{n}\rangle$. We define the *depletion* d_i of the i-th orbital as:

$$d_i = 1 - \rho_i / N. \quad (3.24)$$

The depletion d_i is an informative quantity which measures the relative number of particles that are depleted from the i-th orbital. Throughout this work we extensively use the quantity d_1 and also refer to it as the s-depletion. The diagonal elements

$$\rho_{iiii} = \sum_{\vec{n}} C_{\vec{n}}^* C_{\vec{n}} (n_i^2 - n_i) = \langle n_i^2 \rangle - \langle n_i \rangle \quad (3.25)$$

are related to the *variance* of the distribution of the coefficients C_i of a given state $|\Psi\rangle$, associated with the natural orbitals ϕ_i, as:

$$\tau_i^2 \stackrel{\text{def}}{=} \langle n_i^2 \rangle - \langle n_i \rangle^2 = \rho_{iiii} + \rho_{ii}(1 - \rho_{ii}). \tag{3.26}$$

The norm

$$|\tau| \stackrel{\text{def}}{=} \sqrt{\tau_1^2 + \tau_2^2 + \tau_3^2 + \tau_4^2} \tag{3.27}$$

gives a measure of the variances [5] of all four orbitals of a state $|\Psi\rangle$. The τ_i's and $|\tau|$ are highly useful quantities, as they measure the fluctuations around the occupation numbers of the natural orbital ϕ_i^{NO}. In the case of a mean-field state, where there are no fluctuations, $|\tau|$ is simply zero.

3.8 Example: collapse of the ground state in two and three dimensions

Lastly, we demonstrate in this section how the variational approach presented above can describe the collapse of the gas. We restrict the discussion to the simplest case where only the ground state of the system is populated, i.e., assuming no significant depletion or fragmentation. Excited states and states with non-zero angular momentum are a central concept of this Thesis and are examined separately in Ch. 4 and 5. Moreover, the approach presented here applies to any number of dimensions D. This allows us to draw conclusions on how the behavior of the system depends on its dimensionality.

In the following, we use $\hbar = m = 1$ and so all units are dimensionless. Consider a system of N bosons confined by an anisotropic potential trap

$$V(\mathbf{r}) = \frac{1}{2} \sum_i^D (\omega_i x_i)^2, \tag{3.28}$$

where ω_i is the trap frequency in the i-th direction. The gas is in its ground state which we write as the GP state $\Phi_0 = |N, 0, \dots\rangle$. In other words, N bosons occupy the orbital ϕ_0. This (normalized) orbital, according to the discussion of Sec. 3.6, is the D-dimensional scaled Gaussian [102, 113]:

$$\phi_D(\mathbf{r}) = \pi^{-D/4} \prod_i^D \sigma_i^{-1/2} \exp\left[-x_i^2/(2\sigma_i^2)\right], \tag{3.29}$$

where σ_i is the non-negative parameter that scales the Gaussian profile in the i-th direction. The total (dimensionless) energy per particle and harmonic oscillator is found to

[5] To be precise, the quantity $|\tau|$ is the norm of the *standard deviations* τ_i, commonly defined as the square root $\sqrt{\tau_i^2}$ of the variance τ_i^2. To avoid confusion we make clear that we use in this work the term *variance* to refer to the norm $|\tau|$.

be:

$$\epsilon_D := \frac{\langle \Phi_0 | H | \Phi_0 \rangle}{\frac{D}{4} N \overline{\omega}} = \frac{1}{D} \sum_{i=1}^{D} \frac{\omega_i}{\overline{\omega}} (\sigma_i^{-2} + \sigma_i^2) - \Lambda_D \overline{\omega}^{\frac{D-2}{2}} \prod_{i=1}^{D} \sigma_i^{-1} \tag{3.30}$$

with

$$\Lambda_D = 2|\lambda_0|(N-1)\frac{(2\pi)^{-D/2}}{D} \tag{3.31}$$

and $\overline{\omega} = (\omega_1 \omega_2 \dots \omega_D)^{1/D}$. Without loss of generality, we examine the isotropic case, where $\omega_i = \omega$ and $\sigma_i = \sigma$. Then, Eq. (3.30) becomes:

$$\epsilon_D(\sigma) = \sigma^{-2} + \sigma^2 - \Lambda_D \omega^{\frac{D-2}{2}} \sigma^{-D}. \tag{3.32}$$

We are looking for the value σ_0 that minimizes the above expression. This σ_0 will determine the optimal shape of the Gaussian orbital ϕ_D and hence the solution for each case. The question is if and where such a minimum of the function $\epsilon_D(\sigma)$ exists, as the parameter Λ_D increases. Let us examine the behavior of the found energy at different dimensionalities.

- $D = 1$. The term $\Lambda_1 \sigma^{-1}$ in the energy $\epsilon_1(\sigma)$ is outweighed by the σ^2 term and so there is a minimum at some $0 < \sigma_0 < 1$, for *any* interaction strength Λ_1. Thus, a stable configuration of the 1D gas exists for all Λ_1.

- $D = 2$. There is a well-defined global minimum of the energy ϵ_2: $\epsilon_{2,\mathrm{opt}} = 2\sqrt{1-\Lambda_2}$ at $\sigma_0 = (1-\Lambda_2)^{-1/4}$. At the critical value $\Lambda_{2,c} = 1$ the energy becomes $\epsilon_2(\sigma) = \sigma^2$. Above $\Lambda_{2,c} = 1$ the minimum of the function $\epsilon_2(\sigma)$ does not exist any more; σ goes to zero and the variational orbital ϕ approaches a delta function. We interpret this behavior as implosion and collapse of the gas. It should be noted that in the case of $D = 2$ the interacting energy and the critical parameter $\Lambda_{2,c}$ do not depend on the trapping frequency ω.

- $D = 3$. Similarly to the 2D case, the energy admits a minimum as well, as long as $\Lambda \leq \Lambda_{3,c} = \frac{8}{15 \cdot 5^{1/4}}$. However, this is only a local minimum; no matter how weak the interaction strength is, the kinetic energy cannot completely compensate the interacting one and hence there is always a barrier of finite height separating the stable from the unstable regions in the σ-space (see third panel of Fig. 3.1). This makes the system *metastable* only, meaning that, after a finite time the system will transit to collapse (i.e., $\sigma \to 0$), by either tunneling through the barrier or by 'jumping' over it due to thermal or energy fluctuations.

The above behavior of energy as function of σ for different dimensions D is depicted in Fig. 3.1.

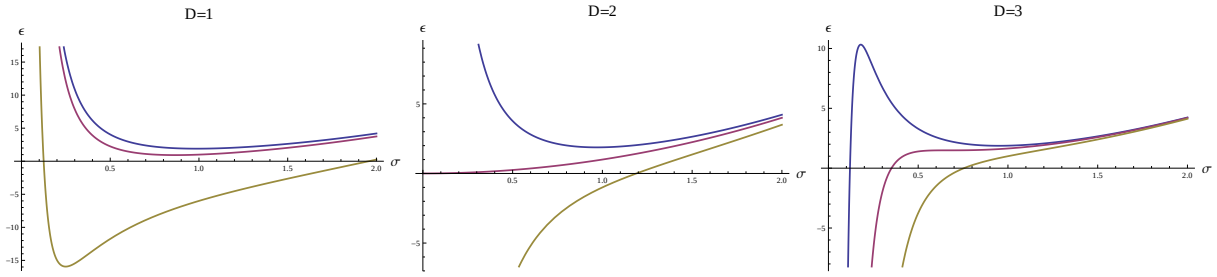

Figure 3.1: Collapse of the GP ground state of an attractive BEC for different dimensionalities and various values of the parameter $\Lambda_D \sim |\lambda_0|(N-1)$. In one dimension (left panel), there is a minimum in the $\epsilon_1(\sigma)$ curve for any attraction strength (plotted are the values $\Lambda_1 = 0.1, 1$ and 8 respectively). The system is always stable. In two dimensions (middle panel), there is a minimum as long as $\Lambda_2 \leq \Lambda_{2,c}$ (upper and middle curve with $\Lambda_2 = 0.12$ and $\Lambda_2 = 1$ respectively). The system is then stable. For larger values than $\Lambda_{2,c}$ the minimum disappears and the system collapses (lower curve with $\Lambda_2 = 3$). In three dimensions (right panel) the only minimum that can exist is a local one; the system is in a metastable state for any interaction less than $\Lambda_{3,c}$ (upper and middle curves with $\Lambda_3 = 0.12$ and $\Lambda_3 = 0.35$ respectively). Otherwise it collapses (lower curve with $\Lambda_3 = 1$).

Chapter 4

The attractive Bose gas in two dimensions

In this chapter we examine the attractive Bose gas in two spatial dimensions and describe the ground state in connection to its angular momentum by using the theoretical methods presented in chapter 3. More specifically, we study the fragmentation of the ground states with some given total angular momentum L, by applying the best-mean-field approach. What makes the two-dimensional attractive gases special is, first, their relatively simple description of the total angular momentum states in terms of single Fock states; and furthermore, the absence of metastability against the collapse of the gas, as it is contrasted to the 3D case.

4.1 Introduction

One of the striking features of ultracold trapped atomic gases, as pointed out in Sec. 1.3, is the deterministic control that can be exerted on the gas and its properties. The density of the gas, the geometry of the trap, as well as the strength and sign of interaction have become fully controllable. Deeper theoretical understanding and advanced experimental tools allow one today to change the sign of the interaction between the bosonic atoms of the gas in a controllable manner and attractive Bose-Einstein Condensates can be formed in the lab [17–19]. Rich novel phenomena in attractive BECs, that are absent in their repulsive counterparts, have given them a special position in contemporary research activity. The collapse and 'Bosenova' phenomenon, for instance, as discussed already in Sec. 1.3, is a good example of such phenomena.

Not accidentally, one of the first case-studies of occurrence of fragmentation in BECs was that of an attractive boson gas in two spatial dimensions [29]. There the authors described the bosonic gas with a many-body ansatz that seemed to be successful at least in the limit where the interparticle interaction is very weak. One of the main results of this work was to find the natural orbitals and their natural occupations in a simple analytic form. Starting from this, it was derived that for a given angular momentum L

the ground state of the system is fragmented. In other words, a non-vanishing angular momentum of the system causes the bosons of the gas to be distributed over a vast number of single-particle states, rather than one. Thus, coherence is lost and this constitutes a system that *cannot* be described by the standard Gross-Pitaevskii theory. In response to this finding it has been suggested that the definition of the single-particle reduced density matrix and the definition of Bose-Einstein condensation should be modified [114] or that in the absence of the symmetry (isotropy) of the trapping potential the fragmentation will vanish [40]. However, these do not clash with a main characteristic of the attractive gas: the angular momentum L is imprinted in the gas in a completely different – fragmented – way, than that in the repulsive case.

Still, the non-weakly attractive two-dimensional gas and its collapse has not been scrutinized in the light of the above findings. In three spatial dimensions on the other hand, it has been shown that fragmentation and participation of the low-lying excited states [27] and the presence of total angular momentum L (see [28] and also next chapter) can postpone the collapse. In this chapter we examine the structure of the ground state of finite systems with non-zero AM and finite non-weak interaction strength λ. We express the energy of this ground state (GS) as a function of L and, moreover, we find an expression for the critical (maximum allowed) value λ_c of the interaction strength. The method used is the Best-Mean-Field, as described in Ch. 3, based on modified (scaled) Gaussian orbitals (single-particle states). We reveal the structure of the ground state with $L > 0$: it is a distribution of the bosons over the M orbitals that above some L, differs from the one derived in the MB treatment [29]. However, the energy that we derive for this state can drop lower than that of the GS of the abovementioned work (also others, see for example Ref. [40]). Asymptotically, in the limit of very weak interaction strength λ and large particle number N, our expression gives back the previously known one.

The structure of this chapter is the following. We introduce the Hamiltonian of the system and the MF ansatz in Sec. 4.2. In Sec. 4.3 we derive an expression for the energy of this ground state as a function of the AM L, for any finite L and non-weak λ. We show that our expression encompasses the energy known from previous asymptotic MB and MF results. Additionally and in connection to this finding, in Sec. 4.4 we derive an expression for the critical value of the interaction strength as a function of the AM L. In Sec. 4.5 we compare our results to those obtained by various MB methods. Lastly, we conclude and discuss the findings in Sec. 4.6.

4.2 The system

We consider the Hamiltonian $H = H_0 + \lambda_0 W$ with

$$H_0 = \frac{1}{2}\sum_i^N \left(-\nabla_{\mathbf{r}_i}^2 + \mathbf{r}_i^2\right) \text{ and } W = \sum_{i<j}^N \delta(\mathbf{r}_i - \mathbf{r}_j). \tag{4.1}$$

This Hamiltonian describes a 2D trapped gas of attractive (that is, $\lambda_0 < 0$) ultracold bosons. To represent the wave function of the system we use the general MF ansatz (Fock

state) of Eq. (3.10):

$$|\Phi\rangle = \mathcal{S}\phi_1(\mathbf{r}_1)\dots\phi_1(\mathbf{r}_{n_1})\phi_2(\mathbf{r}_{n_1+1})\dots\phi_2(\mathbf{r}_{n_2})\dots\phi_M(\mathbf{r}_N) \equiv |n_1, n_2, \dots, n_M\rangle, \tag{4.2}$$

where $\mathcal{S}$ is the symmetrizing operator, accounting for the bosonic nature of the wave function [see also Eq. (3.10)]. The ansatz of Eq. (4.2) describes a fragmented system of N particles, where n_i of them reside in the ϕ_i single-particle state (orbital), with $i = 1, \dots, M$, $\sum_i^M n_i = N$. The total (expectation value of) angular momentum of this state is $L = \sum_i l_i n_i$, where $l_i = \langle\phi_i|\hat{L}_z|\phi_i\rangle$ is the orbital angular momentum of the orbital ϕ_i. Generally, l_i is a function of the anisotropy of the trap. In the case of an isotropically trapped gas, that we examine here, the orbitals are expected to be eigenstates of the (single-particle) operator $\hat{L}_z(\mathbf{r})$ and hence the expectation values l_i equal the eigenvalues $l_i = 0, 1, 2, \dots$. Evaluated on the ansatz the state of Eq. (4.2) the total energy takes on the appearance [96, 101]:

$$E = \langle\Phi|H|\Phi\rangle = \sum_i^M \left(\rho_i h_i + \frac{\lambda_0}{2}\rho_{ii} w_{i,i} + \lambda_0 \sum_{j\neq i}^M \rho_{ij} w_{i,j}\right), \tag{4.3}$$

where $h_i = \langle\phi_i|H_0|\phi_i\rangle$, $w_{i,j} = \langle\phi_i\phi_j|\phi_i\phi_j\rangle$ and $\rho_i = n_i, \rho_{ii} = n_i^2 - n_i$, and $\rho_{ij} = n_i n_j$ are the diagonal matrix elements of the single- and two-particle densities. Our task is to find the Best-Mean-Field; the configuration of Eq. (4.2) that corresponds to the lowest possible energy.

To represent the single-particle states or orbitals ϕ_i, that the bosons of the system occupy, we use the σ-scaled Gaussian solutions of the 2D harmonic oscillator. In the following analysis we choose two different but related orthonormal orbital subsets. At first, we make use of the orbital basis $\{\phi_{lm}\}$, $m = -l, -(l-2), \dots, l-2, l$ consisting of the s, p, d and f-type orbitals that solve exactly the 2D non-interacting problem. The orbitals are scaled by a parameter σ which is to be found variationally and hence optimizes the width of the Gaussian. This particular scaling does not affect the OAM $\{m\} = \{0, 1, -1, 2, 0, -2, \dots\}$ that the orbitals carry, i.e., they are still eigenfunctions of $\hat{L}_z(\mathbf{r})$. Then, and in order to include higher AM, we switch to the basis consisting of the single-particle functions with quantum number $m = l$ only. This basis, which is also referred to as the *lowest Landau levels (LLL)* [29], is explicitly written as:

$$\phi_m(\mathbf{r}) = N_m \left(\frac{r}{\sigma}\right)^m e^{-r^2/(2\sigma^2)} e^{im\theta}, \tag{4.4}$$

where $N_m = (\pi\sigma^2 m!)^{-1/2}$ is the normalization constant and $\sigma > 0$ the scaling parameter. Thus, picking up states only with $m = l$ makes the latter set (LLL) a subset of the former one $\{s, p, d, f \dots\}$. We demonstrate in the following that the BMF for a given non-zero total AM L is the state that includes the LLL only. That is, a variational calculation of the energy of a state built over the orbitals of a general $\{s, p, d, f \dots\}$-basis yields zero occupation numbers for the single-particle states that do not belong to the LLL (non-LLLs). Furthermore, we show that the $L = 0$ ground state, for any number of orbitals,

is a condensed coherent state, while a generic $L > 0$ state is in principle energetically favorable if it is fragmented. However, the fragmentation ratio is found not to be high.

It is known that the GS state of the attractive system will collapse if the parameter $\lambda = |\lambda_0|(N-1)$ exceeds a critical value λ_c [24, 102, 115]. The same holds true for excited states, with the critical value for collapse λ_c now shifted to higher values [26, 28]. Here, the inclusion of the variational scaling parameter into the orbitals allows for a good description of the collapse of the condensate and does not constrain the discussion to the limit where $\lambda \ll 1$, as done in [29, 34], which is far from the collapse.

4.3 Energy of the ground states

By substituting the constraints $N = \sum n_i, L = \sum l_i n_i$ and using the symbols $\alpha_i = n_i/N$ for the relative occupation, the energy functional of Eq. (4.3) takes on the form:

$$\begin{aligned}\epsilon = E/N = (1+\mathcal{L})h_{00} + \frac{\overline{\lambda}}{2}w_{00}\left(\frac{\mathcal{L}^2}{2} - 1 - \frac{\mathcal{L}-2}{2N}\right) + \\ + \sum_{lm}\left\{(l-m)h_{00} + \frac{\overline{\lambda}}{2}\left[\left(2 - \mathcal{L}\ m + \frac{m-2}{2N}\right)w_{00} + 4(\mathcal{L}-1)w_{00,lm} - 4\mathcal{L}w_{11,lm}\right]\right\}\alpha_{lm} + \\ + \frac{\overline{\lambda}}{2}\sum_{lm,l'm'}\left(\mathcal{K}^+_{lm,l'm'} - \mathcal{K}^-_{lm,l'm'}\right)\alpha_{lm}\alpha_{l'm'},\end{aligned} \tag{4.5}$$

with $\overline{\lambda} = |\lambda_0|N$, $\mathcal{L} = L/N$, $h_{00} = (1+\sigma^4)/(2\sigma^2)$, $w_{00} \equiv w_{00,00} = 1/(2\pi\sigma^2)$, $\mathcal{K}^+ = m(\frac{m}{2}+1)w_{00} + 4w_{00,l'm'} + 4mw_{11,l'm'} + 2w_{lm,l'm'}(1-\delta_{lm,l'm'})$ and $\mathcal{K}^- = nw_{00} + 4mw_{00,l'm'}$ the positive and negative prefactor of the square terms $\alpha_{lm}\alpha_{l'm'}$ accordingly. The summations run over $-l \le m \le l$, $0 \le l \le M$ excluding the pairs $l = m = 0$ and $l = m = 1$. It should be noted that we have changed the representation from n_i to α_{lm}. The prefactors $\mathcal{K}^+$ and $\mathcal{K}^-$ depend solely on the indices $lm, l'm'$ and not on the AM L. It is crucial here to explicitly consider the constants of motion L and N in the above expression. To see that consider a vanishing interaction, $\lambda = 0$, or an infinitesimal one, $\lambda \ll 1$. Then the above expression for the energy yields immediately that the optimal distribution is the one with $m = l$, that is the LLL. We ask: what is the optimal distribution of α_{lm} that minimizes the polynomial of Eq. (4.5) for some given finite λ, L and N. To answer this, we first consider only *small oscillations* of the (non-negative) occupations α_{lm} around 0. Since $0 \le \alpha_{lm} \le 1$, for all l and m we can truncate quadratic terms $\mathcal{O}(\alpha^2_{lm})$ and $\mathcal{O}(\alpha_{lm}\alpha_{l'm'})$ and study the behavior of the linearized (in terms of α_{lm}) energy.

4.3.1 Zero Angular Momentum

First, we focus on the states that possess no angular momentum, i.e., $L = 0$. In the case of zero AM the prefactor of α_{lm} of Eq. (4.5) becomes

$$\sum_{lm}\left[(l-m)h_{00} + \overline{\lambda}\left(1 + \frac{m-2}{4N}\right)w_{00} - \overline{\lambda}2w_{00,lm}\right].$$

Its first term is always non-negative ($l \geq m$) while for the integrals $w_{00,lm}$ we found that $0 \leq w_{00,lm} \leq \frac{1}{2}w_{00}$, as long as $lm \neq 00$. Recalling that $\overline{\lambda} > 0$, we see that the prefactor that multiplies λ will always be positive. Hence, any non-zero value for the occupations α_{lm} (excluding α_{00}, α_{11}) will only increase the energy and thus fragmentation is not energetically favorable. That is, for all allowed λ the overall GS of the system with vanishing AM is the condensed state $|\vec{n}_0\rangle = |N, 0, \ldots, 0\rangle$. The energy of Eq. (4.5) for this GS is $\epsilon_0 = h_{00}(\sigma) - \frac{\lambda}{2}w_{00}(\sigma)$. By optimizing the latter with respect to σ we end up with the expression

$$\epsilon_0 = E_0/N = \sqrt{1 - \frac{\lambda}{2\pi}}, \tag{4.6}$$

which is of course the GP energy.

4.3.2 Finite Angular Momentum and Lowest Landau Levels

We now turn to the case of non-vanishing L. As we shall see in this section, the presence of AM can change the picture. First we show that the minimization of Eq. (4.5) yields an optimal distribution of α's (or n_i's) over the LLL only. We stress here that the LLL has been widely used as a basis for the description of the ground state with $L > 0$ and known to be an adequate approximation [116]. However, we are here the first to provide a variational argument for the validity of the LLL. It is clear from Eq. (4.5) that the non-interacting part of the energy admits a minimum when only the $m = l$ single-particle states contribute to the energy functional. The second term ($-\mathcal{L}mw_{00}$) drops linearly with m and hence minimizes the energy when $m = \max = l$. For the matrix elements $w_{00,lm}$ we have noticed (up to $l = 3$) that their value is minimal at $m = l$, while the opposite holds true for the $w_{11,lm}$ elements. That is, they are a non-decreasing function of m (for given l). Taking into account the signs of each of the terms we see that the total energy functional, in a first order approximation to α, admits a minimum when $m = l$. This means that only the LLL orbitals can have non-zero occupations, for non-zero total AM L. We verify this behavior, i.e., that in the GS with given L only orbitals-members of the LLL are occupied, by including terms of second order as well. To do so, we first examine the energy of the state $|\Phi\rangle$ built over three orbitals with different AM quantum numbers. Consider the permanents

$$|n_0, n_+, n_-\rangle \equiv |N(1 - \mathcal{L} - 2\alpha_-), N(\mathcal{L} + \alpha_-), N\alpha_-\rangle, \tag{4.7}$$

where n_0, n_+, n_- are, respectively, the occupations of the $\phi_{00}, \phi_{11}, \phi_{1-1}$ single-particle states (or, equivalently, the s, p_+, p_- orbitals) with $n_0 + n_+ + n_- = N$, $L = n_+ - n_-$ is the total AM of the state, $\mathcal{L} = L/N$ the non-negative AM per particle and $\alpha_- = \frac{n_-}{N}$. In this configurations the states ϕ_{00} and ϕ_{11} comprise the LLL while the ϕ_{1-1} orbital is a non-LLL state. We express the total energy as a function of the occupations n_+, n_- (or equivalently the parameters $\mathcal{L}, \alpha_-$) and the scaling parameter σ. By minimizing this expression with respect to σ we obtain, in the large-N limit, the expression for the total

energy:

$$\epsilon = E/N = \frac{\sqrt{1+\mathcal{L}+2\alpha_-}\sqrt{4\pi(1+\mathcal{L}+2\alpha_-)+(\mathcal{L}^2+2\mathcal{L}\alpha_-+2\alpha_-^2-2)\lambda}}{2\sqrt{\pi}} \tag{4.8}$$

or, in the limit of weak interaction ($\lambda \ll 1$),

$$\epsilon = 1+\mathcal{L}+2\alpha_- + \frac{\mathcal{L}^2+2\mathcal{L}\alpha_-+2\alpha_-^2-2}{8\pi}\lambda + \mathcal{O}(\lambda^2). \tag{4.9}$$

It is easily seen in the last two equations that any non-zero value of the parameter α_- will only increase the total energy and this demonstrates that the non-LLL orbital (here α_-) is not energetically favored for a given $L > 0$. The above expressions for the energy are given for brevity in the large-N limit only. However, the situation is not different if one considers the full expression.

To give some more weight and generality to this claim, we have examined the states $|\vec{n}_{10}\rangle$ which are built over the M=10 σ-scaled orbitals $\{s, p_+, p_-, d_{2+}, d_0, d_{2-}, f_{3+}, f_+, f_-, f_{3-}\}$. We calculated the energy and minimized it simultaneously with respect to the occupations $\alpha_i = n_i/N,\ i = 3, \ldots, 10$ and σ for given $L > 0$ and large N. We found again – both analytically in the large-N limit and numerically – that for all allowed λ, any non-zero occupations of the non-LLL orbitals $\{p_-, d_0, d_{2-}, f_+, f_-, f_{3-}\}$ will only increase the total energy $\epsilon[|\vec{n}_{10}\rangle]$. Hence, the occupation of any non-LLL is not energetically favorable and indeed the Best-Mean-Field, for given L, comprises of LLL only. This is demonstrated in Fig. 4.1. In the left panel, we plot the total energy per particle of the system as a function of each of the six relative occupations of the orbitals that do *not* belong to the LLL, while the rest five of them are set to zero. In the shown case ($\lambda = 5$, $L = 0.6$) any variation of the non-LLL occupation increases the energy. Contrarily, on the right panel, we plot the the energy ϵ versus the occupations $\alpha_{\rm LLL}$, with quantum numbers $l = m = 2$ and $l = m = 3$ respectively. It can be seen clearly that there is a minimum of the energy at a non-zero value of any of the two $\alpha_{\rm LLL}$.

Ground state for given L. Having found that indeed the BMF is built over the LLL orbitals solely, we consider hereafter permanents of Eq. (4.2) built over LLL only [Eq. (4.4)]. With this choice, i.e., $m = l$ and hence using one index m only for each orbital ϕ_m, the energy functional of Eq. (4.8) becomes:

$$\begin{aligned}\epsilon_{\rm LLL} = (1+\mathcal{L})h_0 + \frac{\overline{\lambda}}{2}w_{0,0}\left(\mathcal{L}^2/2 - 1 - \frac{\mathcal{L}-2}{2N}\right) + \\ + \frac{\overline{\lambda}}{2}\sum_m\left[\left(2-\mathcal{L}\ m + \frac{m-2}{2N}\right)w_{0,0} + 4(\mathcal{L}-1)w_{0,m} - 4\mathcal{L}w_{1,m}\right]\alpha_m + \\ + \frac{\overline{\lambda}}{2}\sum_{m,m'}\left(\mathcal{K}^+_{m,m'} - \mathcal{K}^-_{m,m'}\right)\alpha_m\alpha_{m'},\end{aligned} \tag{4.10}$$

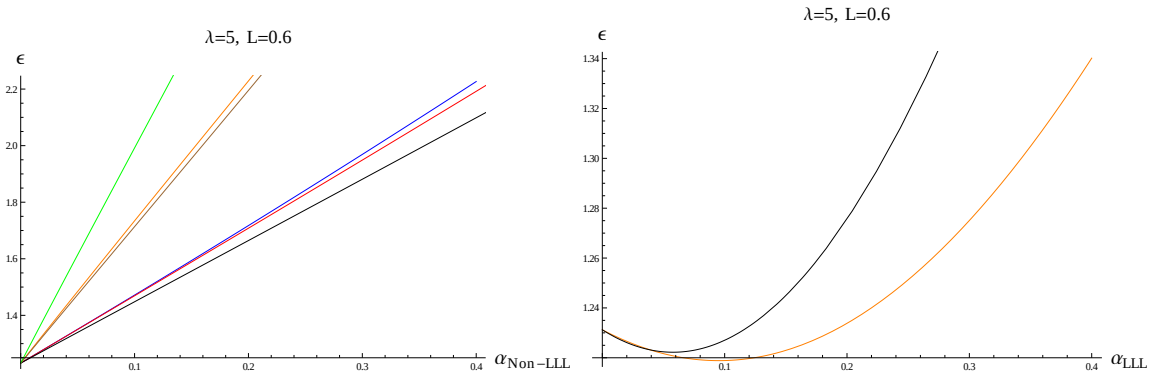

Figure 4.1: LLL is the optimal basis for a given non-zero AM L. The left panel shows the total energy per particle ϵ for $\lambda = 5$ and $L/N = 0.6$ as a function of the each of the six (relative) occupations α_i of the non-LLL, while all the rest are kept to zero. Any variation of these occupations increases the total energy of the system. In the right panel we plot, for comparison, the dependence of the energy, for the same total AM, on the occupations of the LLL with $m = 2$ (orange/lower line) and $m = 3$ (black/upper line). A clear minimum can be seen at a non-zero value of α. All calculations are done at the optimal values of σ for $N = 6000$ particles.

and the matrix elements now take on the explicit form:

$$h_i = (1+i)\frac{1+\sigma^4}{2\sigma^2} \quad \text{and} \quad w_{i,j} = \frac{(i+j)!}{2^{1+i+j}i!j!}\frac{1}{\pi\sigma^2}. \tag{4.11}$$

Our task now is to find this set of parameters $\{n_i, \sigma\}$ that for a given L, minimizes the *total* energy per particle ϵ. We have examined and compared the energies of all different possible Fock states built over $M = 13$ LLL orbitals, with OAM $m = 0, \ldots, 12$, for a particle number up to $N = 18$. Interestingly, we found that above some critical value L_c for the AM the optimal occupations, i.e., the distribution of occupations that minimizes the energy, is given by:

$$n_0 = N-2,\ n_1 = 1,\ n_m = \delta_{m,L-1},\ m = 2, \ldots, M = L, \tag{4.12}$$

where $\delta_{i,j}$ is the usual Kronecker delta. The same state in a Fock representation reads:

$$|N-2, 1, 0, \ldots, 0, 1, 0, \ldots\rangle, \tag{4.13}$$

i.e., only the $m = 0$, $m = 1$ and $m = L-1$ orbitals are populated. We found that this is the optimal distribution of occupations, independent of L, as long as this is larger than the approximate value[1] $L_c \simeq 2\sqrt{N}$. For values lower than L_c either the permanent $|N-L, L, 0, \ldots\rangle$ or the permanent $|N-(L-1), L-2, 1, 0, \ldots\rangle$ are the optimal distributions, depending on the value of $L < L_c$.

[1]Precisely, this critical value is the solution of $L_c^2 - L_c - 4N + 4 + 2^{3-L_c}(L_c + 2N - 4) = 0$.

There is a simple reasoning why such an unexpected distribution of the bosons among three orbitals only is found to be optimal. Both the prefactors of α_m as well as that of $\alpha_m\alpha'_m$ in Eq. (4.10) admit a maximum at $m = M-1$. In other words, the interaction energy is minimized when the 'furthest' orbital is occupied. Due to the attraction, the bosons like to sit close to each other, even in the presence of AM. By exciting only one or two bosons in orbitals with the appropriate OAM, the system achieves the desired non-zero AM L at the lowest energetical cost possible. So, for a given AM L, one boson occupying the orbital with OAM $m = L$ is expected to make up the energetically preferable configuration. The energy of such a configuration is $\epsilon_{\rm e} = h_0(\mathcal{L}+1) + \frac{\lambda_0}{N}\left[\frac{(N-1)(N-2)}{2}w_{0,0} + 2(N-1)w_{L,0}\right]$. However, one can show that if the system excites two bosons, instead of one, to the $m = 1$ and $m = L-1$ orbitals the resulting energy will be lower than the previous case. This additional lowering of the energy comes from the *exchange energy* [included in the last term of Eq. (4.10)] between the two fragments, $\phi_{m=1}$ and $\phi_{m=L-1}$. The energy is now given by $\epsilon_{\rm BMF} = h_0(\mathcal{L}+1) + \frac{\lambda_0}{N}\left[\frac{(N-2)(N-3)}{2}w_{0,0} + 2(N-2)w_{0,1} + 2(N-2)w_{0,L-1} + 2w_{L-1,1}\right]$ and is indeed the ground state energy for some given L. Substituting the matrix elements in the last expression of the energy we get finally:

$$\epsilon_{int} = -\lambda\frac{w_{0,0}}{2N}\left(N - 2 + 2^{2-L}\frac{2N+L-4}{N-1}\right), \tag{4.14}$$

with $h_0 = \frac{1+\sigma^4}{2\sigma^2}$ and $w_{0,0} = 1/(2\pi\sigma^2)$. We minimize the total energy

$$\epsilon = E/N = \epsilon_0 + \epsilon_{int}, \tag{4.15}$$

where

$$\epsilon_0 = (1+\mathcal{L})\, h_0(\sigma) \tag{4.16}$$

with respect to σ to arrive at the expression for the optimal energy of an attractive system with a given number of quanta of AM $L = N\mathcal{L}$. For didactical reasons here we give only the expression in the limiting case where $N \gg 1$ and $\mathcal{L} = L/N$ is fixed, while the full expression can be found in Appendix A. This reads:

$$\epsilon_{int} = -\frac{\lambda}{4\pi\sqrt{1 - \frac{\lambda}{2\pi(\mathcal{L}+1)}}}. \tag{4.17}$$

And the optimal value for the parameter σ, i.e. the optimal width of the orbitals as a function of the interaction strength and the AM is given by:

$$\sigma_0 = \left(1 - \frac{\lambda}{2\pi(\mathcal{L}+1)}\right)^{-1/4}, \tag{4.18}$$

also in the large-N limit. We arrive here at a simple expression for the energy and the single-particle states of the moderately and strongly attractive system, with $L = \mathcal{L}N$

quanta of angular momentum. From Eq. (4.17) one immediately derives the asympotic relation for $\lambda \ll 1$ or, equivalently, for large $\mathcal{L}$. This reads:

$$\epsilon_{int} = -\frac{\lambda}{4\pi} \tag{4.19}$$

and coincides with the expression given in Refs. [29, 40]. What we see is that the energy given in the above references is the large-N, low-λ limit of Eq. (4.17). Moreover, for large N, the energy of Eq. (4.17) is *always* lower than the asymptotic expression $-\lambda/4\pi$, since it takes into account corrections of finite interaction strength λ.

Lastly, the total energy per particle, in the large-N limit, reads:

$$\epsilon = (\mathcal{L}+1)\sqrt{1-\frac{\lambda}{2\pi(\mathcal{L}+1)}}. \tag{4.20}$$

It is interesting to note that the resulting optimized energy, as given above, does *not* equal the sum of the non-interacting plus the interaction energy. They are rather connected through the relation

$$\frac{\partial \epsilon_{total}}{\partial \lambda} = \frac{1}{\lambda}\epsilon_{int}. \tag{4.21}$$

This nonlinearity stems directly from the optimized orbitals; the interaction will change the shape of the orbitals and this will in turn alter the kinetic and potential energies.

Quantized vortices. A well-known rotating excited state of the quantum gas is the vortex state (see Sec. 2.3). A quantized vortex is the coherent state where all particles of the system are in the excited orbital $\phi_m \sim r^m e^{r^2/(2\sigma^2)+im\theta}$ with vorticity $m \in \mathbb{N}$. Here again, σ is the scaling parameter. However, a vortex is a highly excited state of the attractive gas with given total angular momentum $L = m\ N$, as can be seen from the comparison of energies of the above-found ground state and the vortex. Its σ-optimized energy is easily found to be:

$$\epsilon_{\mathrm{VOR}} = (\mathcal{L}+1)\sqrt{1-\frac{\lambda\ \Gamma(\mathcal{L}+\frac{1}{2})}{2\pi^{3/2}(\mathcal{L}+1)\mathcal{L}!}}, \tag{4.22}$$

where $\Gamma(\dots)$ is the Gamma function. This energy, compared to that of Eq. (4.20) is always higher. The vortex state implies a 'hole' in the density of the gas and hence - considering the attractive nature of the interaction - is energetically expensive. The distributions and densities (single-particle RDM) of the $k = 1$ vortex and of the ground state of Eq. (4.13) are compared in Fig. 4.2.

4.4 Stability of the ground states

Next, we calculate the stability of the ground states for some given AM L (or $\mathcal{L} = L/N$) found above. In other words, we are interested in the maximum or critical value of the

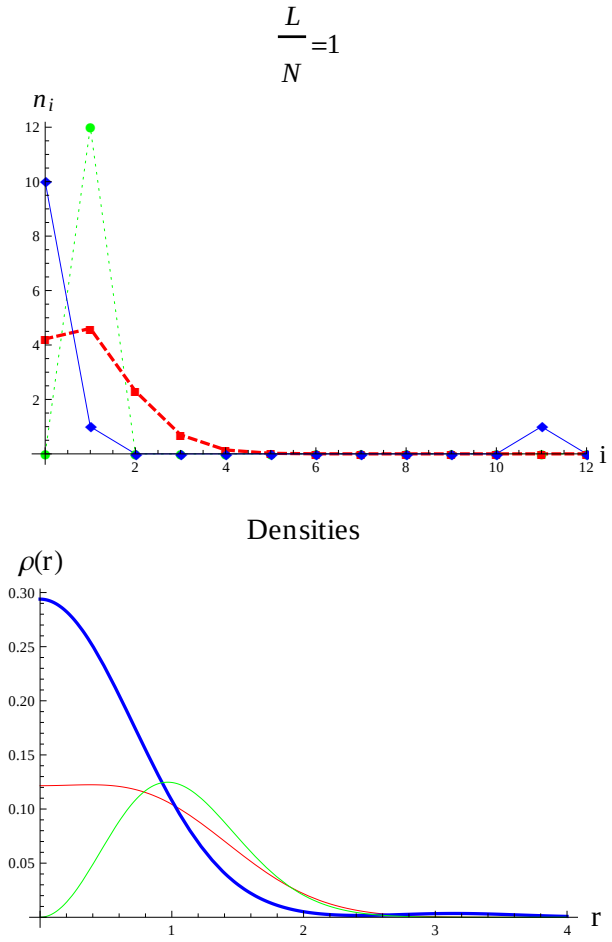

Figure 4.2: Distributions of the occupation numbers (upper panel) and density $\rho_1(r)$, i.e., diagonal of the single-particle reduced density matrix (lower panel) for three different states, all with $\mathcal{L} = 1$ and $N = 12$. The blue line corresponds to the ground state of Eq. (4.13), the red line to the ground state found in Ref. [29] and the green to the vortex state [see Eq. (4.22)].

interaction parameter $\lambda = |\lambda_0|(N-1)$ such that the condensate exists in a non-collapsed state. This is estimated as the maximum value of λ_c such that there is a well defined *global* minimum of the energy as a function of the scaling parameter σ that determines the width of the Gaussian profiles of the orbitals (scaled LLLs). We calculate this value by setting to zero the first and second derivatives of the energy $\epsilon(\sigma)$ of Eq. (4.20) with respect to σ. We arrive at the expression:

$$\lambda_c = \frac{2^{L+1}(N-1)(N+L)\pi}{4L + [8 + 2^L(N-1)](N-2)}, \tag{4.23}$$

which for $N \gg 1$ yields:

$$\lambda_c \simeq 2(\mathcal{L}+1)\pi = (\mathcal{L}+1)\lambda^{GP}, \tag{4.24}$$

where $\lambda^{GP} = \lambda_c(\mathcal{L}=0)|_{N\gg 1} = 2\pi$ is the critical λ of the GP condensed ground state with zero AM. So, as long as N is sufficiently large, practically above a few hundreds of particles, the critical interaction parameter λ_c increases linearly with the AM $\mathcal{L}$. Equations (4.23) and (4.24), together with Eq. (4.17) are the main results of this chapter. Lastly, it should be noted that the corresponding critical value for λ of a vortex state of vorticity $\mathcal{L}$ is higher than the one given above for the GS. Precisely, from Eq. (4.22) we immediately obtain $\lambda_c^{\mathrm{VOR}} = 2\pi\frac{\sqrt{\pi}(\mathcal{L}+1)\mathcal{L}!}{\Gamma(\mathcal{L}+\frac{1}{2})}$. The fact that $\lambda_c^{\mathrm{VOR}} > \lambda_c$ comes to no surprise, since a vortex state is a highly excited state of the attractive system.

4.5 Comparisons with many-body results

Finally, we compare the above found results with results obtained from many-body approaches.

4.5.1 Comparison with known results

We compare the energies and occupations obtained in the preceding sections with known results obtained at the MB level. In the work of Wilkin et al. [29], as well as that of Jackson et al. [40] the following result is given for the total energy of a weakly attractive system:

$$\epsilon_W = \mathcal{L} + 1 - \frac{\lambda}{4\pi}. \tag{4.25}$$

It is interesting that this result is obtained both within a MB approach [29] and a MF ansatz [40]. Wilkin et al. [29] start by writing the (not normalized) solution of the problem as

$$\psi_W = r_c^L e^{-\sum_i^N r_i^2/2}, \tag{4.26}$$

where r_c is the centre of mass coordinate, and find that the natural orbitals ϕ_m of the system are the LLL states. That is, single-particle states $\phi_m \propto re^{-r^2/2+im\theta}$, which unlike

our calculations are not scaled. The respective natural occupations, for N particles and L total AM, are found to be [29]:

$$\rho_m = \frac{(N-1)^{L-m} L!}{N^L (L-m)! m!}. \tag{4.27}$$

The interaction energy of such a configuration equals the interaction energy of the non-rotating system, i.e., $\epsilon_{\mathrm{int,W}} = -\frac{\lambda}{4\pi}$. In the more recent treatment of Ref. [40] the authors built up a GP ansatz out of the fragments ϕ_m and their occupations found in Ref. [29]. Specifically, they expressed the GS of the gas with total AM $\mathcal{L}$ as $\psi_J = \sum c_i \phi_i$, where c_i are the large-N and large-L limits of the occupations ρ_m of Eq. (4.27) and the orbital-basis $\{\phi_i\}$ is again the LLL. The energy thus obtained exactly equals that of Eq. (4.25). We immediately see that the energy found in both of the above approaches is the same as the vanishing-λ limit of Eq. (4.17). Hence, we are able to reproduce the known result and, moreover, give corrections due to finite interaction strength λ. In Fig. 4.3 we plot the occupations of the LLL states for $N = 12$ and different values of $\mathcal{L}$, as calculated in our BMF approach and compare them to those of Eq. (4.27).

4.5.2 Comparison with MCTDHB results

Finally, we compare the energy of our variational ansatz with the energy that is obtained from the MCTDHB exact numerical algorithm (see Ch. 3). For technical reasons, we were able to obtain the energy of the $L = 0$ ground state only. The energies as functions of the interaction strength λ are plotted in Fig. 4.4. We compare there the asymptotic energy of Eq. (4.25), the energy of our variational ansatz for optimized σ [see Eq. (4.6)], the results obtained from a CI expansion over three orbitals ($\{s, p_+, p_-\}$) and last the exact numerical approach (MCTDHB). We can say, that the variational ansatz of the form $\phi \sim e^{-r^2/(2\sigma^2)}$ is a sufficiently good approximation for almost all of the range of λ where a non-collapsed state exists. Furthermore, it captures qualitatively the behavior of the energy $\epsilon(\lambda)$ and the collapse of the system at some λ_c. This critical value for collapse is found close to 2π in the BMF theory [see Eqs. (4.23) and (4.24)] while the MB calculation gives a somewhat lower value. The fixed-orbital (without scaling) approach deviates substantially from the exact energy, past a value of $\lambda \simeq 2$. The MF ansatz, with $L = 0$, is a GP coherent state, while in the MB calculation there is a slight depletion $d_1 = 1 - n_1/N$ of the ground state that depends on λ, but does not exceed $d_1 = 0.02$. The MB calculations are done for $N = 21$ particles.

4.6 Conclusions

The ground states of an attractive 2D BEC with definite total angular momentum have been the subject of this chapter. Starting from a multi-orbital MF description of the state we calculated the energy functional and showed that for given AM only members of the LLL contribute to the ground state. The optimal configuration, i.e., the occupation

numbers of each shape-optimized orbital were found: for given total AM L only two excited modes are populated and carry all AM. For $L \gtrsim 2\sqrt{N}$ it is only one particle with a single quantum of AM and another one with the rest $L-1$ [see Eq. (4.13)]. Our results are valid for weak but also moderately large interaction strength λ. The inclusion of the σ-parameter in our ansatz [Eq. (4.4)] gives an extra flexibility and allows for a description of the collapse. The behavior of the total $L = 0$ energy of the system as a function of λ is sufficiently close to the numerical solution, as this is obtained from MCTDHB calculations, with $M = 6$ orbitals. The energy of the GS possessing some finite AM $\mathcal{L}$ is obtained as a function of $\mathcal{L}$ and λ. This finding constitutes a generalization of the previously known results: indeed from a first order expansion for small λ we get back the relation for the energy as first found by Wilkin et al. and later on by Jackson et al., at the MB [29] and MF [40] levels respectively. Disregarding the σ-scaling, the orbitals that describe the single-particle states are the same in our approach and the above-mentioned works. However, the distribution of the bosons of the system over the LLL states differ substantially. Above some angular momentum ($L \gtrsim 2\sqrt{N}$) the system prefers to excites two bosons only that will carry all the available AM, rather than a vast number of them, as given from relation Eq. (4.27).

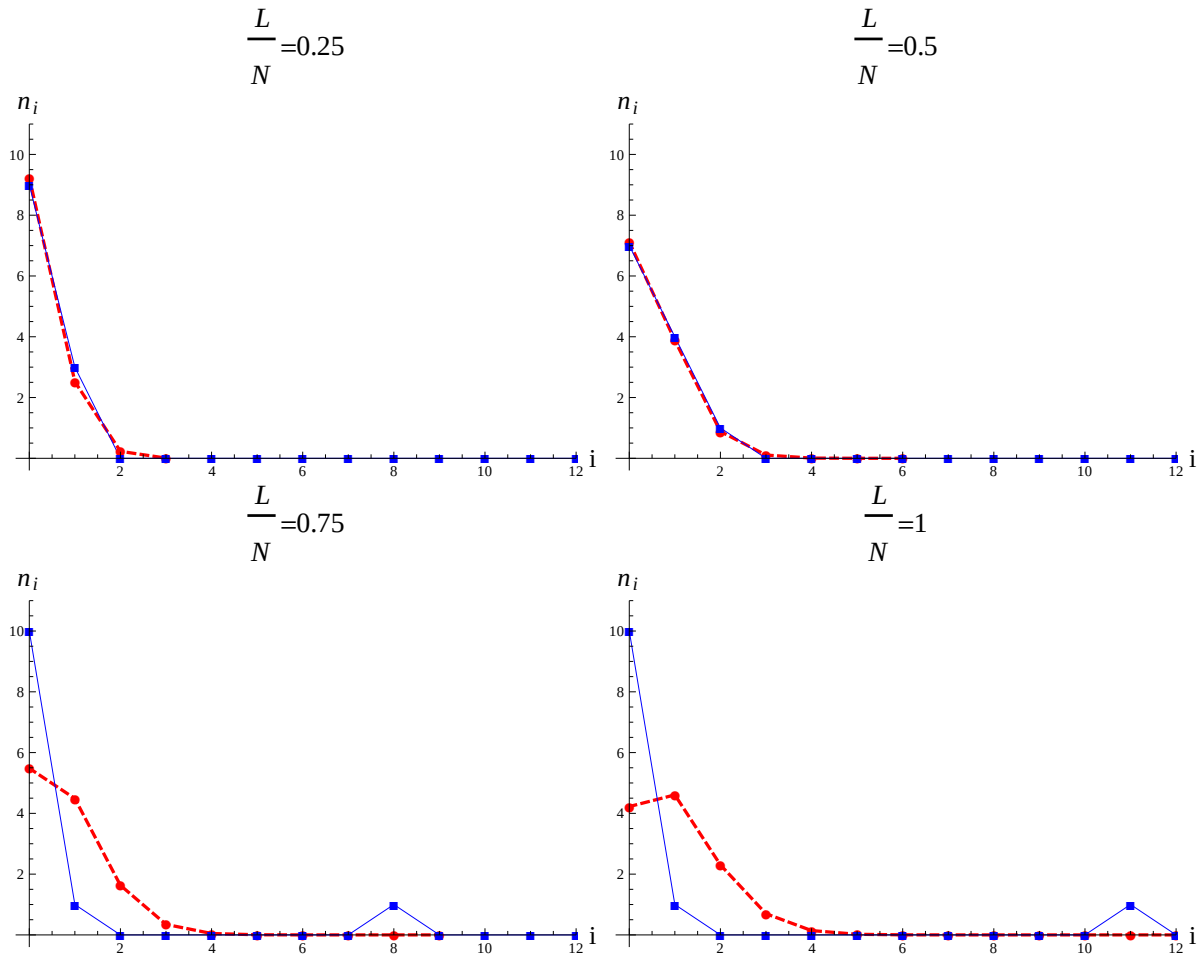

Figure 4.3: Occupation numbers of the ground state for different values of $\mathcal{L}$, as found within the BMF theory (blue) and as given in Wilkin et al. [29] (red-dashed). The agreement is good for an approximate value of $\mathcal{L} \lesssim 0.5$. Above this value the two distributions take on a completely different appearance, even if the energies of the configurations are almost equal. For instance, for a weak interaction $\lambda = 0.01$ the energy difference of the two is $\Delta E \sim 10^{-4}$. The number of particles here is $N = 12$.

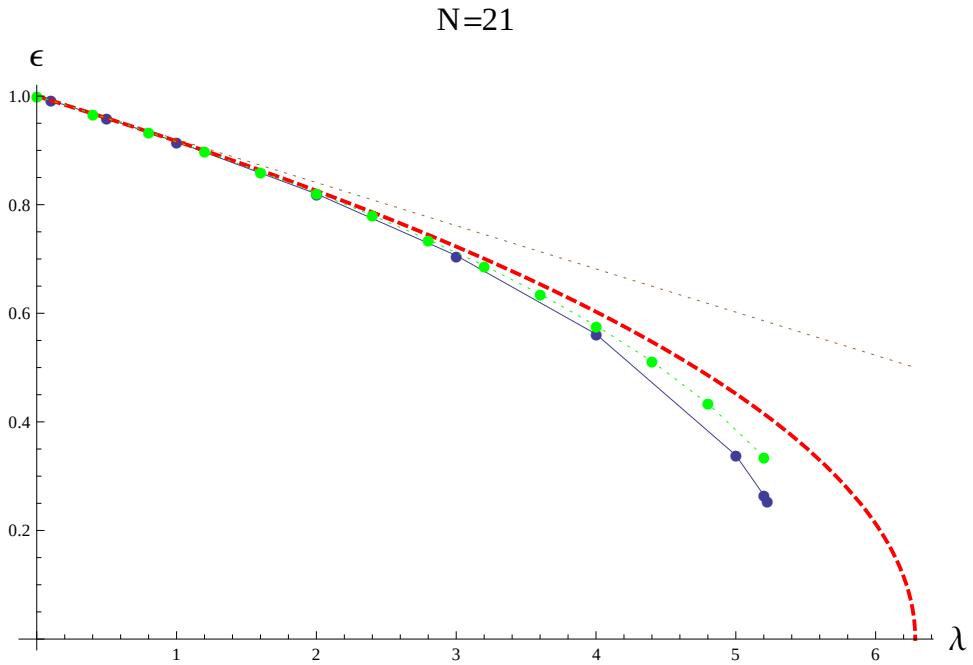

Figure 4.4: Comparison of total energies per particle for the $L = 0$ ground state as calculated from different theoretical models, as a function of λ. Precisely we plot: i) the asymptotic GP energy $\epsilon_{\text{asym}} = 1 - \frac{\lambda}{4\pi}$ (brown dashed line), ii) the GP energy of $\epsilon_{\text{GS}} = \sqrt{1 - \frac{\lambda}{2\pi}}$ Eq. (4.6) (red dashed line), iii) the CI many-body calculations (green line) and iv) the energy as calculated from the MCTDHB with $M = 6$ fully self-consistent orbitals (blue line). The agreement of our variational approach to the exact calculations is good, depending on the strength λ. The energies are plotted until the point λ_c where a stable configuration exists. Past this value the system collapses. In the first (asymptotic) approach (followed in Refs. [29, 40] and others) the orbitals used are fixed and hence no collapse of the system is described. The MF ansatz over scaled Gaussians, as presented in this chapter, predicts a collapse of the $L = 0$ GS of the gas at a critical value $\lambda_c = 2\pi$. Many-body calculations predict a collapse at a value λ_c somewhat smaller. See also text in this and the following chapter for an extensive discussion.

Chapter 5

States of definite total angular momenta in three dimensions and stability of the attractive gas

We continue the study of the attractive Bose gas with a full three-dimensional analysis. We consider systems of different particle numbers and interaction strength and find that even if the overall ground state is collapsed a plethora of fragmented excited states that are still in the metastable region exists. Utilizing the configuration interaction expansion (see Sec. 3.5.1) we determine the spectrum of the ground ('yrast') and excited many-body states with definite total angular momentum quantum numbers $0 \leqslant L \leqslant N$ and $-L \leqslant M_L \leqslant L$, and we identify and examine states that survive the collapse. This opens up the possibility of realizing a metastable system with overcritical numbers of bosons in a ground state with angular momentum $L \neq 0$. The multi-orbital mean-field theoretical predictions about the existence of fragmented metastable states with overcritical numbers of bosons are verified and elucidated at the many-body level. Finally, the descriptions of the total angular momentum within the mean-field and the many-body approaches are compared.

5.1 Introduction

As explained in Sec. 1.3 and Sec. 3.8, a three-dimensional attractive Bose-Einstein Condensate (BEC) is expected to collapse, when the number of the particles N in the ground state or the interaction strength λ_0 exceeds a critical value. The ground state of such a gas is known to be metastable, i.e., to exist in a non-collapsed state for some finite time. Until now, much work has been devoted to exploring the ground state of attractive BECs and its properties (see, for instance, [35, 39, 83, 117, 118]). Furthermore, recent experiments have revealed new phenomena in attractive BECs that seem to go beyond the ground state. In particular, it was found that states with overcritical number of bosons exist [22]. It is natural to assume that excited states of the attractive BECs are involved.

Moreover, disagreements have been reported (see, e.g., [119]) between the experiments and the predictions of the Gross-Pitaevskii (GP) theory on the critical value of the attraction strength, where the gas collapses. This motivates us to study excited states of attractive BECs and to scrutinize their role in the stability of attractive BECs.

The general theoretical approach to (stationary) quantum bosonic gases have been defined in Ch. 3. In this chapter we go beyond a mean-field (MF) description and follow the configuration interaction (CI) expansion. In addition, we present calculations based on the BMF and GP theories and compare the findings to the many-body (MB) results. As explained, within the CI approach, one has to specify the orbitals ϕ_i used to construct the many body states Φ_i, which in turn constitute the basis for the CI expansion, i.e., $\Psi = \sum C_k \Phi_k$. In order to perform real calculations one has to limit down the set $\{\phi_i\} := \mathcal{M}$ to some small number of orbitals (see discussion in Sec. 5.2). This single-particle function set $\mathcal{M}$, i.e., the set of the σ_i-scaled orbitals, see Eqs. (5.3)-(5.5) below, consists of functions that have definite orbital angular momenta, m_l and l, as well as parity (symmetry under spatial inversion). In this way, we take all the symmetries of the problem into account. However, one is more interested in the symmetries of the MB states Φ, since on one hand they are of physical importance and on the other hand they will directly reduce the size of the configuration (Fock) space.

What distinguishes the three-dimensional analysis – in terms of overall symmetries – is the existence of two total angular momentum operators $\hat{L}^2, \hat{L}_z$, instead of one $\hat{L}_z$ in the two-dimensional case. The presence and conservation of $\hat{L}^2$ complicates the algebra (the action of it on a state Ψ) and necessitates, as it will become clear later, a beyond-MF description. Indeed, a single Fock state is not enough for the correct description of eigenstates of $\hat{L}^2$ (see Sec. 5.2).

We principally aim at investigating how the total angular momentum affects the stability and fragmentation of the system. To achieve this we first have to answer on *what the MB states with definite total angular momentum are*. We, therefore, define the MB operators $\hat{L}^2, \hat{L}_z$ and their action on the permanents Φ_i. We then look for a $\{\overline{\Phi}_i\}$-basis of MB states that are common eigenstates of $\hat{L}^2, \hat{L}_z$. Once the new basis $\{\overline{\Phi}_i\}$ is known we can rewrite the state Ψ and the Hamiltonian of the system on this basis for given eigenvalues L, M_L, i.e., over states with the same symmetry. In such a way the size of the new, rotated basis set $\{\overline{\Phi}_i^L\}$, with the index L meaning hereafter that the members of this set have the same angular momentum quantum numbers, is significantly smaller than the original $\{\Phi_i\}$ and the calculations are further facilitated (see also Appendix B.1). We will show that a general state $\overline{\Phi}_k$, with definite angular momentum L, M_L, is a quantum MB state, i.e., a non-MF state.

An equally important goal is to examine the stability and the properties of the ground and excited states of different angular momenta of systems of various λ_0 and N. To do so, we employ the natural orbital analysis; the findings strongly support that states with angular momentum different than zero [large or not, depending on the quantity $\lambda_0(N-1)$] can exist, with a total number of particles well above the critical number of particles N_c^{GP}, as calculated from the GP theory. We verify, therefrom, the predictions of the BMF of Ref. [103], that fragmented excited states exist and survive the collapse and we explain

these features at the MB level.

In an earlier relevant work Elgarøy and Pethick [120] have derived and used a two-mode MB Hamiltonian, borrowed from the nuclear physics Lipkin model, to determine the ground state of an attractive trapped Bose gas. The modes correspond to the s-orbital Y_{00} and the p-orbital Y_{10} and the Hamiltonian matrix is constructed over the set of permanents $|\vec{n}\rangle = |n_0, N-n_0\rangle$, where n_0 bosons reside in the s-orbital and $N-n_0$ in the p-orbital, N being the total number of particles. Then, by rewriting the Hamiltonian in terms of *quasispin operators* $\hat{J}_z, \hat{J}_+, \hat{J}_-$ they calculated the population of each mode, in the ground state. All the configurations $|\vec{n}\rangle$ are eigenstates of what they define as 'quasispin operators' with quantum numbers $J = N/2$ and $J_z = \frac{1}{2}(N-2n_0)$. The ground state, in the range of the parameters where it is not collapsed, was found to be not fragmented. However, the authors did not examine excited states, which as we shall show in the present analysis, can carry angular momentum (or 'non-minimum quasispin' in the case of [120]) and are metastable fragmented states that survive the collapse. Still, the work of Ref. [120] has stimulated the present extended and more complete study. By including *all* three p-orbitals in our configuration space, we are able to write the wave function of the system as eigenfunction of the true total angular momentum operators and hence restore the symmetries of the problem.

In Refs. [35, 39, 83, 118] ultracold bosonic systems are examined with methods beyond the MF approach. However, they pertain to (true or quasi-) two-dimensional systems where, as said, the description of the angular momentum basis is fairly different and simpler than the analysis on a fully three-dimensional system that we present here. In addition, they do not examine the stability of the system with respect to the fragmentation of ground or excited states.

The structure of this chapter is the following. In Sec. 5.2 we define the orbital basis, over which the many-body states are built. In Sec. 5.3 we give the expression for the total angular momentum operator, we derive a MB angular momentum basis, and we show how this partitions the configuration space. In Sec. 5.4 the main results of this chapter, for systems of $N = 12, 60$ and $N = 120$ are presented; in Sec. 5.4.1 MB states belonging to the same subspace $L = 0$ are compared, while in Sec. 5.4.2 we examine ground states of different L-subspaces. In Sec. 5.4.3 we further investigate the properties, namely fragmentation and variance of the expansion coefficients, see Eqs. (3.18) and (3.27), of the previously found metastable MB states. In Sec. 5.5 we study the overall impact of the angular momentum on the state of the system with respect to its collapse, and we compare the role of the angular momentum within the MB and the MF theories. Lastly, Sec. 5.6 summarizes our results and provides concluding remarks. A set of relevant but lengthy derivations are collected in Appendices B.1 and B.2.

5.2 The orbital basis

Consider a gas of ultracold spinless bosons of mass m confined by a three-dimensional potential of oscillator frequency ω, with spherical symmetry and a functional form

$$V(r) = \frac{m\omega^2}{2} \sum_{i=1}^{3} x_i^2 \tag{5.1}$$

and $x_1 \equiv x, x_2 \equiv y, x_3 \equiv z$. The bosons interact pairwise via a contact interaction potential which we represent as a Dirac delta function $\delta(\mathbf{r}_i - \mathbf{r}_j)$, i.e., the interaction in that form depends only on the relative position of the particles. The Hamiltonian of the problem [Eq. (3.1)] now reads:

$$H = H_0 + \lambda_0 W = \sum_{i}^{N} \left[-\frac{1}{2}\nabla_{\mathbf{r}_i}^2 + V(r_i) \right] + \lambda_0 \sum_{i<j}^{N} \delta(\mathbf{r}_i - \mathbf{r}_j). \tag{5.2}$$

The parameter λ_0 measures the interaction strength and is negative for attraction. Here and hereafter we use dimensionless units $\hbar = m = \omega = 1$.

In Sec. 3.5 we explained in detail the methods used. Here we give only the basic ingredients at a glance. The solution of the N-body problem is represented as an expansion $\Psi = \sum_k C_k \Phi_k$, where the functions $\Phi_k(\mathbf{r}_1, \mathbf{r}_2, \ldots, \mathbf{r}_N)$ are the permanents of Eq. (3.11). The permanents are build over the single-particle states that are given below. Then, determining the coefficients of the expansion Ψ is equivalent to diagonalizing the matrix $\mathcal{H}$ that has matrix elements $\mathcal{H}_{ij} = \langle \Phi_i | H | \Phi_j \rangle$.

One notes easily that the Hamiltonian of Eq. (5.2) satisfies the commutation relations $[H, L] = 0$ and $[H, \Pi] = 0$, where L is the total angular momentum and Π the parity (spatial inversion) operator. These symmetries of the Hamiltonian induce a zero $\mathcal{H}$-matrix element between states of different symmetry (angular momentum and parity). Hence ρ_{ij} [see Eq. (3.21)] is diagonal and the ansatz orbital-set that we use [see Eq. (5.3) below] coincides with the set of the natural orbitals $\{\phi_i^{NO}\}$, $i = 1, \ldots, M$.

To complete the picture of our variational solutions, we give the single-particle function basis set, over which the permanents Φ [see Eq. (3.11)] are constructed. This set of *ansätze* consists of the known orbitals that solve the isotropic 3D quantum harmonic oscillator, scaled under a scaling parameter σ_i. Precisely, it consists of four orbitals: the ground $l = 0$ and the three $l = 1$ excited ones, which we scale with two parameters (σ_0, σ_1), as have been already done in Ref. [103]. The parameters σ_i will determine the shape (width) of the orbitals; their optimal values are such that, for a given set of coefficients $\mathbf{C} = \{C_i\}$ [see Eq. (3.20)], the total energy of the system takes an extremum. In this approximative way we restrict the solution of the system to functions that lie inside the monoparametric families of equations, which solve a scaled ordinary Schrödinger equation; the solution of a coupled system of nonlinear differential equations (MCHB equations) boils down to the determination of a set of parameters which minimizes the total energy.

The orbitals have the form:

$$\begin{aligned}
\phi_1(\mathbf{r}) &= \varphi_0(x,\sigma_0)\varphi_0(y,\sigma_0)\varphi_0(z,\sigma_0),\\
\phi_2(\mathbf{r}) &= \frac{1}{\sqrt{2}}(\varphi_1(x,\sigma_1)\varphi_0(y,\sigma_1)\varphi_0(z,\sigma_1) + i\varphi_0(x,\sigma_1)\varphi_1(y,\sigma_1)\varphi_0(z,\sigma_1)),\\
\phi_3(\mathbf{r}) &= \varphi_0(x,\sigma_1)\varphi_0(y,\sigma_1)\varphi_1(z,\sigma_1),\\
\phi_4(\mathbf{r}) &= \frac{1}{\sqrt{2}}(\varphi_1(x,\sigma_1)\varphi_0(y,\sigma_1)\varphi_0(z,\sigma_1) - i\varphi_0(x,\sigma_1)\varphi_1(y,\sigma_1)\varphi_0(z,\sigma_1)),
\end{aligned} \tag{5.3}$$

where

$$\varphi_0(x,\sigma) = \left(\frac{m\omega}{\pi\sigma^2\hbar}\right)^{1/4} e^{-\frac{1}{2}\frac{m\omega}{\sigma^2\hbar}x^2} = \pi^{-1/4}\sigma^{-1/2}e^{-\frac{x^2}{2\sigma^2}} \tag{5.4}$$

and

$$\varphi_1(x,\sigma) = \left[\frac{4}{\pi}\left(\frac{m\omega}{\sigma^2\hbar}\right)^3\right]^{1/4} xe^{-\frac{1}{2}\frac{m\omega}{\sigma^2\hbar}x^2} = \sqrt{2}\pi^{-1/4}\sigma^{-3/2}xe^{-\frac{x^2}{2\sigma^2}} \tag{5.5}$$

are orthonormal orbitals, i.e., $\langle\varphi_i|\varphi_j\rangle = \delta_{ij}$, $i,j = 0,1$.

In terms of spherical harmonics Y_{l,m_l}, i.e., under a change of coordinates, the orbitals of Eq. (5.3) are:

$$\phi_k(\mathbf{r}) = \varphi_l(r,\sigma_l)Y_{lm_l}(\theta,\phi), \tag{5.6}$$

where $l = 0,1$, $-l \leq m_l \leq l$ and $k \equiv k(l,m_l) = 1 + l(l+1) - m_l$.

5.3 Angular momentum basis

It is easy to see that the orbitals of Eq. (5.6) constitute a set of common eigenstates of the orbital angular momentum operators $\hat{L}^2, \hat{L}_z$ together with the parity (inversion) operator $\hat{\Pi}$: $\hat{\Pi}\Psi(\mathbf{r}) = \Psi(-\mathbf{r})$, with eigenvalues $l = \{0,1,1,1\}$, $m_l = \{0,1,0,-1\}$ and $\pi = \{1,-1,-1,-1\}$, respectively.

We now want to express the total angular momentum operators at the MB level. For this purpose we switch to second quantization language and use the bosonic creation (annihilation) operators $b_i^\dagger$ (b_i) [Eqs. (3.12) and (3.13)] associated with the orbital set $\{\phi_i(\mathbf{r})\}$ and which obey the usual bosonic commutation relations: $b_i b_j^\dagger - b_j^\dagger b_i = \delta_{ij}$.

The total angular momentum operators are (see, e.g., [121]):

$$\hat{L}^2 = \hat{L}_z^2 + \frac{1}{2}(\hat{L}_+\hat{L}_- + \hat{L}_-\hat{L}_+), \tag{5.7}$$

$$\hat{L}_z = \sum_{l,m_l} m_l b_{lm_l}^\dagger b_{lm_l}, \tag{5.8}$$

$$\hat{L}_\pm = \sum_{l,m_l} A(l,\mp m_l) b_{lm_l\pm1}^\dagger b_{lm_l}, \tag{5.9}$$

where $A(l,m_l) = [(l+m_l)(l-m_l+1)]^{1/2}$ and $b_{lm_l}^\dagger$ (b_{lm_l}) creates (annihilates) a boson in the state ϕ_{lm_l}, with orbital angular momentum quantum numbers l, m_l.

Applying Eq. (5.7) to the basis of the permanents $\Phi = |\vec{n}\rangle$ with $M = 4$ we get:

$$\begin{aligned}\hat{L}^2|\vec{n}\rangle = \left[n_2(n_3+1) + n_3(n_4+1) + n_3(n_2+1) + n_4(n_3+1) + (n_2-n_4)^2\right]|n_1,n_2,n_3,n_4\rangle + \\ +2\sqrt{n_3(n_3-1)(n_2+1)(n_4+1)}|n_1,n_2+1,n_3-2,n_4+1\rangle + \\ +2\sqrt{n_2 n_4(n_3+1)(n_3+2)}|n_1,n_2-1,n_3+2,n_4-1\rangle.\end{aligned} \tag{5.10}$$

It can be easily seen that each permanent Φ [Eq. (3.11)] is an eigenstate of $\hat{L}_z$ with eigenvalue $M_L = n_2 - n_4$,

$$\hat{L}_z|\vec{n}\rangle = (n_2 - n_4)|\vec{n}\rangle. \tag{5.11}$$

But what happens to the eigenstates and eigenvalues of the $\hat{L}^2$ operator? To answer this, one has to solve the eigenvalue equation:

$$\mathfrak{L}\mathcal{C} = \Lambda\mathcal{C}, \tag{5.12}$$

where $\mathfrak{L}$ is the matrix representation of the operator $\hat{L}^2$ in the basis of permanents [Eq. (3.11)] with matrix elements

$$\mathfrak{L}_{i,j} = \langle\vec{n}_i|\hat{L}^2|\vec{n}_j\rangle, \tag{5.13}$$

$\mathcal{C}$ is the column vector of the coefficients C_i and Λ the eigenvalue in question.

A unitary transformation $\mathcal{U}$ will in general rotate the Φ-basis to a new $\overline{\Phi}$ one. In this basis the secular matrix of Eq. (3.19) becomes:

$$\overline{\mathcal{H}}_{i,j} = \langle\overline{\Phi}_i|H|\overline{\Phi}_j\rangle = \sum_{k,l}\mathcal{U}^{\dagger}_{i,k}\mathcal{H}_{k,l}\mathcal{U}_{l,j}, \tag{5.14}$$

where $\mathcal{U}_{i,j}$ are the matrix elements of $\mathcal{U}$. If $\mathcal{U}$ is simply the matrix of the eigenvectors of $\mathfrak{L}$ then $\overline{\mathcal{H}}$ takes on the desired total-angular-momentum block-diagonal form. The above mentioned vector spaces, that the bases $\{\Phi_i\}, \{\overline{\Phi}_i\}$ span, are homomorphic and can be written as the direct sum of the subspaces $\{\overline{\Phi}_i^L\}$:

$$\{\Phi_i\} \cong \{\overline{\Phi}_i\} = \bigoplus_L \{\overline{\Phi}_i^L\}. \tag{5.15}$$

We have numerically calculated the angular momentum states $\overline{\Phi}_i$ and the matrix transformation $\mathcal{U}$ that transforms to the new basis $\overline{\Phi} = \mathcal{U}\Phi$ of eigenstates of $\hat{L}$ and $\hat{M}_L$, for the cases of $N = 12, 20, 60, 120$ bosons. An analytic approach to the same problem of determining the states $\overline{\Phi}_i$ is presented in Appendix B.2.1. For selected values of L and M_L we construct and diagonalize the block $\mathcal{H}^L$ of the secular Hamiltonian matrix $\overline{\mathcal{H}}$ and find its eigenfunctions $|\Psi^L\rangle$. We use hereafter the index L to stress the fact that the state $|\Psi^L\rangle$ is an eigenstate of $\hat{L}^2$ with quantum number L. The size of the block $\mathcal{H}^L$ is found to be $N_p = \frac{N-L+2}{2}$ (see also Appendix B.1), with the same number of eigenstates. We index the states $|\Psi_i^L\rangle$ with i, to denote the ground ($i = 1$) and the excited ($1 < i \leq \frac{N-L+2}{2}$) states belonging to this block of angular momentum L. When it is not transparent from the context, we will also use $\lambda_{0,c}^L$ or $\lambda_{0,c}^i$, to denote the critical value of the interaction strength where the state $|\Psi_i^L\rangle$ collapses.

5.4 Many-Body Results

In this section we implement the many-body method described above, for systems of trapped ultra-cold gases. We present and discuss calculations regarding systems of $N = 12, 60$ and 120 bosons, embedded in a spherically symmetric trap. First, the interaction strength λ_0 is chosen each time such that the product $|\lambda_0|N$ is kept fixed to the value 10.104 [1]. This choice will permit a direct comparison of our results to those of Ref. [103], where an attractive system of $|\lambda_0|N = 10.104$ was also examined. Later on, also other values of $|\lambda_0|N$ are considered for the shake of completeness. In the following we examine states of definite angular momentum L, M_L and positive parity Π only. The latter makes the total angular momentum of each state increase at an even step, i.e., $L = 0, 2, 4, \ldots, N$.

5.4.1 Ground and excited states of the 'block' L=0

For each of the above systems we examine states with definite angular momentum. We first calculate the energy per particle $\epsilon = \mathcal{E}/N$ [see Eq. 3.20] of those states, as a function of the variational parameters σ_0, σ_1 of the orbitals [see Eqs. (5.4) and (5.5)]. We then look for the minimum ϵ_0 of the energy with respect to these parameters. As mentioned earlier, the total absence of a minimum indicates unbound (total) energy and a collapsing system. Namely, as $\sigma_0, \sigma_1 \to 0$ the orbitals of Eq. (5.3) contract to pointlike distributions. When existent, the minima are expected to be local only; an energy barrier separates the metastability from the collapse regions. The shape of the energy barrier determines the tunneling time of the system through this barrier and − generally − the higher the barrier is, the longer the system is expected to survive in this state. The variation of σ_0, σ_1 takes place over states of the same symmetry and hence the surfaces ought not to cross (see Fig. 5.1. See also the theoretical discussion on no-crossing of energy surfaces in [122, 123] and references therein). Notice that, owing to the attractive interparticle interaction, the wave function of the system has to be spatially shrunk, compared to that of the non-interacting system; indeed the optimal scaling parameters of the orbitals, are always found to obey $\sigma_0, \sigma_1 < 1$.

The first system studied is that of $N = 120$ bosons, with attractive interaction of strength λ_0=-0.0842. The energies per particle $\epsilon(\sigma_0, \sigma_1)$ of three distinct states of this system are collectively presented in Fig. 5.1. We first pick the state with quantum numbers L=0 and M_L=0 of the operators $\hat{L}^2, \hat{L}_z$, respectively. We find that the ground state is collapsed (lowest surface in Fig. 5.1). As the introduction of Sec. 5.1 suggests, we expect to find excited, fragmented states that can survive this collapse. Indeed, an examination of the spectrum of the states of the Hamiltonian of Eq. (3.19) reveals that the $|\Psi^{L=0}_{i=20}\rangle$ excited state is the first to demonstrate a minimum in the energy (middle surface in Fig. 5.1) and this makes it the yrast state, for this λ_0 and L. The optimal values of

[1] The reader should not get the impression that this choice conflicts the $|\lambda_0|(N-1)$ scaling in the subsequent analysis of Secs. 5.4 and 5.5. The value $|\lambda_0|N = 10.104$ is chosen just to ensure that the GP ground state of systems of *any* number of bosons N will be collapsed. We would not have obtained fairly different results if the choice $|\lambda_0|(N-1) = const.$ was made instead.

the sigmas are $\sigma_0 = 0.72, \sigma_1 = 0.70$, the minimum energy per particle for these values of sigmas is $\epsilon_0 = 1.37$ and the s-depletion is $d_1 = 0.33$. However, the energy barrier, that prevents the system from collapse, is extremely low, $h \sim 10^{-3}$, making the state only marginally metastable. On the other hand, the $|\Psi^{L=0}_{i=30}\rangle$ excited state of the system exhibits a clear minimum (energy barrier height $h = 0.23$), with energy per particle $\epsilon_0 = 1.60$ and s-depletion $d_1 = 0.48$ at the optimal values of the sigmas $\sigma_0 = 0.82, \sigma_1 = 0.81$ (upper surface in Fig. 5.1).

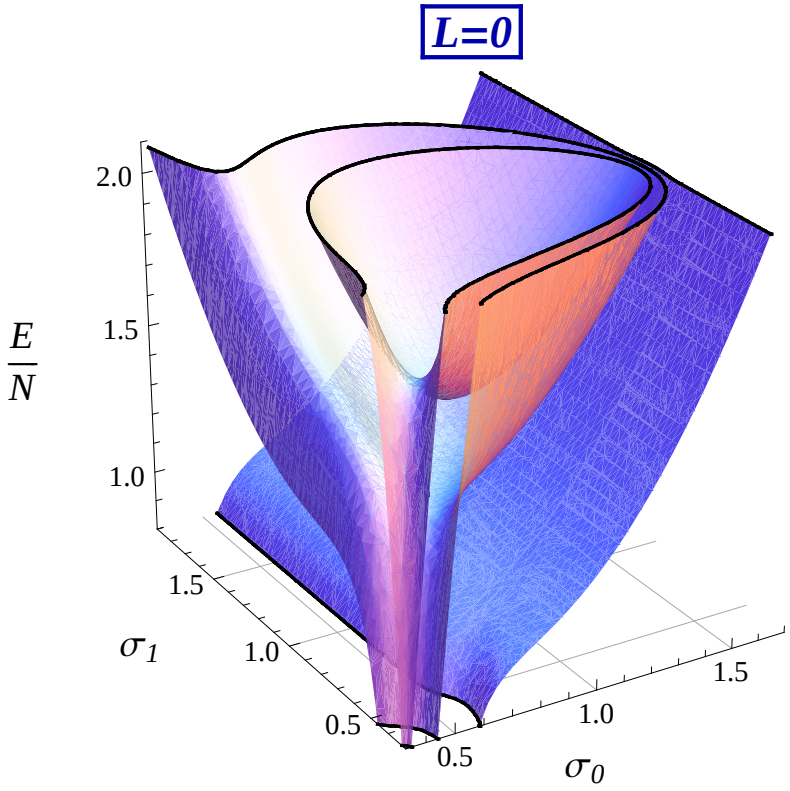

Figure 5.1: Energy landscape $\epsilon(\sigma_0, \sigma_1)$ for a system of $N = 120$ bosons, $\lambda_0 = -0.0842$. Shown are energy surfaces of the ground ($i = 1$), the $i = 20$ and the $i = 30$ excited MB states, all with $L = M_L = 0$. The lowest surface corresponds to the ground state of the coherent system, where almost all 120 bosons reside in the s-orbital. It exhibits no minimum and hence the system collapses. The middle surface barely exhibits a minimum, at $\sigma_0 = 0.72, \sigma_1 = 0.70$, with barrier height $h = 3.83 \cdot 10^{-3}$. The natural occupations are $\rho_1 = 80.82$, $\rho_2 = 13.06$, $\rho_3 = 13.06$ and $\rho_4 = 13.06$. In the third surface a clear minimum in the energy, $\epsilon_0 = 1.60$, is shown, at $\sigma_0 = 0.82, \sigma_1 = 0.81$, with barrier height $h = 0.23$. The occupation numbers, at this point, are $\rho_1 = 62.13, \rho_2 = 19.29, \rho_3 = 19.29, \rho_4 = 19.29$. All quantities are dimensionless.

For $L = 0$ a metastable fragmented state can decay by two channels. The first, as mentioned above by tunneling through the barrier. The second, by coupling to lower surfaces with the same $L = 0$ which do not have a minimum. Since all these surfaces do not have a minimum are energetically far below, the coupling between them is not

expected to induce a quick collapse. Consequently, metastable excited states with $L = 0$, with parameter values tuned at the collapse region of a GP state, exist at higher energies.

5.4.2 Ground states for various angular momenta L

Next, we perform the same analysis as in section 5.4.1 for the system of $N = 120$ bosons, this time over states of significantly higher angular momentum. Precisely we choose states with $L = 52, M_L = 0$. We recall that the maximum allowed quantum number for the total angular momentum, within the present analysis, is $L_{max} = N = 120$. We want to compare the stability and the properties of the two systems, namely that of $L = 0$ to that of $L = 52$. The energy surface $\epsilon(\sigma_0, \sigma_1)$ as a function of the scaling parameters σ_0, σ_1 is plotted in Fig. 5.2. A clear minimum can be seen, at $\sigma_0 = 0.82, \sigma_1 = 0.81$ and $\epsilon_0 = 1.59$ manifesting a metastable ground state with $L = 52$, for the same system whose $L = 0$ ground state is found to be collapsed. We should stress here that the state we examine is the *lowest* in energy state of this L and so this makes it the ground (yrast) state of the problem.

In Fig. 5.3 we plot the energy surface of the same state, examined above, for different values of the interaction strength, $\lambda_0 = (-0.010, -0.056, -0.100)$. For small values of $\lambda_0 = (-0.010, -0.056)$ the energy surface exhibits a clear minimum, with its energy barrier being higher than in the case of $\lambda_0 = -0.0842$. In the third picture, the energy surfaces shows no minimum, meaning that this state is collapsed, though the critical value $\lambda_{0,c}^{L=52}$ is much higher than the corresponding $\lambda_{0,c}^{L=0}$ of the $L = 0$ state.

Following Fig. 5.1, a plot of energy surfaces of ground (yrast) states, $i = 1$, with different angular momentum and hence different stability behavior, would be intuitive. If one would plot the energies of the group of ground states $|\Psi_{i=1}^{L=0}\rangle$, $|\Psi_{i=1}^{L=38}\rangle$ and $|\Psi_{i=1}^{L=58}\rangle$ on the (σ_0, σ_1) plane, they would see that the resulting graph would look very much like that of Fig. 5.1. This means that the energy surfaces of the pairs of states $|\Psi_{i=1}^{L=38}\rangle$ and $|\Psi_{i=20}^{L=0}\rangle$ as well as $|\Psi_{i=1}^{L=58}\rangle$ and $|\Psi_{i=30}^{L=0}\rangle$ are almost the same, for all σ_0, σ_1. This coincidence is not an accident. Indeed, as we shall show later, one can find states that are very close − almost degenerate − in energy but have different angular momentum quantum number L (see discussion at the end of Sec 5.4.3).

As a direct generalization of the above, we can say that if, for some λ_0 the ground state with $L = 0$ of the N-boson system is collapsed, then there will be a ground state with angular momentum $L > 0$, large enough so as to survive the collapse. Further, if the interaction strength is increased, past some new critical value, this state will also collapse.

5.4.3 Analysis and structure of the energy surfaces

To thoroughly analyze the properties of the MB states we examine the findings of the previous sections under the light of the natural orbital analysis and the use of RDMs. For given ground and excited metastable states $|\Psi\rangle$ we want to answer on: (i) what the natural occupations are, (ii) how much fragmented the states are and (iii) how much they deviate from MF states, in a range of the parameters σ_0, σ_1 as well as λ_0, L, M_L.

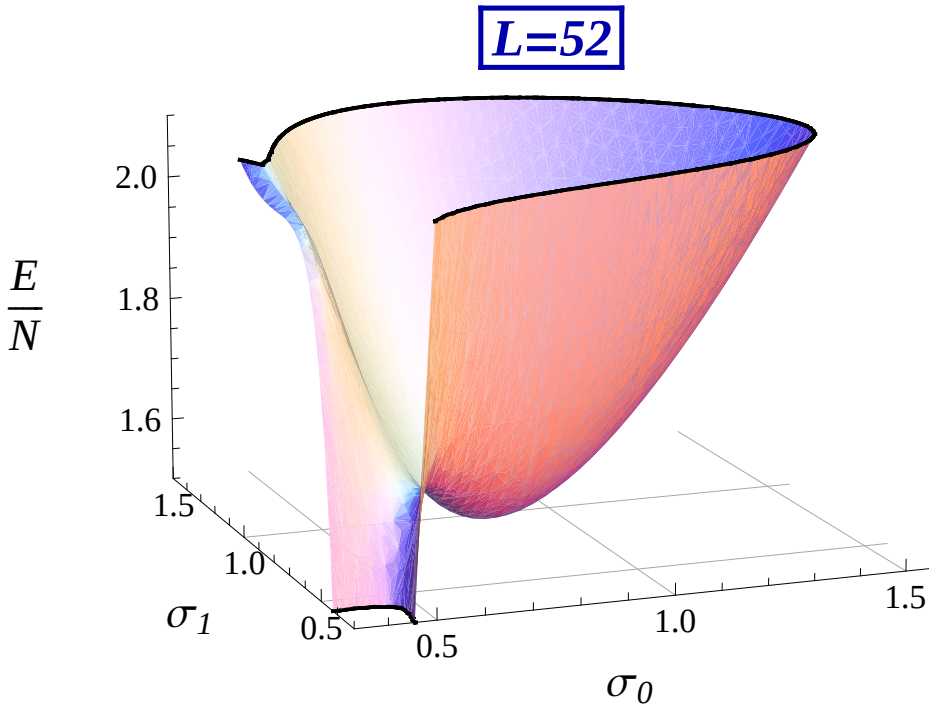

Figure 5.2: For the same system as in Fig. 5.1, i.e., $N = 120, \lambda_0 = -0.0842$ we plot the energy surface of the ground state with angular momentum $L = 52, M_L = 0$. Clearly there is a minimum in the surface, which manifests metastability of the system. Contrarily, when $L = 0$ (Fig. 5.1) the ground state is found to be collapsed. The minimum energy per particle is $\epsilon_0 = 1.59$, at point $\sigma_0 = 0.82, \sigma_1 = 0.81$ and the occupation numbers $\rho_1 = 62.30, \rho_2 = 14.30, \rho_3 = 29.10, \rho_4 = 14.30$. All quantities are dimensionless.

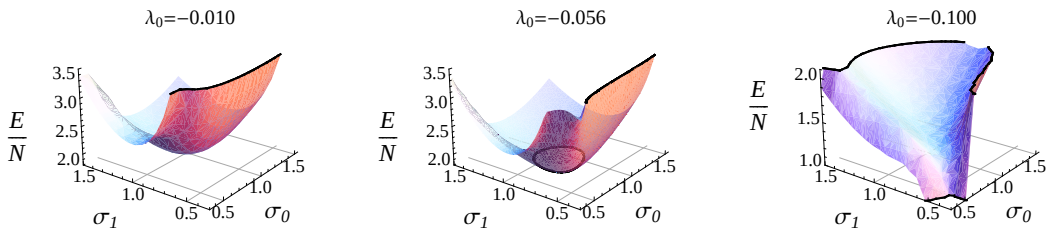

Figure 5.3: Energy surfaces for the state of Fig. 5.2 for values of interaction strength $\lambda_0 = -0.010, \lambda_0 = -0.056$ and $\lambda_0 = -0.100$. The first two surfaces exhibit minima, i.e., metastability, while the third one does not and hence the system collapses. See text for more details. All quantities are dimensionless.

The systems examined in this section consist of $N = 12$ and $N = 60$ bosons and the interaction strength is set to $\lambda_0 = -0.842$ and to $\lambda_0 = -0.1684$, respectively.

Fragmentation

As mentioned, due to the symmetry of the Hamiltonian, the natural orbitals of Eq. (3.21) coincide with those defined in Eq. (5.3), for all $\lambda_0, \sigma_0, \sigma_1$. It is interesting to see how the occupations ρ_i, defined in Eq. (3.23), of the ground and excited metastable states of definite L, vary in the (σ_0, σ_1) plane or change with λ_0. Unlike ρ_2, ρ_3 or ρ_4, the quantity ρ_1 (or d_1) is invariant − for given L − under changes of the quantum number M_L of the operator $\hat{L}_z$. Furthermore, as long as solely ground states are considered, i.e., $i = 1$, ρ_1 determines the total angular momentum L. These properties make ρ_1 a quite informative and representative quantity of the state $|\Psi\rangle$.

For a system of $N = 60$ bosons in the ground metastable state with $L = 26, M_L = 2$, we calculate the depletion of the ϕ_1-orbital (s-depletion d_1), see Eq. (3.24), as a function of the parameters σ_0, σ_1. In Fig. 5.4 we plot the contour lines $\rho_1 = const.$, versus the parameters σ_0, σ_1. The energy landscape of this particular state, for this choice of parameters would look very much like the one of Fig. 5.2. To allow a monitoring of the energy surface, we also plot in Fig. 5.4 the contours (light grey) of constant energy ϵ. The dashed line is the highest-in-energy contour that corresponds to a metastable state. It splits the graph into four parts; in the upper right one the 'trajectories' are bounded, while they are not in the other parts of the space (hyperbolic trajectories). Thus it resembles a *separatrix* of a phase space, whose trajectories meet asymptotically only in a saddle point. The energy per particle has a local minimum $\epsilon_0 = 1.55$ at $\sigma_0 = 0.81, \sigma_1 = 0.79$ and at this point the s-depletion is found to be 0.45, i.e., 55% of the particles of the system are excited to the orbitals $\phi_j,\ j = 2, 3, 4$.

Of special interest is also the change of the s-depletion as the system moves towards the collapse. To make this evident we have plotted on Fig. 5.4 an arrow marking the 'collapse path', i.e., the line that connects the minimum (green dot) with the saddle point (green square) of the energy surface, i.e., the maximum of the energy barrier. Along this path the system moves over the energy barrier towards collapse and it crosses contours of different ρ_1; as collapse takes place the s-depletion of the state increases. We note that for large values of the scaling parameters, i.e., $\sigma_0, \sigma_1 > 1$ the s-depletion remains practically unchanged.

Every state $|\Psi^L\rangle$ with definite angular momentum L is $(2L + 1)$-fold energetically degenerate, due to the quantum number M_L. This means that the energy landscape of a state would not feel any change in M_L. Recall from Eq. (5.11) that the eigenvalue of $\hat{L}_z$ of a permanent $|\Phi\rangle$ is simply $M_L = n_4 - n_2$. Similarly it can be shown that, for a general state $|\Psi\rangle$, $M_L = \rho_4 - \rho_2$ holds. Not surprisingly, this suggests that the occupations ρ_1, ρ_3, i.e., the occupations of the two $m_l = 0$ orbitals, do not contribute to the z-projection of the total angular momentum $\hat{L}$. However, as the quantum number M_L of a state with a given L varies, only the occupation ρ_1 remains unchanged, while ρ_3 varies accordingly to keep the total number of particles fixed, i.e., $\rho_3 = N - \rho_2 - \rho_4 - \rho_1 = N - M_L - 2\rho_4 - const.$.

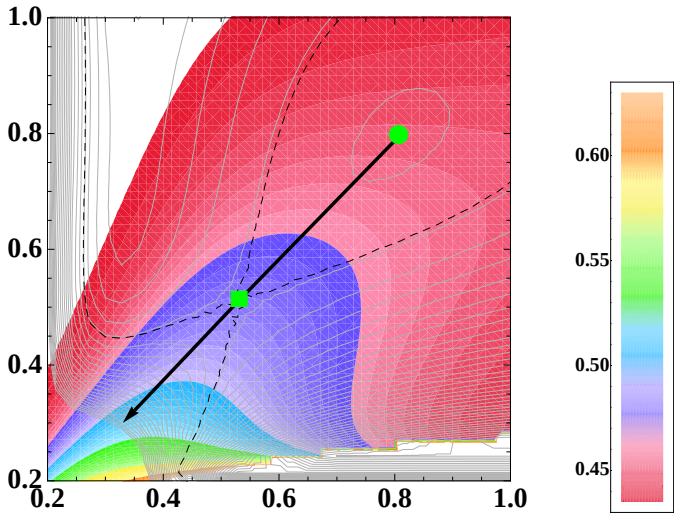

Figure 5.4: Change in the s-depletion of the condensate ($d_1 = 1 - \rho_1/N$) on the (σ_0, σ_1) plane for a metastable ground state with $L = 26, M_L = 2$ of an $N = 60$, $\lambda_0 = -0.1684$ system. Plotted are contour lines of fixed $\rho_1 = const.$. The minimum of energy (green dot in the plot) is $\epsilon_0 = 1.55$ at $\sigma_0 = 0.81, \sigma_1 = 0.79$ and the s-depletion is $d_1 = 0.45$. The saddle point (green square) on the energy surface gives the maximum energy that a metastable state can have. Along the 'collapse path' (arrow) d_1 increases; by moving the system − over the energy barrier − it becomes more and more fragmented. All quantities are dimensionless.

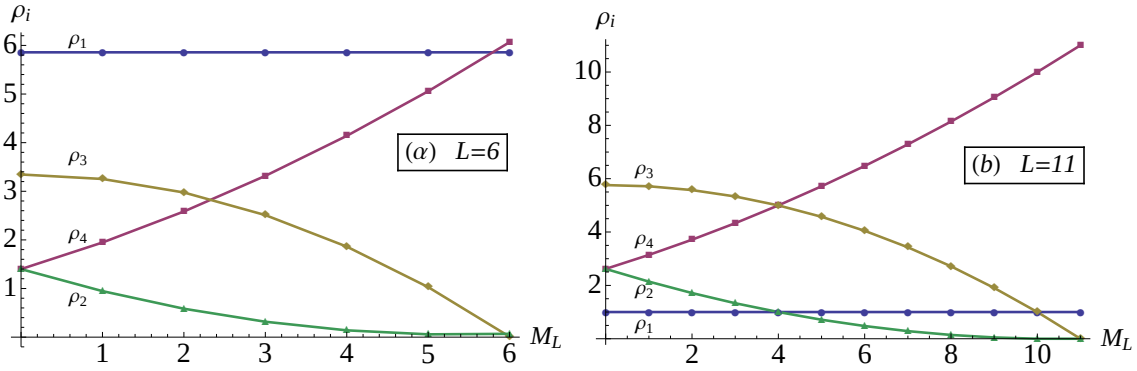

Figure 5.5: Occupations with respect to M_L, for a system of $N = 12$ bosons, with interaction strength set to $\lambda_0 = -0.842$, in the ground state of angular momentum (a) $L = 6$ and (b) $L = 11$. The occupations of the three excited natural orbitals differ significantly when, inside the $L = const.$ subspace, we increase the projection M_L of the angular momentum. The occupation numbers presented here are calculated at the optimal values of σ_0, σ_1. Both the energy and the optimal σ_i, $i = 0, 1$, are invariant under changes of M_L. It should be noted that, for different values of L, the same pattern on the occupations ρ_i persists, though ρ_1 is fixed at different values, according to $\rho_1 \simeq N - L$ [see Eq. (5.19)]. All quantities are dimensionless.

This behavior is depicted in Fig. 5.5 for a system of $N = 12$ bosons in its ground state, for $L = 6$ on the first and $L = 11$ on the second panel. On panel 5.5(a), at point $M_L = 1$, the first from above line (blue) corresponds to the occupation ρ_1, the second (yellow) to ρ_3, the third (purple) to ρ_4 and the fourth one (green) to ρ_2. On panel 5.5(b) the sequence is $\rho_3, \rho_4, \rho_2, \rho_1$, with the same coloring. The occupation numbers presented here are calculated at the optimal values of σ_0, σ_1, that minimize the total energy of the system. Both the energy and the optimal σ_i, $i = 0, 1$, are invariant under changes of M_L. By comparing the two panels we see that the same pattern on the changes of the occupations is repeated, with ρ_1 fixed at different values; at $L = 6$, $\rho_1 \simeq 6$ while at $L = 11$, $\rho_1 \simeq 1$. We infer that the behavior of the occupations against M_L is a general feature, independent of L, N.

In Fig. 5.6, for a system of $N = 12$, we show how the depletion d_1 varies with increasing absolute value of interaction strength. In the left panel the dotted lines correspond to the six excited states, $i = 2, \ldots 7$, of $L = 0$. The solid line marks the depletion of the lowest-in-energy metastable state (ground state), at each value of λ_0, at the optimal σ_0, σ_1. The successive 'jumps' of this line take place at the critical values λ_0^i where the state collapses. Thus the plane of the figure is divided into the right 'collapsed half-plane' and the left 'metastable half-plane'. Similar tendencies persist for states of different angular momenta. This is shown in the right panel, where we plot three curves that correspond to MB states of different angular momenta; the lowest one with $L = 0$, the middle one $L = 2$, and the upper one with $L = 8$, all with $M_L = 0$. Each curve is the value of the s-depletion of the lowest-in-energy metastable state with specific L against $\lambda = |\lambda_0|(N - 1)$. For low interaction strength ($\lambda < 7$) the ground state is the state with $L = 0$ and (almost) zero

fragmentation. For larger values of the interaction strength the condensed state cannot support a metastable state anymore. Though, the first excited (and fragmented) state $|\Psi_{i=2}^{L=0}\rangle$ is found to be non-collapsed.

An examination of the s-depletions of the different ground states of the right panel of Fig. 5.6 allows one a comparison of the respective energies; indeed, two states $|\Psi_i^L\rangle$ with the same s-depletion are expected to have the same energy. For example, the s-depletions of the states $|\Psi_{i=2}^{L=0}\rangle$ and $|\Psi_{i=1}^{L=2}\rangle$ (first and second from below lines, respectively) are very close to each other for the whole range of λ_0 that they exist and their energies $E[|\Psi_{i=2}^{L=0}\rangle]$ and $E[|\Psi_{i=1}^{L=2}\rangle]$ are found to behave accordingly. In fact, those two states belong to a family of states $\{|\Psi_{i=i_k}^{L=L_k}\rangle\}_k$, whose members, defined by:

$$i_k + \frac{L_k}{2} = q,\ q \in \mathbb{N}^*, \tag{5.16}$$

have, for $\lambda_0 = 0$, the same energy, i.e.,

$$E[|\Psi_{i=i_k}^{L=L_k}\rangle] \overset{\lambda_0=0}{=} const. \tag{5.17}$$

for all possible L_k, i_k. That is, all the states with $L = L_k, i = q - L_k/2$, for some positive $q \in \mathbb{N}^*$, are degenerate in the absence of interaction. The degeneracy of such a group of states has been already noted in Ref. [34] and subsequent works. However, the states considered there are those of $M_L = L$ and hence the description becomes essentially two-dimensional. In the case of $\lambda_0 < 0$ and $L_1 < L_2$ Eq. (5.17) transforms to:

$$E[|\Psi_{i_1}^{L_1}\rangle] \overset{\lambda_0<0}{<} E[|\Psi_{i_2}^{L_2}\rangle]. \tag{5.18}$$

Namely, the decrease in the energy is larger in the state with the lowest angular momentum, when the attraction is switched on. This behavior can be seen in the comparison of the states of different angular momentum L, on the right panel of Fig. 5.6.

Summarizing, we see that the s-depletion is an informative quantity of the state, as it reveals information about the energy and the angular momentum, that $|\Psi\rangle$ carries. The s-depletion of a particular metastable state remains almost fixed for $\sigma_1, \sigma_0 \gg 1$, while it changes rapidly as the system is driven to the collapse region of the surface. The s-depletion does not depend on the angular momentum M_L. Among states with different symmetries (quantum numbers) that are energetically degenerate at $\lambda_0 = 0$, the attractive interaction favors energetically the one with lower L, hence smaller M_L-degeneracy.

Variance

Besides the s-depletion of the condensate, the variances τ_i and $|\tau|$, defined in Eqs. (3.26) and (3.27), give information about both the structure of the stationary states and the dynamical behavior of them. Although the calculation of time-dependent states are beyond the scope of this work, one can, based on the present results, comment on the expected dynamical stability of the states. In a fully variational time-dependent multi-configurational approach [105, 108] both the permanents and the expansion coefficients

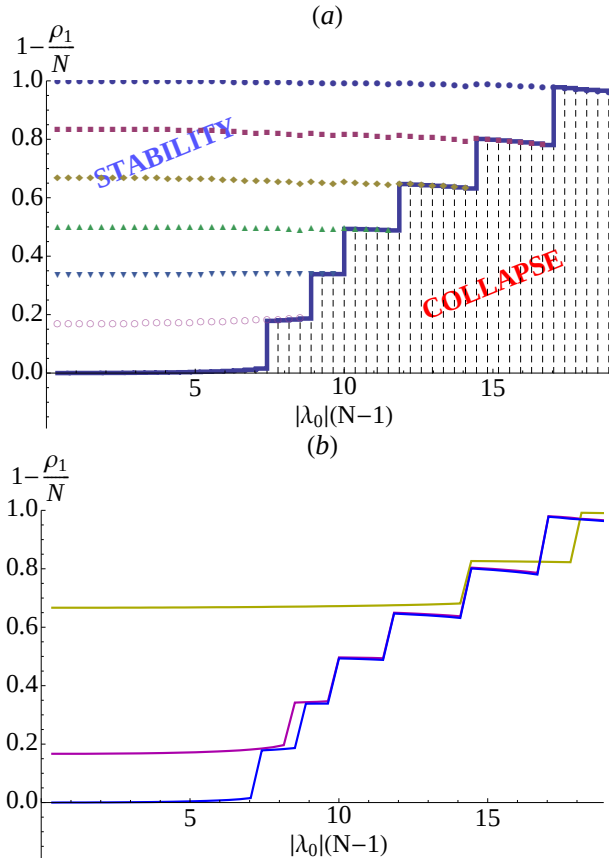

Figure 5.6: s-depletion, $d_1 = 1 - \frac{\rho_1}{N}$, varying with the (absolute value of the) interaction strength for a system of $N = 12$ bosons. In panel (a) the dotted lines correspond to the ground and the six excited states of the $L = 0$ block of the Hamiltonian. The solid line marks the lowest-in-energy metastable (yrast) state that was found at each λ_0 point. In panel (b), shown are three curves corresponding to the MB (yrast) states of different angular momentum L; the lowest one with $L = 0, M_L = 0$ (blue), the middle one with $L = 2, M_L = 0$ (magenta), and the upper one with $L = 8, M_L = 0$ (yellow line). For weak interaction strength the ground state is the $|\Psi_{i=1}^{L=0}\rangle$ state with (almost) zero fragmentation. For $\lambda = |\lambda_0|(N-1) \simeq 8$ the lowest-in-energy state that survives the collapse is the fragmented state $|\Psi_{i=2}^{L=0}\rangle$ with $d_1 \simeq 0.2$. Its energy is very close to that of the *ground state* $|\Psi_{i=1}^{L=2}\rangle$ of the $L = 2$ block. Compare also the three states $|\Psi_{i=1}^{L=8}\rangle$, $|\Psi_{i=4}^{L=2}\rangle$ and $|\Psi_{i=5}^{L=0}\rangle$ at point $\lambda \simeq 15$ (see text for more details). All quantities are dimensionless.

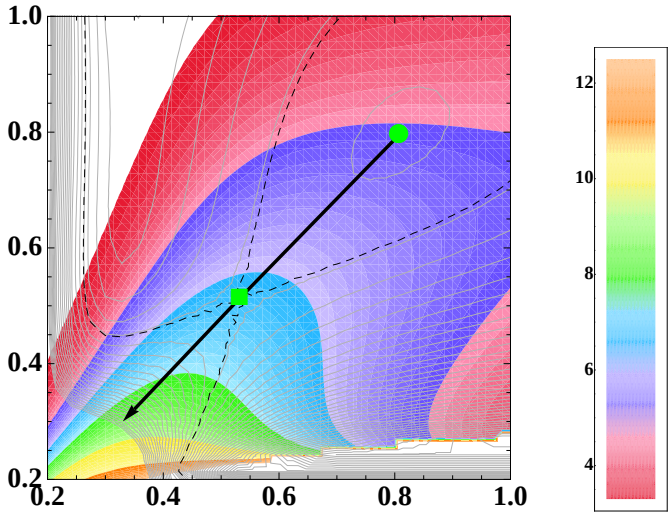

Figure 5.7: Change in variance $|\tau|$ on the (σ_0, σ_1) plane for a $N = 60$ bosons system, for the same state as in Fig. 5.4. Plotted are the contours of $|\tau| = const.$ as well as the contours of constant energy (grey curves). At the minimum of energy (green dot) $\epsilon_0 = 1.55$, $\sigma_0 = 0.81, \sigma_1 = 0.79$, the variance of the system is $|\tau| = 4.79$. The arrow joins the minimum (dot) and the saddle point (square) of the energy surface, i.e., it depicts the 'collapse path'. As the system moves along this 'collapse path' the change of the variance grows moderately large (see text for more details). All quantities are dimensionless.

are time-dependent, i.e., $|\Psi(t)\rangle = \sum_k C_k(t)|\Phi_k(t)\rangle$. As shown in Ref. [101] the expansion coefficients C_k in $|\Psi\rangle = \sum_i C_i|\Phi_i\rangle$ comprise a Gaussian distribution on their own, of width characterized by variance $|\tau|$. So, a state with a large value of $|\tau|$ will include a large number of coefficients C_k in its expansion. For this reason it is expected to be dynamically more unstable than a state with small $|\tau|$.

To study the variance of the states $|\Psi^L\rangle$ we plot in Fig. 5.7 the contours of fixed variance $|\tau| = const.$ on the (σ_0, σ_1) plane for a system of $N = 60$ bosons in the ground state with $L = 26, M_L = 2$. We also draw the 'collapse path' (arrow) as defined before, the minimum (dot) and the saddle point (square) of the energy surface as well as the contours of constant energy ϵ (grey lines). At the minimum of energy, at point $\epsilon_0 = 1.55$, $\sigma_0 = 0.81, \sigma_1 = 0.79$, the variance of the system is $|\tau| = 4.79$. As the systems moves along the 'collapse path' on the energy surface it crosses contours of different variance $|\tau|$ towards larger values. Since a zero (or almost zero) value of $|\tau|$ is indicative of a MF state, we see that the system moves, in this way, towards less and less MF states. On the other hand, for large values of the scaling parameters, i.e., $\sigma_1, \sigma_0 \gg 1$, the variance $|\tau|$ remains practically unchanged.

We have also examined the case of a non-collapsed GP ground state of zero angular momentum. For values of parameters $N = 12$ and $\lambda_0 = -0.5052$ the ground state of the system is the condensed state with $L = 0$ and the variance $|\tau|$, as well as the s-depletion d_1, at the optimal σ_0, σ_1 is almost zero. The same as before scenario is found to

hold; in a neighborhood of the minimum of the energy, in the (σ_0, σ_1) plane, the variance remains very close to zero but as the system moves over the energy barrier the variance grows larger, i.e., the system moves towards non-MF states. The same happens to the s-depletion d_1. It should be noted that, in all cases, the minimum value of $|\tau|$ and the optimum one (i.e., the value of $|\tau|$ at the minimum of energy) do not coincide.

In Fig. 5.8 we plot the change in variance $|\tau|$ of ground states $|\Psi^L\rangle$, against the quantum number L, for six different values of the interaction strength λ_0. The number of particles is $N = 60$ and L varies from $L = 0$ to $L = 58$ or $0 < L/N < 0.97$. As we increase the value of $|\lambda_0|$ the L-states, starting from $L = 0$ upwards, collapse and hence cease to exist. We denote with L_{min} the minimum value of L with which, at a given value of λ_0, a metastable ground state of angular momentum L_{min} can exist. For small values of $|\lambda_0|$, where $L_{min} = 0$, the variation of the states increases monotonously with L. For larger values of $|\lambda_0|$ ($\lambda_0 \lesssim -0.15$) a minimum in the curve $\tau(L)$ appears, at a point $L > L_{min} > 0$. The variances for all different values of the interaction strength meet at one point, as $L \to N$. Generally we detect two competing tendencies on $|\tau|$ as L increases; first, since the size of the configuration space N_p drops linearly with L ($N_p = 1$ when $L = N$) the number of coefficients in the expansion of Eq. (3.18) decreases with L and so will $|\tau|$. On the other hand, as L grows larger, the configurations $\overline{\Phi}$ include more basis-functions Φ in their expansion and hence their variance $|\tau|_{\overline{\Phi}}$ increases. The 'dominance' of the one or the other tendency seems to be conditioned by the value of the interaction strength λ_0. However, for large values of L, the dependence of $|\tau|$ on λ_0 is not significant.

We, next, study the dependence of the variance $|\tau|$ of the states $|\Psi^L\rangle$ on the quantum number M_L. We recall that the maximum angular momentum L_{max} that a MB state can possess is, due to the orbital subspace used here, always equal to the total number of particles N. The $(2L + 1)$ M_L-states, of different z-projection of $\hat{L}$, make every L-eigenstate $(2L + 1)$-fold degenerate.

In Fig. 5.9 we plot the variance $|\tau|$ as a function of M_L for various states. For systems of (a) $N = 12$ and (b) $N = 60$ bosons we choose three different ground states $|\Psi^L_{i=1}\rangle$ with $L = 5, 8, 11$ and $L = 26, 40, 58$ (first and second panels, respectively). In the figure, at $M_L = 4$ for the left and $M_L = 20$ for the right panel, the lowest, middle and upper curves correspond to the lowest, middle and upper values of L, respectively (blue, purple and yellow colors). As the quantum number M_L increases the variance $|\tau|$ drops, contrary to the fact that the size of the configuration space N_p does not depend on M_L (see Appendix B.1). However, the size of the expansion of the basis functions $\overline{\Phi}$ scales like $(N - |M_L|)^2$ and this results in the decrease of the variance $|\tau|_{\overline{\Phi}}$ of each of the functions $\overline{\Phi}$, as M_L increases. In the 'edge' of each L-block, where $M_L = \pm L, \pm(L - 1)$, the variance takes always its minimum value (see also Appendix B.2.2). If, further, $L = N$ and $M_L = \pm L = \pm N$ the variance $|\tau|$ is zero, since there is only the permanent $|0, N, 0, 0\rangle$ (or $|0, 0, 0, N\rangle$) that contributes to the state $|\Psi\rangle$.

It should be noted that the shown dependence of the variance $|\tau|$ on M_L is connected to the size of the (truncated) space of single-particle basis functions that we use. In similar calculations over an extended (i.e., less truncated) ϕ-space, there would be more terms

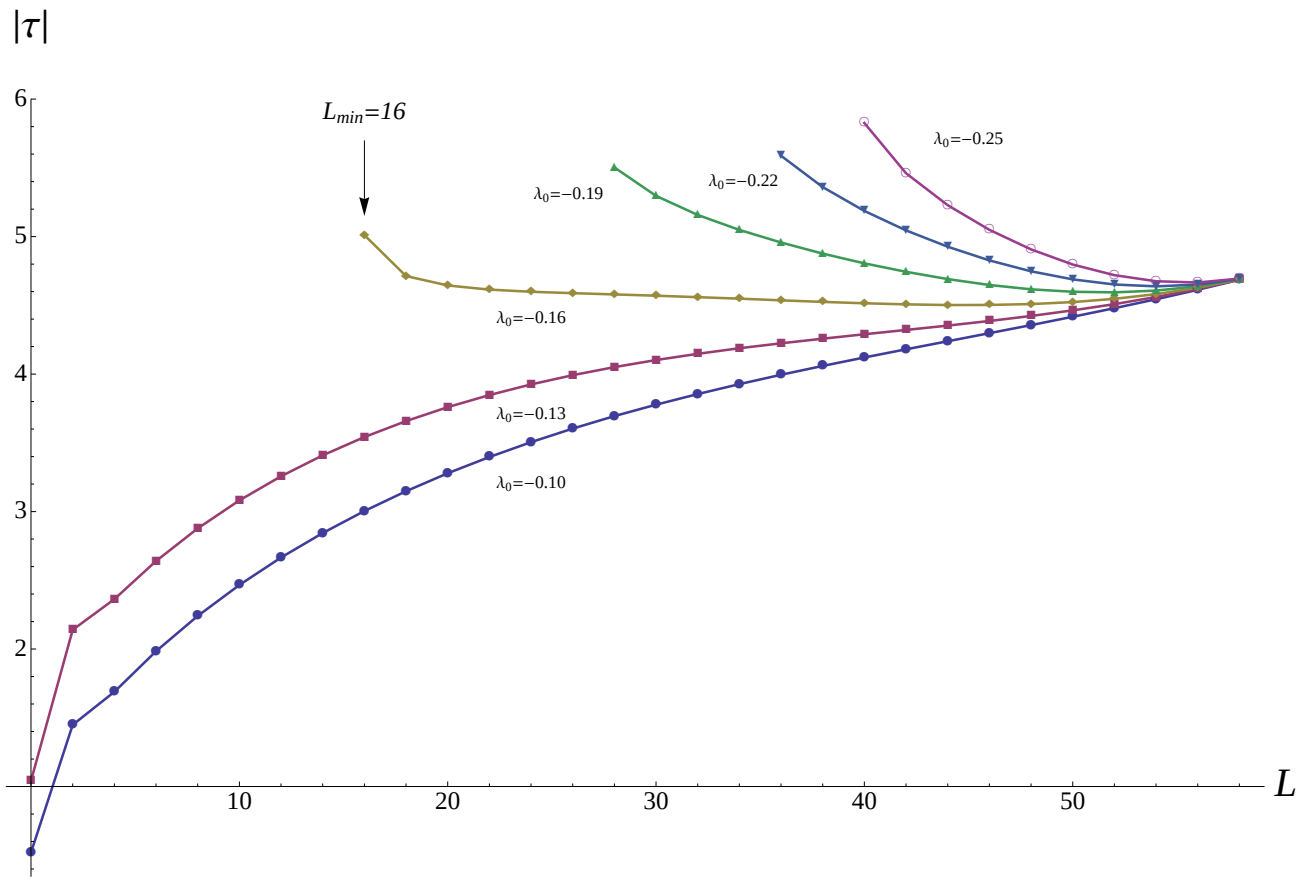

Figure 5.8: Change in the variance $|\tau|$ of ground states $|\Psi^L_{i=1}\rangle$ against the quantum number L, for six different values of the interaction strength λ_0. The number of particles is $N = 60$ and the maximum angular momentum is $L_{max} = N$ (in the diagrams up to $L = 58$). The curves shown are for metastable states which do exist. As the value of λ_0 grows larger the L-states, starting from $L = 0$ upwards, collapse and hence cease to exist. L_{min} is the minimum value of L that, at each value of $|\lambda_0|$ a metastable ground state of angular momentum L_{min} exists. As an example L_{min} is indicated by an arrow for the $\lambda_0 = -0.16$ curve. For small values of λ_0, where $L_{min} = 0$, the variance of the states increases monotonously with L. For larger values of λ_0 a minimum of $|\tau|$ appears at some $L > L_{min}$. All quantities are dimensionless.

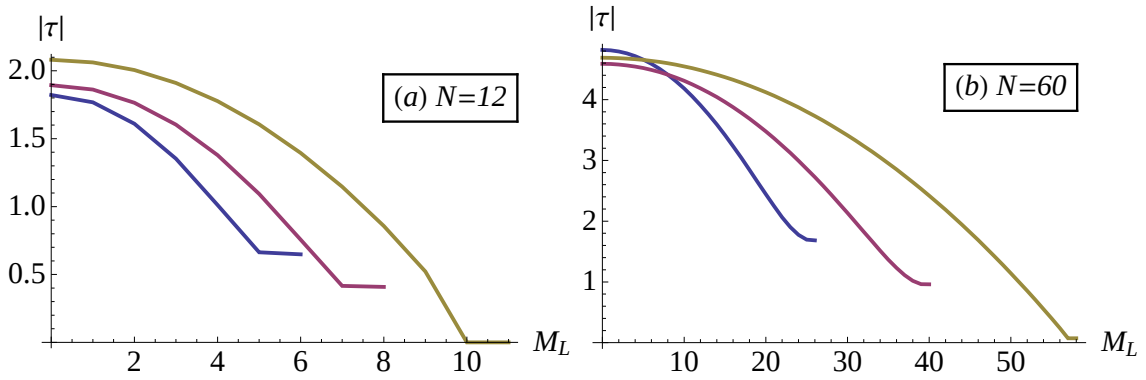

Figure 5.9: Change in the variance $|\tau|$ of MB states $|\Psi^L_{i=1}\rangle$ against the quantum number M_L. Precisely, for a system (a) of $N = 12$ bosons and interaction strength $\lambda_0 = -0.842$ and (b) of $N = 60$ bosons and interaction strength $\lambda_0 = -0.1684$ we pick three ground states $|\Psi^L_{i=1}\rangle$ with different values of L. On the left panel, at $M_L = 4$, the bottom line (blue) corresponds to $L = 5$, the medium one (purple) to $L = 8$ and the upper (yellow) one to $L = 11$. On the right panel, at $M_L = 20$, the bottom line (blue) corresponds to $L = 20$, the medium one (purple) to $L = 40$ and the upper (yellow) one to $L = 58$. In the 'edge' of each L-block of the Hamiltonian matrix $\mathcal{H}$, where $M_L = \pm L, \pm(L-1)$, the variance takes always its minimum value. For $M_L = \pm L = \pm N$ the variance $|\tau|$ is zero and the state is a MF state (see Appendix B.2.2). The shown decrease of the variance is attributed to the decreasing number of available permanents Φ that comprise the basis functions $\overline{\Phi} = \mathcal{U}\Phi$, as the number M_L increases (see text for more details). All quantities are dimensionless.

in the expansions of $\overline{\Phi}$ and the variances shifted to higher values. However, the general tendencies, as shown in Figs. 5.8 and 5.9 are not expected to change.

In this section we have studied the dependence of the variance $|\tau|$ of a state on the parameters σ_0, σ_1 and the quantum numbers L and M_L. Generally, as the system moves towards collapse (i.e., $\sigma_1, \sigma_0 \to 0$) the variance $|\tau|$ increases. Moreover, the variance as a function of L can increase monotonously or exhibit a minimum, depending on the value of λ_0. The variance $|\tau|$ decreases with increasing M_L.

5.5 Angular momentum and collapse: Many-Body vs. Mean-Field

As already discussed, any three-dimensional attractive condensate is expected to collapse when the product $\lambda = |\lambda_0|(N-1)$ exceeds a critical value λ_c. However, fragmented metastable states can survive the collapse for a much greater value $\lambda > \lambda_c$. In this section we examine the behavior of MB states $|\Psi^L\rangle$, as well as these of the MF states $|\Phi\rangle$ of various angular momenta − exact or expectation values − in the onset of collapse. Combining the findings of the previous discussion we show how the angular momentum can stabilize an overcritical condensate. We first discuss the impact of angular momentum on the stability of MB states. We then give an account of the estimated angular momentum within the MF approximation by deriving relevant quantities (expectation value of the angular momentum operator) that will allow us comparisons with the MB results.

5.5.1 Many-Body predictions

In the previous section, we described the structure of MB states that have a definite angular momentum $0 \leq L \leq N$. We showed that, generally, these states are fragmented and, moreover, are non-MF states. This suggests that a MB state $|\Psi^L\rangle$ with definite L can, depending on its s-depletion and the value of $|\lambda_0|$, survive the collapse. Additionally, the condition $[H, \hat{L}] = 0$ necessitates the conservation of the total angular momentum and thus the stability of the state $|\Psi^L\rangle$.

Figure 5.10 summarizes and aggregates the main results of this chapter. We first focus on the upper connected dotted lines, which are the results for the MB states. For systems of different particle numbers $N = 12, 20, 60$ and 120 (see the legend of the figure for the correspondence to the different colors) we plot the s-depletion d_1 versus the quantity $\lambda = |\lambda_0|(N-1)$. Each plotted point, at each value of λ, is the depletion d_1 of the ground (yrast) state $|\Psi^L_{i=1}\rangle$ of some angular momentum L which is still non-collapsed. As the absolute value of the interaction strength increases, the lowest-in-energy states $|\Psi^L\rangle$ start to collapse. The energies and occupations (depletions) are calculated at the optimal values of the parameters σ_0, σ_1. As we have already seen in Sec. 5.4.3, at a given λ_0, the s-depletion of a MB ground state gives also the angular momentum L/N of this state.

Qualitatively, for the ground state of each L-block, one can write

$$\frac{L}{N} = 1 - \frac{\rho_1}{N} + O\left(\tau(\lambda_0)\right) \equiv d_1 + O\left(\tau(\lambda_0)\right), \tag{5.19}$$

i.e., the angular momentum of a ground state $|\Psi^L\rangle$ and the depletion of it differ only to some term $O(\tau)$, that depends on the fluctuation (variance) of that state, which in turn depends on the strength of the interaction. In a non-interacting system the fluctuations are zero and $d_1 = \frac{L}{N}$ exactly.

Interpreting the results of Fig. 5.10 we can say that for any value of the factor λ there will be some $L > 0$ such that the (ground) state $|\Psi^L_{i=1}\rangle$ is metastable. The critical angular momentum L increases monotonously with λ. The stability behavior seems not to depend significantly on the number of bosons in the following sense: for small particle numbers the curves of Fig. 5.10 are slightly different, while for $N \gg 1$ all curves converge, rendering in such a way the obtained results universal and independent of a particular choice of λ_0 or N.

5.5.2 Mean-Field predictions

Any MB state $|\Psi^L\rangle$, as we saw, is an eigenfunction of the operator $\hat{L}^2$. At the MF level, however, every state $|\Phi\rangle$ of the system is represented by only one permanent Φ. Hence, with the exceptions of states with $M_L = \pm L, \pm(L-1)$, a MF state $|\Phi\rangle$ is by construction incapable of describing eigenstates of $\hat{L}^2$ (see Appendix B.2.2 for the possible MF states that are eigenstates of the total angular momentum operator). This incapability comprises a major difference between the two descriptions. Within the multi-orbital BMF [96] theory the occupations n_i of each orbital of the ground state are varied to extremize the energy functional of this state. However, in the description of excited states [103] they serve as parameters that are externally determined. In such a way one is free to choose the values for the set of the occupations $\{n_1, n_2, n_3, n_4\}$ or $\{n_2, n_3\}$ for given depletion d_1 and total particle number N. So, for example, the choice $n_2 = n_3 = n_4 \neq 0$, made in Ref. [103], guarantees the sphericallity of the single-particle density [i.e., $\rho(\mathbf{r}) = \rho(r)$], but breaks the L-symmetry of the state. We recall that in the present MB approach the natural occupation numbers, for *all* the ground and excited states, are determined variationally from the eigenvectors $\mathcal{C}$ of the optimized Hamiltonian matrix $\mathcal{H}$, see Eq. (3.23). As a result, the rotational symmetries of the system are restored.

So, what is the angular momentum that MF states have? It is a matter of fact that at a MF level one can only speak of expectation values and not exact values/quantum numbers of L. It can be shown (Appendix B.2.2) that the expectation value $\langle \hat{L}^2 \rangle$ of the angular momentum of a MF state with equally distributed excited bosons $n_2 = n_3 = n_4$ is the statistical average (mean) of the exact total angular momentum of the MB states with the same value of depletion d_1:

$$\tilde{L}_{MF} = \langle L_{MB} \rangle_{d_1}, \tag{5.20}$$

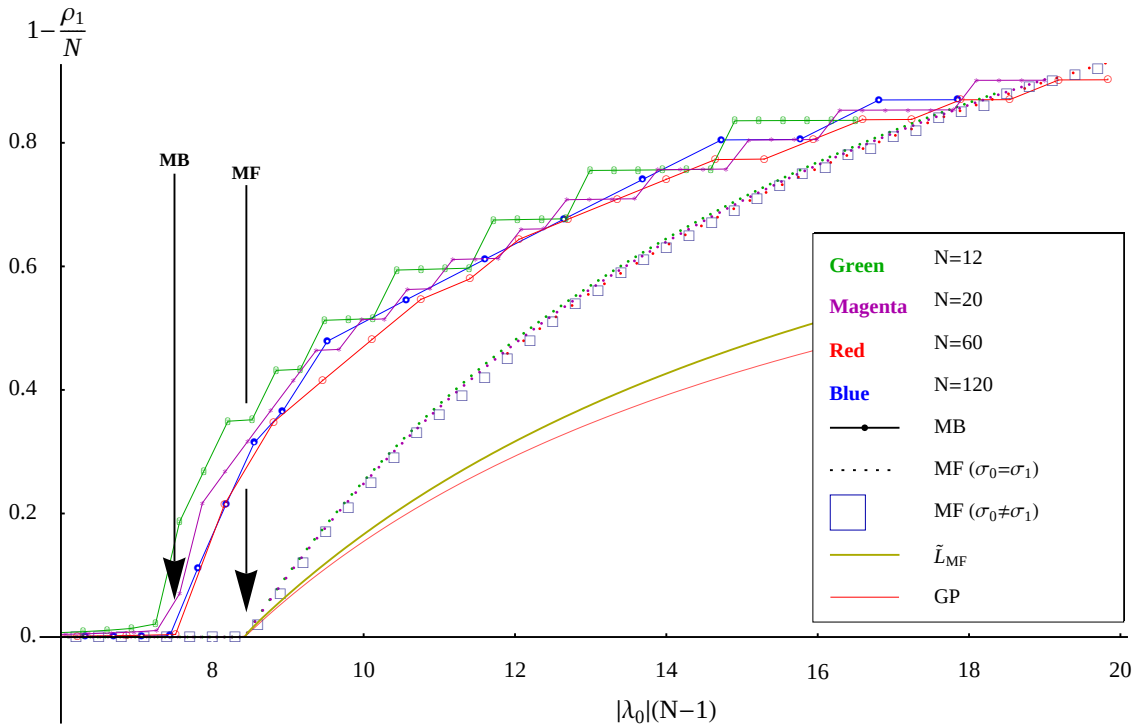

Figure 5.10: Stability plot for systems of different number of bosons $N = 12, 20, 60, 120$. As the interaction strength $|\lambda_0|$ increases the lowest-in-energy states start to collapse; here we plot, at each value of λ_0, the depletion of the lowest-in-energy state, that is still non-collapsed. The connected dotted lines (upper 'band' of curves) are the many-body calculations. Every point of the MB plots corresponds to a ground (yrast) state $|\Psi^L_{i=1}\rangle$ which, unlike the mean-field states, have a definite value of angular momentum L. The angular momentum L/N and the depletion of the ground states $|\Psi^L_{i=1}\rangle$ are almost equal, depending on the fluctuations of the state. The dotted unconnected lines are the critical s-depletions, as estimated from MF theory; the calculations here are done for the permanents $|n_1, n, n, n\rangle$, built over four orbitals, with equal occupations of the p-orbitals. The second lowest continuous line (yellow) determines the expectation value of the angular momentum $\tilde{L}_{MF}/N$, over (generally fragmented) MF states, which is given by the depletion $\frac{2}{3}(1-\rho_1/N)$, here $\rho_1 \equiv n_1$. The lowest continuous line (red) on the diagram depicts the maximum number of bosons N_c^{GP} that can be loaded in a Gross-Pitaevskii condensate (marked as GP in the graph) without collapsing. For this curve one has to identify the axis $1-\frac{\rho_1}{N}$ with $1-\frac{N_c^{GP}}{N}$, i.e., ρ_1 plays the role of the critical GP particle number at a given $|\lambda_0|(N-1)$. The difference in the estimation of the factor $\lambda_c = |\lambda_{0,c}|(N-1)$ where the $L = 0$ ground state collapses is evident; the overestimated value of λ_c from the GP approach is larger than the MB one and puts the latter closer to the experimentally measured one [119]. The depicted stability behavior does not significantly depend on the particle number N, making this behavior universal (see text for more details). All quantities are dimensionless.

where $\tilde{L}_{MF}(\tilde{L}_{MF}+1) = \langle \hat{L}^2 \rangle$. So, in accordance to its name, the *mean-field* state can provide only the *mean* angular momentum of the corresponding (i.e., same d_1) MB states. Furthermore, one can calculate (Appendix B.2.2) the average momentum over, first, all the MF states $|\Phi\rangle$ and, second, over all MB states. It turns out that they are connected through:

$$\langle \tilde{L}_{MF} \rangle_{all\ states} = \frac{N}{\sqrt{5}} = \frac{3}{\sqrt{5}} \langle L_{MB} \rangle_{all\ states}. \tag{5.21}$$

So, the average angular momentum over MF states is found to be $\frac{\sqrt{6}}{2} \simeq 1.22$ times higher than the average one over MB states.

Since, within the MF theory, the states $|\Phi\rangle$ do not possess a definite quantum number L we cannot write any exact correspondence between the depletion d_1 of the state and the angular momentum L, as we did in the case of MB ground states. Instead, we can use $\tilde{L}_{MF}$ and relate it to d_1 through:

$$\frac{\tilde{L}_{MF}}{N} = \frac{2}{3}\left(1 - \frac{n_1}{N}\right) = \frac{2}{3} d_1. \tag{5.22}$$

This result is taken in the limit $N \gg 1$ (see Appendix B.2.2). It should be noted that it does not depend on the value of λ_0. This reflects the absence of fluctuations on a MF state, which do depend on the interaction strength λ_0.

How is $\tilde{L}_{MF}$ related to the stability of the condensate? Recall first, that a system will survive the collapse if, for a given λ_0, the number of particles that occupy the s-orbital stays below a critical number N_c [2]. This, however, does not forbid the total number N of bosons of the system to be larger than this critical number. Indeed a system can exist in a state with $n_1 < N_c$ bosons occupying the s-orbital and $N - n_1$ occupying higher-in-energy orbitals. More precisely, any excitations of bosons to p-orbitals may increase the total energy of the system but will contribute to the total stability of it, since the excited p-bosons 'feel' less the interaction energy than the s-bosons. This is the reasoning behind the metastability of fragmented states with an overcritical number of bosons, already demonstrated in Ref. [103]. Here we further show that a MF state $|\Phi\rangle$ with non-zero expectation value of angular momentum $L_{MF} > 0$ exhibits fragmentation, Eq. (5.22), which increases the overall stability of the system. However, the impact of the angular momentum in the stability of the condensate is overestimated at the MF level. A comparison of Eq. (5.22) with the corresponding MB one, Eq. (5.19), convinces us of this claim.

To allow a better comparison to the MB results of Fig. 5.10 we plot on the same graph the data obtained from the MF states (second group of dotted unconnected lines in Fig. 5.10). More precisely, for systems of $N = 12, 20$ and $N = 60$ bosons, we plot at each value of $|\lambda_0|(N-1)$ the s-depletion $d_1 = 1 - \rho_1/N$, with ρ_1 now given by the critical

[2] This should not be restricted to the s-orbital. The system will − also − collapse if the numbers of bosons that reside in the $p, d, f \ldots$ orbitals exceed the corresponding critical numbers. However, these numbers are quite larger than the critical one of the s-orbital and the collapse of the excited orbitals is therefore not of primary significance.

number of particles N_c (i.e., maximum number of particles so that the state $|\Phi\rangle$ is not collapsed) calculated from the relation:

$$N_c = N_c^{GP} \frac{(-64 \cdot 5^{3/4} - 128 \cdot 5^{3/4} \frac{n}{N} + 300\Lambda_0 - 375\Lambda_0 \frac{n}{N})}{\left[-4 + 13(\frac{n}{N})^2\right](16 \cdot 5^{3/4} - 75\Lambda_0)}, \tag{5.23}$$

at $\sigma_0 = \sigma_1$, with $\Lambda_0 = \frac{\lambda_0}{4\pi}\left(\frac{2}{\pi}\right)^{1/2}\frac{4}{3}$, $N_c^{GP} = 1 - \left(\frac{1}{5}\right)^{1/4}\frac{16}{15}\frac{1}{\Lambda_0}$ and $n = n_2 = n_3 = n_4$ the occupations of the p-orbitals. Equation (5.23) in the limit $N \gg 1$ gives back Eq. (7) of Ref. [103]. Also, the numerical MF calculations for the critical numbers of a $N = 120$ bosons system, without using the assumption $\sigma_0 = \sigma_1$, are presented in Fig. 5.10 with the 'boxed' line (blue). The second from below continuous line (dark yellow) determines the angular momentum expectation value $\tilde{L}_{MF}/N$ [Eqs. (5.22) and (B.34)], over MF states. The lowest continuous line (red) of Fig. 5.10 is the calculations from the Gross-Pitaevskii theory. In this case one has to identify $1 - \frac{\rho_1}{N}$ with $1 - \frac{N_c^{GP}}{N}$, where N_c^{GP} is the maximum number of bosons that, for a given λ_0, can be loaded in a GP state without collapse. Here we use $N = 60$ bosons. The total particle number N_c^{GP} is, of course, the number of s-bosons of the system. Obviously this critical number is decreased, as we move to the right of the x-axis of the diagram and hence we call this curve the 'critical GP'.

The 'bands' of MF and MB states depicted in Fig. 5.10 substantially deviate one from each other at small and moderately larger values of λ. This is nicely manifested in the difference between the MF and MB predictions of the collapse of the $L = 0$ ground state. The collapse of the MB state appears to happen at a smaller value of the product λ than the one that the MF theory estimates. This reflects the overestimation of the impact of the angular momentum within the MF and puts the MB prediction closer to the experimentally measured values of λ (see Ref. [119] and also the discussion in Refs. [124–127] about the discrepancies between MF predictions and experimental values of the critical numbers and the collapse times).

We see that the form of the curves for the s-depletion of the MF states seems not to be affected from the number N of the particles of the system. The various plotted MF curves for different N, like the MB ones, tend to converge for $N \gg 1$, making thus the described stability behavior a universal and independent of N phenomenon. For the MF case convergence has been noticed already for $N \sim 10^2$ bosons. It should be noted, though that unlike the MB states, the MF ones with $L = 0$ collapse all *at the same* critical value $\lambda_c = |\lambda_{0,c}|(N-1)$, regardless of the total number N of bosons. We also see in Fig. 5.10 a divergence of the angular momentum $\tilde{L}_{MF}$ (dark yellow line) from the s-depletion of the MF states (dotted lines); this is exactly the relation of the two quantities, that Eq. (5.22) provides. The 'critical GP' curve significantly diverges from both the multi-orbital MF and the MB predictions.

Conclusively, we presented a way, Eq. (5.20), to connect the angular momenta of a MF state of the form $|n_1, n, n, n\rangle$ to that of the MB states with the same depletion d_1. A non-zero angular momentum will result in a fragmented condensate [Eq. (5.22)] which in turn will render the system more stable, with respect to the parameter λ. Those results are in agreement with the MB ones of the previous section.

5.6 Conclusions

In this chapter we constructed many-body states with definite angular momentum quantum numbers L and M_L, for systems of N isotropically trapped bosons in three dimensions, interacting via an attractive two-body potential. These many-body states are written as an expansion (configuration interaction expansion) over orthogonal many-body basis functions (permanents). We represented the Hamiltonian and angular momentum operators as matrices on this basis and we looked for the states that simultaneously diagonalize them. In this representation the Hamiltonian has a block-diagonal form, with each block consisting of many-body states, with the same eigenvalue of angular momentum. The single-particle basis functions that we used are the wave functions (s- and p-orbitals) that solve exactly the linear (non-interacting) problem, each scaled under a parameter σ_i, which we determined variationally. The rotational symmetries as well as symmetries under spatial inversion that the single-particle basis functions possess are also present in the many-body states and reduce significantly the size of the configuration space. Due to the truncated single-particle basis set, the total angular momentum is restricted to $0 \leq L \leq N$. To our knowledge this is the first time that a fully three-dimensional Bose gas in isotropic trapping potential is studied, with the many-body wave function of the system expressly written as an eigenfunction of both total angular momentum operators $\hat{L}^2$ and $\hat{L}_z$, for $L \geq 0$.

For a value of the parameter $\lambda = |\lambda_0|(N-1)$ such that the $L = 0$ ground state of the system is collapsed, we have plotted the energy per particle $\epsilon(\sigma_0, \sigma_1)$ of the ground and the excited many-body states, as a function of the parameters σ_0, σ_1. We have shown that metastable excited states of the same angular momentum can exist. Furthermore, for the same system, we demonstrated the existence of metastable ground states with angular momentum $L > 0$ that can survive the collapse. These states would also collapse, if the (absolute value of the) interaction strength is further increased. The examination of the above states, in terms of the natural orbital analysis, revealed that the states are fragmented, with a substantial number of particles being excited to the p-orbitals.

We discussed why the s-depletion of a many-body state $|\Psi\rangle$ bears information about the energy and the angular momentum of $|\Psi\rangle$. We found that the s-depletion of a metastable state remains practically fixed for $\sigma_0, \sigma_1 \gg 1$, while it changes rapidly as the system is driven to collapse. We have shown also that the z-projection of the angular momentum M_L does not affect the occupation of the first natural orbital.

We have studied the dependence of the variance $|\tau|$ of a state on the parameters σ_0, σ_1 and the quantum numbers L and M_L. We saw that along the 'collapse path' the variance increases. The variance as a function of L − depending on the value of λ_0 − can increase monotonously or exhibit a minimum. We also found that as the quantum number M_L increases the variance $|\tau|$ decreases.

To further investigate the impact of the angular momentum on the stability of the system, we plotted the critical s-depletion of the metastable ground states $|\Psi^L_{i=1}\rangle$ (yrast states) as a function of the quantity $\lambda = |\lambda_0|(N-1)$. We showed the connection of the s-depletion to the critical angular momentum L, in both the mean-field and the many-

body cases. We demonstrated that for any value of the factor λ there is some angular momentum $L > 0$ such that the (ground) state $|\Psi^L_{i=1}\rangle$ is metastable. The critical angular momentum L increases monotonously with λ and this behavior is found to be independent of the particle number N, as long as $N \gg 1$. We derived analytical relations for the expectation value of the angular momentum of a mean-field state, with equally distributed excited bosons, which allowed us to compare it with the corresponding results from the many-body approach. We have further demonstrated that the angular momentum of this mean-field state equals the average angular momentum of many-body states, with the same s-depletion.

Conclusively, we can say that for any particle number N and interaction strength λ_0 of an attractive condensate, there is some well defined quantum number L of the many-body angular momentum operator $\hat{L}^2$ such that the *ground state* of this system is metastable, i.e., exhibits a clear minimum in energy as a function of the shapes of the orbitals. Moreover, since the total angular momentum of the system is conserved, once the system is prepared in a ground state with $L > 0$ it can survive the collapse, and that for a particle number/interaction strength much beyond the corresponding ones of the $L = 0$ ground state. We hope that our results will stimulate experimental research.

Chapter 6

The attractive Bose gas under external rotation

In the last two chapters the ground and excited states of the attractive gas with the constraint $L > 0$ were studied. In the present chapter we ask what happens to the 3D gas, initially prepared at an $L = 0$ ground state, when it is set to external rotation. We look at the properties of the ground state and its stability for different rotating frequencies Ω and different trap geometries and find that the ground state is not stabilized against the collapse. Our findings are compared to known results.

6.1 Introduction

The collapse of the attractive BECs – as discussed – has been the research subject of various works in the past, but, in addition, situations where the collapse can be hindered have been proposed the past two decades (see, for instance, Refs. [66, 113, 128]). It has been furthermore known that the attractive gas, once prepared in a vortex configuration, will be more stable against collapse [26, 66, 129]. Moreover, fragmented metastable excited states [103] and ground states with definite non-zero angular momentum [28] have also been found to postpone the collapse.

On the other hand, it is known that rotating (stirring) condensates is a way of imprinting angular momentum in a gas and nucleating vortices [52, 130]. In repulsive gases rotating with a frequency smaller than the trapping frequency there can exist configurations where the system is well described by a stationary state with some finite non-zero vorticity. Vortices [50], vortex lattices [130] and highly correlated – fractional quantum Hall – states [58], as well as giant-vortices [55] have all been experimentally observed in repulsive gases. In sharp contrast, the behavior of the attractive system under rotation is quite different [63, 131, 132]. The question of how rotation would affect the stability and collapse of the attractive condensate in harmonic traps has recently been addressed [133]. In Ref. [133] it has been found at the Gross-Pitaevskii (GP) mean-field (MF) level that the attractive gas can be stabilized against collapse for rotation frequencies smaller

than the trap frequency. These findings have motivated us to attack the same problem at the many-body (MB) level. We show herein that rotating an attractive condensate, confined by a harmonic isotropic or slightly anisotropic trap, with a frequency below the trap frequency, does not have an impact on the stability as well as on the angular momentum of the ground state. We then analyze the problem on the GP (MF) level and find as well that no stabilization of the ground state occurs. We stress at this point that it has been previously shown that there is no stabilization of the attractive gas in an isotropic anharmonic trap with a slight anharmonicity for rotation frequencies below the trapping one (see [63]).

6.2 The system.

We consider an attractive BEC of N atoms of mass m, confined by a generally anisotropic trapping potential

$$V(\mathbf{r}) = \frac{1}{2}m\omega^2\left[(1-\varepsilon)x^2 + (1+\varepsilon)y^2 + \zeta^2 z^2\right] = V_0(x,y,z) - \varepsilon V_a(x,y), \tag{6.1}$$

where ω, ε and ζ are real non-negative parameters that determine the frequencies of the trap and its deformation, namely $\omega_x = \omega\sqrt{1-\varepsilon}, \omega_y = \omega\sqrt{1+\varepsilon}$ and $\omega_z = \omega\zeta$, $V_0 = \frac{m\omega^2}{2}(x^2+y^2+\zeta^2 z^2)$ is the axially symmetric part of the potential and $V_a = \frac{m\omega^2}{2}(x^2-y^2)$ the rotating anisotropy. Since we are interested in the rotating problem we will work in the corotating frame of reference, where the MB Hamiltonian takes on the time-independent appearance:

$$H = \sum_i^N \left[-\frac{\hbar^2}{2m}\nabla^2(\mathbf{r}_i) + V(\mathbf{r}_i) - \Omega\hat{L}_z(\mathbf{r}_i)\right] + \lambda_0\sum_{i<j}^N \delta(\mathbf{r}_i - \mathbf{r}_j), \tag{6.2}$$

where Ω is the frequency of the rotation around the z-axis, $\hat{L}_z$ the z-projection of the angular momentum operator and λ_0 measures the interaction strength and takes on negative values for attraction. Again, we set $\hbar = m = \omega = 1$ so as to work in dimensionless units.

The Hamiltonian of Eq. (6.2) admits exact solutions in the absence of interaction, i.e., when $\lambda_0 = 0$. In the case of isotropic system ($\varepsilon = 0$, $\zeta = 1$) and in the limit of fast rotation ($\Omega \to \omega$) the energy levels are organized into what is known as *Landau Levels*. The same holds true for weak interparticle interactions [29, 116, 134]. Thus, in the fast rotation and weak interaction limit the *Lowest Landau Level* (LLL) is particularly designated for the description of the ground state of the system. The orbitals that comprise the (scaled) LLL have the form $\psi_k^{LLL}(\mathbf{r}) = N_k r^k e^{-r^2/2\sigma^2} Y_k^k(\theta,\phi)$, $k = 0,1,2,\ldots$, where Y_k^k is the spherical harmonic with $l = m_l = k$ and N_k is the normalization constant. The scaling parameter σ defines the width of the Gaussian part and will be treated variationally, i.e., so as to minimize the total energy. Of course, if $\lambda_0 = 0$ then $\sigma = 1$. At the resonance, $\Omega_r = \omega$, all (infinitely many) orbitals of this set become degenerate in energy.

The above orbitals can also be expressed in Cartesian coordinates as appropriate linear combinations of the solutions $\phi_i(x,y,z) = \varphi_{n_x}(\omega_x,x)\varphi_{n_y}(\omega_y,y)\varphi_{n_z}(\omega_z,z)$ of the three-dimensional harmonic oscillator, i.e., the scaled Hermite-Gauss functions, $\varphi_{n_x}(\omega_x,x) = \frac{(\omega_x/\sigma^2\pi)^{1/4}}{\sqrt{2^{n_x}n_x!}} H_{n_x}\left(\frac{\sqrt{\omega_x}}{\sigma}x\right) e^{-\omega_x x^2/2\sigma^2}$, where $H_n(\dots)$ denotes the Hermite polynomial of degree n. Namely, for the isotropic case $\omega_x = \omega_y = \omega_z$, we rewrite the orbitals as

$$\psi_k(\mathbf{r}) = \sum_{n_x+n_y=k} c_i \phi_i, \tag{6.3}$$

with $c_i = \langle \psi_k^{LLL} | \phi_i \rangle$, $n_x+n_y = k$, $k = 0,1,2,\dots$, and $i = i(n_x,n_y) = \frac{1}{2}[n_x+3n_y+(n_x+n_y)^2]$ is a function that we employ to uniquely map the pair $\{n_x,n_y\}$ to the single parameter i. Once we depart from the isotropy of the trap the infinite degeneracy, now at $\Omega_r = \omega_x < \omega_y$, is *not* lifted [87] and the above LLL states are not solutions of the anisotropic system. Since the radial symmetry of the trap is broken the orbitals do not possess exact angular symmetries and one cannot express the solutions in terms of pure spherical harmonics anymore. Instead, one should resort to the orbitals ψ_k expressed as a mixture of functions ϕ_i. The same transformation coefficients c_i, that are defined above for the isotropic case, can also be used for generic $\omega_x \neq \omega_y \neq \omega_z$. This transformation maps the functions from the Hermite-Gauss representation to that with non-zero (expectation value of) orbital angular momentum. Of course, for $\varepsilon = 0$ and $\zeta = 1$ (i.e., for isotropic traps) the mapped orbitals give back the spherical harmonics. The expectation values of $\hat{L}_z$ for the orbitals ψ_k, for ε small enough, are $\langle \psi_k | \hat{L}_z | \psi_k \rangle \equiv l_k = \left[1 + \frac{\varepsilon^2}{8} + \mathcal{O}(\varepsilon^4)\right] k$, with $k = 0,1,2,\dots$. It should be noted that, when $\varepsilon \neq 0$, the orbital set $\{\psi_k\}$ is also not an exact solution of the non-interacting anisotropic Hamiltonian, since the linear combination $\psi_k = \sum c_i \phi_i$ mixes non-degenerate states. However, in the limit of small ε, this choice is justified on account of working with single-particle states ψ_k that have non-zero (expectation value of) angular momentum l_k and thus allows for a possible coupling to the rotation.

6.3 Many-body approach.

We study our system at the MB level, i.e., beyond a MF description, with a general variational MB method that allows the system to fragment and takes into consideration fluctuations of the states. To this end we follow the configuration interaction (CI) expansion, that is introduced in Sec. 3.5.1. The MB wave function $|\Psi\rangle$ of the system is expanded over a set of functions $|\Phi_i\rangle$ (permanents),

$$|\Psi\rangle = \sum C_i |\Phi_i\rangle, \tag{6.4}$$

each describing a MF state of a condensed or fragmented Bose gas of N atoms. The permanents are built over a certain set of M single-particle functions (orbitals). In this work $M = 4$ and the set of orbitals comprise the LLL and its anisotropic extension, as described above. The permanents can be written in an occupation-number-representation

as $|\Phi_i\rangle = |\vec{n}\rangle = |n_0, n_1, \dots n_{M-1}\rangle$, where it is meant that n_i bosons occupy the ϕ_i orbital, satisfying $\sum_i n_i = N$. The Hamiltonian of the problem is then represented as a matrix $\mathcal{H}$ over the permanents $|\Phi_i\rangle$ and diagonalized. The eigenvalues E_i of $\mathcal{H}$ are the energies of the states. The eigenvectors $\{C_i\}$ of $\mathcal{H}$ provide us with the wave functions with which one can compute various quantities like the *natural occupation numbers* ρ_i of the ground and excited states, with $\sum_i \rho_i = N$. It should be noted that the *natural orbitals* and the orbitals described and used in the expansion above coincide. This holds for the isotropic case (due to the symmetry of the problem) and has been found (numerically) to be well satisfied for the slightly anisotropic case discussed below. From the natural occupations we can calculate the total angular momentum of the ground state as $L = \sum_{l=0}^{3} l\rho_l$. By varying the parameter σ (i.e., the Gaussian width of the orbitals), we minimize the energies per particle $\epsilon = E/N$ as a function of the rotation frequency Ω, for some fixed value of $\lambda = |\lambda_0|(N-1)$ and determine the optimal value σ_0. The analysis of the system that follows is always done for optimal states, i.e., at σ_0. The number of particles is hereafter set to $N = 12$.

As before, we denote with λ_c the critical value of the parameter λ where the ground state of the condensate ceases to exist. This is calculated as the largest value of λ where there is a (local) minimum in the energy E as a function of σ. The absence of such a minimum denotes a collapsed state (see also Secs. 1.3 and 3.8 and Refs. [28, 30, 102, 103]). We are interested in the dependence of λ_c on the rotation frequency Ω. In Fig. 6.1 we plot the critical value λ_c against Ω for the isotropic $\varepsilon = 0,\ \zeta = 1$ and the slightly anisotropic case $\varepsilon = 0.1,\ \zeta = 1$. [1] The values of Ω range from 0 to $\Omega_r = \omega_x = \sqrt{1-\varepsilon}$. At exactly the resonance frequency Ω_r, the energy diverges and the gas becomes mechanically unstable. We notice no change in the stability of the ground state of the isotropic system as the rotation frequency Ω increases from 0 up to Ω_r, and only a negligible increase in $\lambda_c(\Omega)$ of less than 0.1% for $\varepsilon = 0.1$. The value of the critical parameter $\lambda_c = 8.425(9)$ remains unchanged when $\varepsilon = 0$ for the whole allowed region of Ω, and marginally increases from $\lambda_c(0) = 8.436(2)$ to $\lambda_c(\Omega_r) = 8.440(7)$ for $\varepsilon = 0.1$. [2] These results, obtained at the MB level, obviously contradict the GP results of Ref. [133] (see analysis and discussion below).

Next, to analyze the MB results, we chose $\lambda = 3$ as a representative value of the interaction parameter of an isotropic system ($\varepsilon = 0$) with non-collapsed ground state and calculated the energy per particle ϵ, the angular momentum per particle L/N and the natural occupations $\rho_i,\ i = 0, \dots, 3$ for the ground state. We found that the above quantities remain constant for any $\Omega \in [0, \Omega_r)$. The state remains condensed ($\rho_0 = N$), carries no angular momentum ($L/N = 0$) and has energy $\epsilon = 1.396(8)$. For the anisotropic case of $\varepsilon = 0.1$ we also found that the above quantities practically do not change. Namely, ρ_0 marginally decreases from $\rho_0(0) \simeq 12$ to $\rho_0(\Omega_r) = 11.998(9)$, and the rest of the natural occupations change from $\rho_1(0) \simeq 10^{-8}, \rho_2(0) \simeq 10^{-5}, \rho_3(0) \simeq 10^{-13}$ to $\rho_1(\Omega_r) \simeq 10^{-7}, \rho_2(\Omega_r) = 10^{-3}, \rho_3(\Omega_r) \simeq 10^{-12}$. There is an insignificant decrease in the

[1] It is important that even smaller trap anisotropies are sufficient to nucleate vortices in experimental setups, like $\varepsilon = 0.025$ for instance, in the rotating repulsive gas of Ref. [52].

[2] Here and hereafter, when we write $\lambda_c(\Omega_r)$ it is meant, mathematically, $\lambda_c(\Omega)$ in the limit of the resonance frequency $\Omega \to \Omega_r$. The same is meant for other system's properties at the resonance frequency.

energy [from $\epsilon(0) = 1.395(8)$ to $\epsilon(\Omega_r) = 1.395(4)$] and a corresponding increase in the angular momentum [from $L(0)/N \simeq 0$ to $L(\Omega_r)/N = 2 \cdot 10^{-4}$].

The fact that the ground state of the isotropic system is found to be fully (i.e., 100%) condensed deserves some discussion. The total absence of depletion and fluctuations in this case is explained if one considers the MB orbital set used: since each orbital ψ_k^{LLL} has different angular symmetry a coupling between the different modes is forbidden due to the symmetry of the problem. Any non-zero occupation of the $i = 1, 2, 3$ orbitals would result in the change of the total angular momentum of the system. Naturally, such a coupling is induced in the system when the anisotropy ε is turned on and hence the occupations $\rho_i, i = 1, 2, 3$ can be non-zero. Nonetheless, as we have found above, for attractive systems in three-dimensional isotropic and slightly anisotropic traps, coupling of the ground zero-angular-momentum state to excited-states with non-vanishing angular momentum essentially does not occur, even for rotation frequencies as high as the resonance frequency Ω_r. In other words, for rotating attractive BECs none of the $\psi_{k>0}^{LLL}$ (or, for slightly anisotropic traps, $\psi_{k>0}$) states becomes the state lowest-in-energy, even for rotation frequencies as high as the resonance frequency Ω_r.

Do the above findings change for a MB basis set that does allow for ground-state depletion? The answer is negative. Having used, in place of the LLL, the set consisting of the s, p_+, p_0 and p_- orbitals (see in this respect Ref. [28]), we found the ground state of the isotropic system slightly depleted (i.e., about 98% condensed for $\lambda \simeq \lambda_c$), but its angular momentum zero for all rotation frequencies up to the resonance frequency Ω_r. Side by side, the depletion and fluctuations of the ground state do not depend on the rotation frequency. Importantly, the critical value λ_c for the collapse does not depend on the rotation frequency as well. The same conclusion holds for slightly anisotropic traps ($\varepsilon = 0.1$). In summary, we have shown by a MB approach that the critical value of the interaction for collapse, λ_c, of rotating three-dimensional attractive BECs does not depend on the frequency of rotation.

The fact that the ground states of both the isotropic ($\varepsilon = 0$) and the slightly anisotropic system ($\varepsilon = 0.1$) were found at the MB level to be essentially fully condensed for any rotation frequency Ω smaller than the resonance frequency Ω_r, means that the GP theory should be valid here and reproduce the MB conclusions.

6.4 The Gross-Pitaevskii approach.

We now want to turn from the MB to the GP (MF) description and address the same question, namely how the stability of the attractive gas is affected as the system is rotated externally. The GP theory assumes that all particles reside in the same single-particle state and hence the wave function for the state of the whole system is given by a single permanent $\Psi_{GP} = \prod_i^N \psi_{GP}(\mathbf{r}_i)$. The GP orbital ψ_{GP} for the ground state of the rotating gas should be represented with an ansatz that takes into consideration orbitals with non-zero angular momentum, as done in the MB treatment. To this end we expand ψ_{GP} as a

linear combination

$$\psi_{GP}(\mathbf{r},\sigma)=\sum_k c_k\psi_k(\mathbf{r},\sigma), \tag{6.5}$$

where the basis ψ_k is the same as the one used in the MB computations reported above. The coefficients c_k and parameter σ (Gaussian width of the orbitals) are determined variationally with the normalization constraint $\sum_k |c_k|^2=1$ and the summation running over from $k=0$ to $k=3$. We calculate the expectation value $E=\langle\Psi_{GP}|H|\Psi_{GP}\rangle$ with the above GP ansatz and minimize it with respect to the parameters $c_i, i=1,2,3$ and σ, for different values of the interaction parameter $\lambda=|\lambda_0|(N-1)$ and for given values of $\Omega\in[0,\sqrt{1-\varepsilon})$ and the (small) trap anisotropy ε. The expectation value of the angular momentum operator for ψ_{GP} is $l=\sum_{i,j}\mathfrak{l}_{ij}c_i^*c_j$, $i,j=1,\ldots,4$, where the matrix elements $\mathfrak{l}_{ij}=\langle\psi_i|\hat{L}_z|\psi_j\rangle$ are given, in second order approximation, as $\mathfrak{l}_{ii}=l_{i-1}=\left(1+\frac{\varepsilon^2}{8}\right)\cdot(i-1)$, $\mathfrak{l}_{13}=\mathfrak{l}_{31}=\frac{\varepsilon}{2\sqrt{2}}$, $\mathfrak{l}_{24}=\mathfrak{l}_{42}=\frac{\sqrt{3}\varepsilon}{2\sqrt{2}}$ and the rest of the elements are zero. The total angular momentum is $L=Nl$.

We calculate the critical value of the interaction λ_c as a function of the rotation frequency Ω, for the cases of $\varepsilon=0,\ \zeta=1$ and $\varepsilon=0.1,\ \zeta=1$. As anticipated from the MB analysis, we again found no essential change in the stability of the gas, as Ω varies from 0 to $\Omega_r=\sqrt{1-\varepsilon}$. Namely, in the isotropic case, the GP ansatz of Eq. (6.5) yields the value $\lambda_c=8.425(9)$ which coincides with that obtained from the MB analysis, and remains fixed for any $\Omega\in[0,\Omega_r)$. In the case of anisotropic trap ($\varepsilon=0.1$) we found $\lambda_c(0)=8.436(3)$ and a negligible increase as Ω increases, i.e., $\lambda_c(\Omega_r)\simeq 1.0005\cdot\lambda_c(0)$. We then fix the interaction parameter to $\lambda=3$ as before. In the isotropic case, $\varepsilon=0$, the energy $\epsilon=1.396(8)$ and angular momentum $L/N=0$ remain constant for all $\Omega\in[0,\Omega_r)$ and, as above, the values coincide with those of the MB ansatz. For $\varepsilon=0.1$, we found $\epsilon(0)=1.395(8)$, $\epsilon(\Omega_r)=1.391(8)$, $L(0)/N\simeq 0$ and $L(\Omega_r)/N=0.045(2)$. Namely, the energies found in the MB and GP approaches are almost identical while the angular momentum computed within the GP theory at the resonance frequency Ω_r is somewhat above the value that the MB theory gives. Nonetheless, both values of angular momentum can be considered practically zero. In conclusion, the rotation does not increase the stability of the ground state described by the GP ansatz of Eq. (6.5).

Lastly, we re-examine the attractive rotating gas using a different GP ansatz that has been previously used in the literature, namely the ansatz of Ref. [133] (see also references therein). The authors of Ref. [133] considered a GP ansatz for the ground state of the system, which they expressed – depending on the geometry of the confining potential – either as a Gaussian-sech single-particle wave function:

$$\phi(\mathbf{r})=\left[N(2l_xl_yl_z\pi)^{-1}\right]^{1/2}e^{-x^2/2{l_x}^2}e^{-y^2/2{l_y}^2}sech\left(\frac{z}{l_z}\right)e^{i\alpha xy} \tag{6.6}$$

or as a Gaussian:

$$\phi(\mathbf{r})=\left[N(l_xl_yl_z)^{-1}\pi^{-3/2}\right]^{1/2}e^{-x^2/2{l_x}^2}e^{-y^2/2{l_y}^2}e^{-z^2/2l_z^2}e^{i\alpha xy}. \tag{6.7}$$

The parameters l_x, l_y, l_z and α were to be determined variationally. The phase αxy put in Eqs. (6.6)-(6.7) is referred to as the 'quadrupolar flow' term; a non-zero value of α increases the energy of the isotropic system in this state.

In Ref. [133] it is found that, using the ansatz of Eq. (6.6) or (6.7), the stability of the gas is significantly increased with increasing frequency Ω. However, an algebraic error in the above work is responsible for this (erroneous) behavior of the energy per particle ϵ as a function of the rotation frequency Ω. Already in Eq. (4) of Ref. [133] there is a sign error; redoing carefully the calculations we convinced ourselves that in the true expression the sign in the last term of the integrand is a plus instead of a minus. This sign error gives rise to an extra (negative) term in the GP energy functional which overestimates the dependence of the energy on Ω and artificially reduces the energy of the system (see the Appendix for more details).

In fact, also with the ansätze of Eqs. (6.6)-(6.7) the external rotation does not practically affect the stability of the condensate, in the sense that the critical value of the interaction parameter λ_c does not essentially change with Ω. We have verified this by calculating the energies and critical parameters λ_c by varying all three parameters l_x, l_y, l_z of Eqs. (6.6)-(6.7) for $\zeta = 0, 1, 5$ and $\varepsilon = 0, 0.1$, as it is originally done in Ref. [133] (the parameter α is expressed as a function of l_x and l_y and absorbed into the GP energy functional as in [133]). The Gaussian-sech ansatz of Eq. (6.6) is used in the case $\zeta = 0$, while the Gaussian ansatz of Eq. (6.7) is used when $\zeta = 1$ and 5. The critical λ_c of the radially symmetric systems (i.e., $\varepsilon = 0$, $\zeta = 0, 1, 5$) remains fixed, while in the slightly anisotropic systems (i.e., $\varepsilon = 0.1$, $\zeta = 0, 1, 5$) λ_c does not increase more than 0.2% as Ω increases from 0 to Ω_r. The computed values of λ_c for different values of ζ and ε are presented in Table 6.1. We then fix $\lambda = 3$ and calculate the energies and angular momenta of the ground state. For $\varepsilon = 0$, irrespective of the choice of ζ, the energy has been found to be independent of the rotation frequency Ω. For instance, we found $\epsilon(\varepsilon = 0, \zeta = 1) = 1.396(8)$. For $\varepsilon = 0.1$ the energy $\epsilon(\Omega_r)$ was found to decrease by 1.5% for $\zeta = 0$, by 0.32% for $\zeta = 1$, and by 0.04% for $\zeta = 5$ with respect to the corresponding energy $\epsilon(0)$ of the non-rotating system. Lastly, the expectation values of the angular momentum of the two ansätze are (almost) exactly zero for $\varepsilon = 0$ ($\varepsilon = 0.1$), regardless of the value of ζ.

Finally, we point out that, for the cases examined, the optimal value of parameter α is practically zero. It should be noted that the minimization of the GP energy functional with the ansatz of Eq. (6.5) yields a distribution for the coefficients c_i ($c_0 \simeq 1$ and $c_i \simeq 0,\ i = 1, 2, 3$) which essentially includes only the first of the LLL Gaussian-shaped orbital. I.e., the ansätze of Eqs. (6.7) and (6.5) essentially coincide with the respective orbital of isotropic systems.

6.5 Discussion and conclusions

In this chapter we have studied the stability under rotation of attractive ultracold Bose gases, confined by an isotropic as well as a slightly anisotropic harmonic trap. The problem has been mapped to and calculated in the corotating frame. Both many-body and Gross-

Pitaevskii approaches revealed that the rotation does not affect the stability of the gas against the collapse. Namely, the maximum value of the interaction strength λ_c where the attractive gas collapses remains essentially unchanged as the rotation frequency Ω varies within the extreme values 0 and $\Omega_r = \omega_x = \sqrt{1-\varepsilon}$, where ω_x is the frequency of the trap in the direction of the weakest confinement.

We have found here on both the MB and the GP (MF) levels that the ground state of the rotating attractive system carries zero (or almost zero in the anisotropic case) angular momentum for the whole range of the allowed values of Ω. Obviously, no vortex states are created. In the MB treatment, this means that no transition between LLL states of different angular symmetries has been found for the rotating attractive system. In the GP (MF) analysis this means that no symmetry broken states were found to be energetically favorable as the rotation frequency Ω increases from 0 to Ω_r. In both MB and GP approaches, the energy of the ground state remains practically unchanged and the attractive gas is condensed in the nodeless s-orbital as the rotation frequency increases. Hence, the GP description agrees well with the MB computation. These results conflict the findings of Ref. [133].

We revisited then the problem using the ansatz that incorporates a 'quadrupolar flow' term, used in Ref. [133]. The energy and stability of the system were again found not to be affected by the rotation of the trap. The resolution of this discrepancy lies in a sign error in the expectation value of the Hamiltonian of Ref. [133], which leads to a qualitatively different behavior of the properties of the system as a function of the rotation frequency Ω. Our results are in agreement with findings in the literature for isotropic harmonic (see [132]) and isotropic anharmonic traps with slight anharmonicity [63, 131].

We should, finally, stress that the present variational approach to the stationary ground state is not an extensive study of the rotating attractive gas. Even though we can rule out the stability-enhancement of the stationary ground state and the vortex nucleation in the attractive gas rotating with a frequency Ω smaller than the resonance frequency Ω_r, there is more physics beyond that. For instance, the stability of low-lying excited states with non-zero total angular momentum is expected to depend on Ω. [3] We have shown elsewhere [28] that ground states with $L > 0$ are generally fragmented states and thus more stable against collapse. A ground state with $L = 0$ will not couple to the external rotation and hence the ground-state symmetry will not change as Ω increases. On the other hand, a ground state initially with non-zero L *will be* affected by the rotation. The critical parameter λ_c in that case could increase as a function of Ω, before the latter reaches the extreme value Ω_r, and this will further stabilize the rotating $L \neq 0$ state against collapse. It is still to be investigated whether and for which parameters' values crossings of energy levels and symmetry changing of the (non-collapsed) rotating ground-state might occur. Lastly, based on the found absence of symmetry breaking of the ground state in the examined region $\Omega < \Omega_r$ and the divergence of the energy and angular momentum for $\Omega \geq \Omega_r$, we may speculate that, in the rotating attractive gas a vortex ground state – if at all can exist – may only appear as a giant-vortex (i.e., a single vortex at the center of the

[3] Indeed, we have some numerical indication for such a dependence in a MB treatment of the problem involving ground states of $L > 0$.

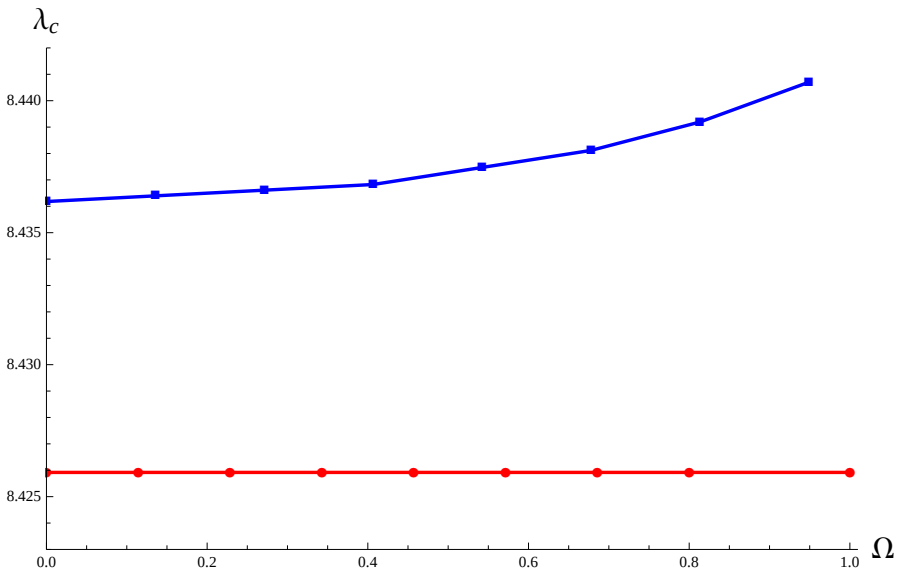

Figure 6.1: Many-body calculations for the critical parameter λ_c as a function of the frequency of the external rotation Ω, for the cases of isotropic [$\varepsilon = 0$, $\zeta = 1$; lower (red) line] and slightly anisotropic [$\varepsilon = 0.1$, $\zeta = 1$; upper (blue) line] confining traps. The critical interaction λ_c remains practically unaffected (the scale should be noted!) for the whole region of $\Omega \in [0, \Omega_r = \sqrt{1-\varepsilon})$. The number of particles is $N = 12$. See text for more details. All quantities are dimensionless.

trap whose radius and vorticity are increasing functions of time) and this only for rotation with frequency $\Omega \geq \Omega_r$. A time-dependent many-body treatment, for instance using the multiconfigurational time-dependent Hartree for bosons (MCTDHB) method [105, 108] that has described successfully many-body dynamics of attractive BECs [109, 111], should shed light on this interesting problem and uncover the response mechanisms of attractive gases to rotations.

λ_c			
	ζ=0	ζ=1	ζ=5
ε=0	9.547(7)	8.425(9)	5.522(8)
ε=0.1	9.554(9)	8.429(0)	5.523(2)

Table 6.1: Critical parameter λ_c for different values of the anisotropy ε and the z-deformation ζ of the trapping potential calculated in the GP theory, using the 'quadrupolar flow' ansätze, see Eqs. (6.6)-(6.7) and text below it. The parameter λ_c in the radially symmetric ($\varepsilon = 0$) cases does not depend on the frequency Ω of the rotation, while the change in λ_c as Ω varies from 0 (for which λ_c values are collected in the table) to $\Omega_r = \sqrt{1-\varepsilon}$ is negligible (less than 0.2%) when the trap is slightly anisotropic ($\varepsilon = 0.1$). All quantities are dimensionless.

Chapter 7

Outlook

The present Thesis dealt with static properties of ultracold trapped atomic gases of attractive bosons in two and three spatial dimensions. The connection of the angular momentum to the fragmentation and stability of the states of the systen was a central subject matter.

It is known from theoretical studies and experimental observations that the attractive bosonic gas is prone to collapse, meaning that such a system cannot sustain itself due to the overriding attraction. Nevertheless, the collapse or not of the gas strongly depends on its dimensionality: a gas confined to one dimension will never collapse, while the two- and three-dimensional gases will collapse, once the strength of the interaction (or, equivalently, the number of particles) is set sufficiently high. The analysis of the present Thesis focused on the collapse of the 2D and 3D gases possessing definite total angular momentum (Chs. 4 and 5 respectively) as well as the 3D externally rotated gas (Ch. 6).

It has been found more than a decade ago [29] that, in the limit of vanishing interaction, a two-dimensional attractive gas bearing total angular momentum L is fragmented over a vast number of single-particle states, which are the members of the LLL. Moreover, its interaction energy should not depend on this L. In the present analysis, the GS of the two-dimensional attractive gas with AM L was reexamined. It was found, by utilising the multi-orbital BMF, that for some given $L > 0$ the GS of the system is indeed described by members of the LLL only. For the GS with definite $L > 0$ the optimal distribution of the occupations was found and a simple analytic expression for the energy of this state as a function of L and the interaction strength λ was derived. In contrast to previous works (for instance [29, 40]) the results presented herein incorporate non-vanishing λ. At the low-λ and large-N limits the found energy coincides with the known expression. On top of that, it gives the appropriate (higher-order) corrections on λ and, for larger λ and fixed N, drops below the known expression. Interestingly, our results signified a distribution of the bosons among the LLL different than the one reported in [29] or in [40]. This distribution was identified as a second rotating phase of the attractive gas, where none but two bosons absorb all the available AM. It should be, however, noted that the above described novel distribution of the particles, for finite N and infinitesimal λ, yields – regarding only first order terms in λ – an energy that is slightly higher than the previously known forms. For increasing N our expression approaches (from above) the known one [29, 40]. Lastly, an

analytic expression for the critical λ of the GS as a function of its AM L was given; it is an increasing function of L that becomes linear in the large-N limit.

In three spatial dimensions, the situation, regarding the angular symmetries is rather different. The existence of two compatible operators, namely the operators $\hat{L}^2$ and $\hat{L}_z$ of the total angular momenta, complicates the structure of the common MB eigenstates of the two operators. In particular, an eigenstate of $\hat{L}^2$ and $\hat{L}_z$ was generally found to be a MB state, i.e., a superposition of Fock states. A symmetric (isotropic) Hamiltonian H, as the one examined in Ch. 5, suggests that there are eigenstates of H with good AM quantum numbers. Hence, such eigenstates of H are also not MF states. To our knowledge, little has been known in the literature in this respect, before the work of Ref. [28]. In the present analysis a basis of MB functions that preserve all the angular and spatial symmetries of the isotropically confined gas was initially found. Using this set the energies and the properties (fragmentation, depletion, variance) of the ground and excited states of the system were calculated. It was shown that the angular momentum L (and not necessarily L_z) stabilizes the gas, in the sense that λ_c increases with L. The found MB results were compared to those obtained from (symmetry broken) MF and GP descriptions and it was shown that for increasing λ GP theory fails in the correct description of the stability of the gas.

Lastly, in Ch. 6, the dependence of the properties of the ground state of the 3D gas when the harmonic trap is set into rotation was questioned. Both the isotropic and slightly anisotropic cases were analyzed, by mapping the problem to the corotating frame of reference. It was shown that neither symmetry breaking nor symmetry changing take place as the frequency of the external rotation Ω is increased. As a consequence the stability of the gas remains unaffected. Past a resonant value $\Omega_r = \omega_{\text{trap}}$ the gas ceases to exist in a stable configuration, for any λ_0. It was found, both at the MB and MF levels and in sharp contrast to the repulsive case, that no vortex can be nucleated and the possible origin of this absence was discussed.

In the light of the above findings, it would be interesting to examine the dynamical-stability of the described states. Exact numerical studies of ground and excited states – by utilizing the MCTDHB method – would help in this directions. Specifically, in the two-dimensional system it could be clarified whether the distribution of particles found in Ch. 4 are indeed energetically favorable and, furthermore, stable in time. Intriguing implication will arise if condensates made out of charged particles are considered. Then, the dipole magnetic moments of the atoms will depend on the angular momentum quantum numbers, as found in Chs. 4 and 5. The magnetic field induced to the charged particles by their AM could in turn impact on the stability of the gas through Feshbach self-resonances. Regarding Ch. 6, it is an open question whether an analysis of the externally rotated (harmonically trapped) gas in the laboratory – and not in the corotating – frame would yield the same result, namely that no vortex is nucleated.

Ultracold gases is an exciting research field of modern physics and can function as an inexhaustible lab for testing theories of many-body physics. Quantum mechanical behavior exposed at large scales is a unique situation of ultracold gases and liquids and could be further utilized. The approaches herein rely on the fact that such quantum gases

should not be treated clasically or semi-classicaly (as, for instance, within the GP theory). Indeed, as explained, going one step beyond MF theories one is able to correctly describe AM eigenstates, fragmentation, fluctuations and variance[1] of the states and various MB phenomena, that are otherwise 'rounded' and smeared out. Closing this Thesis, the author wishes to express his hope that the present work will stimulate experimental research and make a tiny step towards acquiring a better insight and control of the quantum world.

[1] Also correlations, that are related to variances, but were not the subject of the present Thesis.

Appendix A

Full expression for the energy of the 2D gas

We give the full expressions of the total and interaction energy for a 2D attractive system, as calculated within the BMF theory. These expressions are complementary to Ch. 4. Total energy, optimized for σ for any L, N and λ:

$$\epsilon_f = (\mathcal{L}+1)\sqrt{1-\frac{\lambda}{2\pi(\mathcal{L}+1)}A(L,N)}, \tag{A.1}$$

where

$$A(L,N) = 1 - \frac{2}{N} + 2^{2-L}\frac{2N+L-4}{N(N-1)} \tag{A.2}$$

and $\mathcal{L} = L/N$. For $N \to \infty$ we get $A \to 1$ and $\epsilon_f \to \epsilon$, i.e,, the above expression reduces to the energy of Eq. (4.20). The optimum σ, i.e., the value σ_0 where the total energy obtains a minimum is:

$$\sigma_0 = \sqrt[4]{1-\frac{\lambda}{2\pi(\mathcal{L}+1)}A(L,N)}. \tag{A.3}$$

The optimized interaction energy reads:

$$\epsilon_{\mathrm{int},f} = -\frac{\lambda A(L,N)}{4\pi\sqrt{1-\frac{\lambda A(L,N)}{2\pi(\mathcal{L}+1)}}} \tag{A.4}$$

Similarly, this is the general expression for the energy as given the Eq. (4.17) but without taking the large-N limit.

Appendix B

Angular momentum in 3D

B.1 Size of Fock Space

The total number of the N-body basis functions (permanents) that can be constructed over a basis of M one-particle wave functions of Eq. (5.3) is [101]:

$$N_p = \begin{pmatrix} M+N-1 \\ N \end{pmatrix} = \frac{(M+N-1)!}{N!\,(M-1)!}, \tag{B.1}$$

which for $M = 4$ becomes

$$N_p = \frac{1}{6}(N+1)(N+2)(N+3) \simeq \frac{N^3}{6}. \tag{B.2}$$

Using the symmetries of the system we can reduce significantly this number and hence the complexity of the problem. Without loss of generality we assume that the particle number N and the quantum number M_L are even integers.

Total angular momentum $\hat{L}_z$: Since $[\hat{L}_z, \hat{H}] = 0$ the state $|\Psi\rangle = \sum_i^{N_p} C_i|\Phi_i\rangle$ can be chosen to be a common eigenfunction of the two operators. This transforms $\mathcal{H}$ to a block diagonal form, with every block consisting of states of distinct M_L. The number of states $|\Psi\rangle$ in a block with some M_L is

$$N_p = \frac{(N+2-|M_L|)^2}{4} \lesssim \frac{N^2}{4}. \tag{B.3}$$

Parity $\hat{\Pi}\Psi(\mathbf{r}) = \Psi(-\mathbf{r})$: Similarly, $[\hat{\Pi}, \hat{H}] = 0$ and $\mathcal{H}$ block diagonalizes into two blocks, each with distinct parity $\Pi = +1$ or $\Pi = -1$. The number of states $|\Psi\rangle$ in the block with $\Pi = 1$ is

$$N_p = \frac{[N+4+2M_L-3M_L H(M_L)]\,[N+2-M_L H(M_L)]}{8} \lesssim \frac{N^2}{8}, \tag{B.4}$$

where $H(x)$ is the unit-step function.

Total angular momentum $\hat{L}^2$: Last, the commutator $[\hat{L}^2, \hat{H}] = 0$, diagonalizes the matrix $\mathcal{H}$ into blocks of states that have definite angular momentum quantum number L. The number of states $|\Psi^L\rangle$ in the block with some L is

$$N_p = \frac{N - L + 2}{2} \lesssim \frac{N}{2}, \tag{B.5}$$

where L is the quantum number of $\hat{L}^2$ and here it is assumed to be an even number. In case L is odd Eq. (B.5) should read: $N_p = (N - L + 1)/2$. Note that these relations hold for any M_L.

B.2 Angular momentum in Many-Body and Mean-Field theories

B.2.1 Many-body eigenstates of the total angular momentum operator $\hat{L}^2$

We now return to the question of explicitly finding the eigenstates of the operator $\hat{L}^2$, as discussed in Sec. 5.3.

A general permanent $|\Phi\rangle = |\vec{n}\rangle$, representing a system of a total number of bosons $N = n_1 + n_2 + n_3 + n_4$ and z-projection of the angular momentum $M_L = n_2 - n_4$, takes on the form:

$$|\vec{n}\rangle = |n_1, n_2, n_3, n_4\rangle = |N - 2n_2 - n_3 + M_L, n_2, n_3, n_2 - M_L\rangle, \tag{B.6}$$

where n_2, n_3 are integers, such that $M_L H(M_L) \leqslant n_2 \leqslant (N + M_L)/2$, $0 \leqslant n_3 \leqslant N - 2n_2 + M_L$, where $H(x)$ is the unit-step function. An expansion $|\Psi\rangle$ over these (orthogonal) permanents $|\Phi\rangle$ is:

$$|\Psi\rangle = \sum_{n_2,n_3} C_{n_2,n_3} |\vec{n}\rangle \tag{B.7}$$

where n_2, n_3 run over all possible permanents of Eq. (B.6). Acting operator Eq. (5.7) on Eq. (B.7) we get:

$$\hat{L}^2|\Psi\rangle = \hat{L}^2 \sum_{n_2,n_3} C_{n_2,n_3}|\vec{n}\rangle = \Lambda \sum_{n_2,n_3} C_{n_2,n_3}|\vec{n}\rangle, \tag{B.8}$$

or

$$\Lambda \sum_{n_2,n_3} C_{n_2,n_3}|\vec{n}\rangle = \sum_{n_2,n_3} C_{n_2,n_3}\Big(A(n_2,n_3)|\vec{n}\rangle + B(n_2,n_3)|\vec{n}+2\rangle + \Gamma(n_2,n_3)|\vec{n}-2\rangle\Big), \tag{B.9}$$

where $\Lambda = L(L+1)$ are the eigenvalues of $\hat{L}^2$, $|\vec{n}+2\rangle = |n_1, n_2 - 1, n_3 + 2, n_4 - 1\rangle$ and $|\vec{n}-2\rangle = |n_1, n_2+1, n_3-2, n_4+1\rangle$, i.e., they are the double 'excitations' of the permanent

$|\vec{n}\rangle$. The functions A,B,Γ are:

$$\begin{aligned} A(n_2,n_3) &= n_2(n_3+1)+n_3(n_4+1)+n_3(n_2+1)+n_4(n_3+1)+(n_2-n_4)^2, \\ B(n_2,n_3) &= 2\left[n_2n_4(n_3+1)(n_3+2)\right]^{1/2}, \\ \Gamma(n_2,n_3) &= 2\left[n_3(n_3-1)(n_2+1)(n_4+1)\right]^{1/2}. \end{aligned} \tag{B.10}$$

The problem is focused in calculating the coefficients C_{n_2,n_3} such that Eq. (B.8) is fulfilled. We will show how one can reduce this equation to a simpler form. By multiplying Eq. (B.9) with $\langle\vec{n}|$ and using orthogonality of permanents and the relation

$$\Gamma(n_2-k,n_3+2k) = B(n_2-k+1,n_3+2k-2),\ k\in\mathbb{N}, \tag{B.11}$$

we obtain:

$$\Lambda C_{n_2,n_3} = A(n_2,n_3)C_{n_2,n_3}+\Gamma(n_2,n_3)C_{n_2+1,n_3-2}+B(n_2,n_3)C_{n_2-1,n_3+2}. \tag{B.12}$$

This is a homogeneous, second order recurrence (or difference) equation of the two independent variables n_2, n_3, with known non-constant coefficients.

In the above equations there are two free parameters n_2, n_3 which are varied independently and these are also the independent variables of Eq. (B.12). To reduce the dimensionality of the problem one can proceed by switching the representation of the permanents and their coefficients. Precisely, we can use a simpler representation for indexing the vectors $|\Phi\rangle$ in the expansion of $|\Psi\rangle$. Noticing that the action of the operator $\hat{L}^2$ on a state of Eq. (B.7) involves only permanents of the form

$$|\vec{n}_i\rangle = |n_1,\alpha-i,\beta+2i,\alpha-i+M_L\rangle, \tag{B.13}$$

where $\alpha,\beta\in\mathbb{N}$ and $-(N+M_L)/2\leqslant i\leqslant -M_LH(M_L)$, we can work with permanents of the above type only, for fixed α,β. In fact the action of $\hat{L}^2$ partitions the configuration space into invariant subspaces, with permanents of the form of Eq. (B.13). Permanents with $\alpha\neq\alpha'$ or $\beta\neq\beta'$ will not contribute to the same eigenstate $|\Psi\rangle$. This allows us to move from the *two-parametric* $\{n_2,n_3\}-$ to the *one-parametric* $\{i\}-$ representation. We write now again Eqs. (B.7)-(B.12) in the new representation.

A general state becomes:

$$|\Psi\rangle = \sum_i C_i|\vec{n}_i\rangle, \tag{B.14}$$

where i runs again over all permanents (B.13). Similarly, acting operator Eq. (5.7) on Eq. (B.14) we get:

$$\hat{L}^2|\Psi\rangle = \hat{L}^2\sum_i C_i|\vec{n}_i\rangle = \Lambda\sum_i C_i|\vec{n}_i\rangle \tag{B.15}$$

$$= \sum_i C_i\Big(A_i|\vec{n}_i\rangle + B_i|\vec{n}_i+2\rangle+\Gamma_i|\vec{n}_i-2\rangle\Big), \tag{B.16}$$

with $A_i = A(\alpha - i, \beta + 2i), B_i = B(\alpha - i, \beta + 2i)$ and $\Gamma_i = \Gamma(\alpha - i, \beta + 2i)$. Equations (B.11) and (B.12) become:

$$\Gamma_{i+2k} = B_{i+2(k-1)}, \tag{B.17}$$

and

$$(A_i - \Lambda)C_i + \Gamma_i C_{i-1} + B_i C_{i+1} = 0, \tag{B.18}$$

respectively. The above is a homogeneous second-order recurrence (difference) equation of one independent variable [cf. Eq. (B.12)].

For some choices of the parameters $\alpha, \beta, \Lambda, M_L$ Eq. (B.18) can be easily solved. In particular, for $\alpha = 0, \beta = N$ and $M_L = 0$ we obtain:

$$\Lambda = 0 \ (L = 0), \qquad C_i = \frac{(-1)^{2N+1-i} 2^{N+2-2i} \Gamma(\frac{N}{2}+2-i)\Gamma(\frac{N+1}{2})}{\Gamma(i-1/2)} C_0, \tag{B.19}$$

$$\Lambda = 2 \ (L = 1), \qquad C_i = \frac{(-1)^{2N+1-i} 2^{N+3-2i} N \Gamma(\frac{N}{2}+2-i)\Gamma(\frac{N+1}{2})}{(6i-N-6)\Gamma(i-1/2)} C_0, \tag{B.20}$$

$$\Lambda = 6 \ (L = 2), \quad C_i = \frac{(-1)^{2N+1-i} 2^{N+5-2i} (N-2) N \Gamma(\frac{N}{2}+2-i)\Gamma(\frac{N+1}{2})}{(140i^2-60(N+5)i+3N(N+18)+160)\Gamma(i-1/2)} C_0, \tag{B.21}$$

where C_0 is to be determined from the normalization condition $\sum_i |C_i|^2 = 1$ and $-N/2 \leqslant i \leqslant 0$. Equations (B.19)-(B.21) give three of the states $\overline{\Phi}^L$, that are eigenstates of $\hat{L}^2$ and belong to the rotated basis $\{\overline{\Phi}_i^L\}$ of Sec. 5.3.

B.2.2 Mean-field and average many-body angular momentum

We show here that the total angular momentum of a mean-field state, with equally distributed excited bosons $n_2 = n_3 = n_4 \equiv n$ is the statistical average of the exact total angular momentum of the many-body states with the same depletion $d_1 = 1 - \frac{\rho_1}{N}$, i.e.,

$$\tilde{L}_{MF} = \langle L_{MB} \rangle_{d_1}. \tag{B.22}$$

Recall that $0 \leqslant L \leqslant N$. Then, for a total number of N bosons there are $N + 1$ blocks (L-blocks) of the Hamiltonian matrix $\mathcal{H}$, each with a distinct value of L. We want to calculate the average angular momentum $\langle L \rangle$, among states $|\Psi^L\rangle_{n_1}$ with a given natural occupation $\rho_1 = n_1$. We assume that in each L-block this occupation n_1, as we move from the highest-excited state to the ground state, increases like

$$\begin{cases} n_1(k) = 2k, & \text{if } L \text{ is even} \\ n_1(k) = 2k + 1, & \text{if } L \text{ is odd,} \end{cases} \tag{B.23}$$

where $k \in \mathbb{N}$ indexes the state $|\Psi^L_{i=k}\rangle$. The above relations hold exactly in the absence of interaction, i.e., $\lambda_0 = 0$, and in a satisfactory approximation when $\lambda_0 \neq 0$. Then, as we have numerically verified, each L-block with $L \lesssim N - n_1$ contains exactly one state $|\Psi^L\rangle_{n_1}$ with the desired n_1 (or very close to it). Recall that the size of an L-block drops linearly with L, as in Eq. (B.5). So there are $N + 1 - n_1$ L-blocks that contain one state

$|\Psi^L\rangle_{n_1}$. The occupation n_1, in the case of $\lambda_0 = 0$, is even in half of the blocks, odd in the other half ones. The total number of states with occupation n_1 is:

$$N(n_1) = \sum_{i=0}^{N+1-n_1,2} (2i+1) \tag{B.24}$$

due to the $\hat{L}_z$ degeneracy. To include only even (or approximately even) occupations n_1 we sum on a step of two (the added term ', 2' in the upper limit of the sum denotes that step). These states have total angular momentum:

$$L_{total} = \sum_{i=0}^{N+1-n_1,2} (2i+1)L_i. \tag{B.25}$$

The quantum number L_i of each block simply increases like $L_i = i$ and hence

$$\langle L_{MB}\rangle_{n_1} = \frac{\sum L_i(2i+1)}{\sum(2i+1)} = \frac{N'(4N'+7)}{6(N'+1)} \simeq \frac{2}{3}(N-n_1), \tag{B.26}$$

where $N' = N - n_1$. In the limit $N \gg 1$ we get:

$$\langle L_{MB}\rangle_{d_1} \simeq \frac{2}{3}Nd_1. \tag{B.27}$$

The average over all MB $|\Psi\rangle$ states, of all n_1 simply gives:

$$\langle L_{MB}\rangle_{all\ states} = \frac{N}{3}. \tag{B.28}$$

On the other hand, a MF state, with equidistributed excited bosons:

$$|\Phi\rangle = |n_1, n, n, n\rangle, \tag{B.29}$$

with $n_1 + 3n = N$, has no well-defined angular momentum quantum number L (except from the single case $|N, 0, 0, 0\rangle$). We can, though, calculate the expectation value on a state $|\Phi\rangle$ from Eq. (5.10) as:

$$\langle \hat{L}^2\rangle = \langle \vec{n}|\hat{L}^2|\vec{n}\rangle = n_2(n_3+1) + n_4(n_3+1) + n_3(n_4+1) + n_3(n_2+1) + (n_2-n_4)^2 \tag{B.30}$$

for a general permanent

$$|\Phi\rangle = |n_1, n_2, n_3, n_4\rangle, \tag{B.31}$$

or

$$\langle \hat{L}^2\rangle = 4n(n+1) \tag{B.32}$$

for the permanent of Eq. (B.29). For comparison purposes, we define a *pseudo-quantum number* $\tilde{L}_{MF}$, such that

$$\tilde{L}_{MF}(\tilde{L}_{MF}+1) = \langle \hat{L}^2\rangle. \tag{B.33}$$

Hence:

$$\tilde{L}_{MF} = \frac{1}{2}\left(-1+\sqrt{16n^2+16n+1}\right) = \frac{1}{2}\left[-1+\sqrt{\frac{16}{9}\left(N-n_1\right)^2+\frac{16}{3}\left(N-n_1\right)+1}\right]. \tag{B.34}$$

For $N \gg 1$, we get:

$$\tilde{L}_{MF} = \frac{2}{3}\left(N-n_1\right) \simeq \langle L_{MB}\rangle_{n_1}. \tag{B.35}$$

So, indeed the angular momentum of the MF state (B.29) equals, under the assumption $N \gg 1$, the mean angular-momentum of the MB states with the same s-depletion. Equation (B.35) immediately gives back Eq. (5.22):

$$\frac{\tilde{L}_{MF}}{N} = \frac{2}{3}\left(1-\frac{n_1}{N}\right) = \frac{2}{3}d_1. \tag{B.36}$$

Now, the average angular momentum over the permanents of Eq. (B.31) with the same n_1 is:

$$\langle \tilde{L}_{MF}\rangle_{n_1} = -\frac{1}{2}+\sqrt{\frac{3N-8n_1}{6}N}, \tag{B.37}$$

for $N \gg 1$ and $N > 3n_1$, whereas the average over all the permanents of Eq. (B.31) reads:

$$\langle \tilde{L}_{MF}\rangle_{all\ states} = \frac{N}{\sqrt{5}} = \frac{3}{\sqrt{5}}\langle L_{MB}\rangle_{all\ states}, \tag{B.38}$$

also at $N \gg 1$.

Last, we prove the condition for a MF state of Eq. (B.31) to be eigenstate of the angular momentum operator $\hat{L}^2$, already given in Sec. 5.5.2. Let $|\Phi^L\rangle$ be a single-permanent eigenstate of $\hat{L}^2$ of Eq. (5.7). Then it must

$$\hat{L}^2|\Phi^L\rangle = L(L+1)|\Phi^L\rangle, \tag{B.39}$$

where $L(L+1)$ is the eigenvalue of $\hat{L}^2$ for this permanent. Then from Eq. (5.10) we get that the conditions:

$$\begin{cases} n_3 = 0 \quad \text{or} \quad n_3 = 1 \quad \text{and} \\ n_2 = 0 \quad \text{or} \quad n_4 = 0 \end{cases} \tag{B.40}$$

must hold simultaneously. From here it turns out that the permanents that can satisfy Eq. (B.39) are:

$$|\Phi^L\rangle = |N+M_L,0,0,-M_L\rangle, \quad \text{with} \quad M_L = -L, \tag{B.41}$$
$$|\Phi^L\rangle = |N-M_L,M_L,0,0\rangle, \quad \text{with} \quad M_L = L, \tag{B.42}$$
$$|\Phi^L\rangle = |N+M_L-1,0,1,-M_L\rangle, \quad \text{with} \quad M_L = -L+1, L \geq 1, \tag{B.43}$$
$$|\Phi^L\rangle = |N-M_L-1,M_L,1,0\rangle, \quad \text{with} \quad M_L = L-1, L \geq 1, \tag{B.44}$$

where N the total number of particles and $M_L = n_2 - n_4$ the quantum number of $\hat{L}_z$, as usual. Thus we see that the only permanents that can be eigenfunctions of the operator $\hat{L}^2$ are the permanents with quantum numbers restricted to:

$$M_L = \pm L, \pm(L-1). \tag{B.45}$$

Unless $\lambda_0 = 0$, Eq. (B.45) serves as a necessary but not sufficient condition, for a MF state to be eigenstate of both the angular momentum operators $\hat{L}^2, \hat{L}_z$ and also the Hamiltonian $\hat{H}$. In the case of $\lambda_0 = 0$ there are no couplings among states with the same L and M_L and condition (B.45), hence, suffices to determine a MF eigenstate of $\hat{L}^2, \hat{L}_z$ and $\hat{H}$. The same is expected to happen for small values of λ_0.

Appendix C

The Gross-Pitaevskii energy functional with the 'Quadrupolar Flow' Ansatz

We re-derive and discuss the expression for the energy functional of Ref. [133]. The GP energy functional in the co-rotating frame reads:

$$E = \int \left[\frac{\hbar^2}{2m} |\nabla \phi|^2 + V(\mathbf{r}) |\phi|^2 + \frac{\lambda_0}{2} |\phi|^4 + i\hbar\Omega(\phi^* x \frac{\partial \phi}{\partial y} + \phi y \frac{\partial \phi^*}{\partial x}) \right] d\mathbf{r}, \tag{C.1}$$

where λ_0 measures the strength of the interaction, m is the mass of the particle and Ω is the frequency of the rotation around the z-axis. In Ref. [133] there is an algebraic error in the above expression (Eq. (4) of Ref. [133]). There, the sign of the last term of the integrand is a minus instead of a plus. This sign error remains further in the calculations of Ref. [133] and is seen in Eq. (8) and (10) therein. Indeed, in the last term of Eq. (10) of Ref. [133] the '-2' term has to be omitted and so the corrected expression would read:

$$\epsilon_G = \frac{1}{4} \left[\frac{1}{\gamma_x^2} + \frac{1}{\gamma_y^2} + \frac{1}{\gamma_z^2} + (1-\varepsilon)\gamma_x^2 + (1+\varepsilon)\gamma_y^2 + \zeta^2 \gamma_z^2 \right] - \frac{k}{\sqrt{2\pi}\gamma_x\gamma_y\gamma_z} - \frac{\Omega^2}{4} \frac{\left(\gamma_x^2 - \gamma_y^2\right)^2}{\gamma_x^2 + \gamma_y^2} \tag{C.2}$$

(for the $\alpha > 0$ branch), where $\gamma_{x,y} = l_{x,y}/\sqrt{\hbar/m\omega}$ and $k = |\lambda_0|N/4\pi$. The same correction is required for Eq. (8) of Ref. [133] as well. The presence of this extra term gives rise to an artificial dependence of the critical value of λ_c on the rotation frequency Ω, qualitatively different from the correct one. Indeed, a first order expansion of the (correct) energy, Eq. (C.2), around $\gamma_x = \gamma_y$, i.e., for small deformations, will result in an expression of the energy that does not depend on the frequency Ω. According to this, for zero or small ellipticity ε of the trapping potential, the resulting shape of the orbital ϕ is symmetric around the z-axis, i.e., $\gamma_x = \gamma_y$, and the energy of the system, as well as the critical interaction strength, practically do not depend on the frequency Ω. On the other hand, the (incorrect) energy ϵ_G as it is calculated in Ref. [133] strongly depends on Ω. Furthermore, it can be easily seen that the 'quadrupolar flow' ansatz of either Eq. (6.6) or (6.7) gives, for

small ε, an expectation value of almost zero angular momentum $\langle \hat{L}_z \rangle = \frac{1}{2} \frac{(l_x^2 - l_y^2)^2}{l_x^2 + l_y^2} mN\Omega \overset{\varepsilon \to 0}{=} 0$, and hence cannot describe any state with nonzero angular momentum that can in principal increase the stability of the system. For zero or small ε the energy and the critical parameter λ_c cannot change as a function of Ω and this reflects the cylindrical symmetry of the ansätze used, since $l_x \simeq l_y$ if $\varepsilon \simeq 0$.

Bibliography

[1] W. Ketterle, http://www.nobelprize.org/nobel_prizes/physics/laureates/2001/ketterle-lecture.html.

[2] R. P. Feynman, *Prog. Low Temp. Phys* **1**, 17 (1955).

[3] Bose, *Z. Phys. A* **26**, 178 (1924).

[4] A. Einstein, *Sitzungsberichte der Preussischen Akademie der Wissenschaften* **1**, 3 (1925).

[5] M. Fierz, *Helv. Phys. Acta* **12**, 3 (1939).

[6] W. Pauli, *Phys. Rev.* **58**, 716 (1940).

[7] R. F. Streater and A. S. Wightman, *PCT, Spin and Statistics, and all that*, Princeton University Press, 5th edition, 2000.

[8] A. J. Leggett, *Quantum Liquids*, Oxford University Press, 2006.

[9] K. B. Davis, M. O. Mewes, M. R. Andrews, N. J. van Druten, D. S. Durfee, D. M. Kurn, and W. Ketterle, *Phys. Rev. Lett.* **75**, 3969 (1995).

[10] C. C. Bradley, C. A. Sackett, J. J. Tollett, and R. G. Hulet, *Phys. Rev. Lett.* **75**, 1687 (1995).

[11] M. H. Anderson, J. R. Ensher, M. R. Matthews, C. E. Wieman, and E. A. Cornell, *Science* **269**, 198 (1995).

[12] A. E. Leanhardt, T. A. Pasquini, M. Saba, A. Schirotzek, Y. Shin, D. Kielpinski, D. E. Pritchard, and W. Ketterle, *Science* **301**, 1513 (2003).

[13] Scientific perspectives for ESA's future programme in Life and Physical sciences in space, Technical report, European Science Foundation, 2005.

[14] O. Penrose and L. Onsager, *Phys. Rev.* **104**, 576 (1956).

[15] A. J. Coleman and V. I. Yukalov, *Reduced Density Matrices*, Springer, 2000.

[16] P. Noziéres, in *Bose-Einstein Condensation,* edited by A. Griffin, D. W. Snoke, and S. Stringari, Cambridge University Press, Cambridge, England, 1996.

[17] S. Inouye, M. R. Andrews, J. Stenger, H.-J. Miesner, D. M. Stamper-Kurn, and W. Ketterle, *Nature (London)* **392**, 151 (1998).

[18] J. L. Roberts, N. R. Claussen, J. P. Burke, C. H. Greene, E. A. Cornell, and C. E. Wieman, *Phys. Rev. Lett.* **81**, 5109 (1998).

[19] P. Courteille, R. S. Freeland, D. J. Heinzen, F. A. van Abeelen, and B. J. Verhaar, *Phys. Rev. Lett.* **81**, 69 (1998).

[20] S. L. Cornish, N. R. Claussen, J. L. Roberts, E. A. Cornell, and C. E. Wieman, *Phys. Rev. Lett.* **85**, 1795 (2000).

[21] P. G. Kevrekidis, G. Theocharis, D. J. Frantzeskakis, and B. A. Malomed, *Phys. Rev. Lett.* **90**, 230401 (2003).

[22] S. L. Cornish, S. T. Thompson, and C. E. Wieman, *Phys. Rev. Lett.* **96**, 170401 (2006).

[23] C. C. Bradley, C. A. Sackett, and R. G. Hulet, *Phys. Rev. Lett.* **78**, 985 (1997).

[24] E. V. Shuryak, *Phys. Rev. A* **54**, 3151 (1996).

[25] E. A. Donley, N. R. Claussen, S. L. Cornish, J. L. Roberts, E. A. Cornell, and C. E. Wieman, *Nature (London)* **412**, 295 (2001).

[26] S. K. Adhikari, *Phys. Rev. E* **65**, 016703 (2001).

[27] L. S. Cederbaum, A. I. Streltsov, and O. E. Alon, *Phys. Rev. Lett.* **100**, 040402 (2008).

[28] M. C. Tsatsos, A. I. Streltsov, O. E. Alon, and L. S. Cederbaum, *Phys. Rev. A* **82**, 033613 (2010).

[29] N. K. Wilkin, J. M. F. Gunn, and R. A. Smith, *Phys. Rev. Lett.* **80**, 2265 (1998).

[30] C. Pethick and H. Smith, *Bose-Einstein Condensation in Dilute Gases*, Cambridge University Press, Cambridge, England, 2002.

[31] C. Cohen-Tannoudji, B. Diu, and F. Laloë, *Quantum Mechanics*, volume 1, Wiley-Interscience, 1977.

[32] W. Thompson, *Angular Momentum*, Willey-Interscience, 1994.

[33] J. R. Grover, *Phys. Rev.* **157**, 832 (1967).

[34] B. Mottelson, *Phys. Rev. Lett.* **83**, 2695 (1999).

[35] G. F. Bertsch and T. Papenbrock, *Phys. Rev. Lett.* **83**, 5412 (1999).

[36] G. M. Kavoulakis, B. Mottelson, and C. J. Pethick, *Phys. Rev. A* **62**, 063605 (2000).

[37] M. Ueda and T. Nakajima, *Phys. Rev. A* **64**, 063609 (2001).

[38] M. S. Hussein and O. K. Vorov, *Phys. Rev. A* **65**, 035603 (2002).

[39] A. D. Jackson and G. M. Kavoulakis, *Phys. Rev. Lett.* **85**, 2854 (2000).

[40] A. D. Jackson, G. M. Kavoulakis, and M. Magiropoulos, *Phys. Rev. A* **78**, 063623 (2008).

[41] L. Onsager, *Nuovo Cimento* **6**, Suppl. 2, 249 (1949).

[42] A. Abrikosov, *Zh.Eksp.Teor.Fiz.* **32**, 1442; Sov.Phys. JETP **5**, 1174 (1957).

[43] M. Ueda and A. J. Leggett, *Phys. Rev. Lett.* **83**, 1489 (1999).

[44] D. Butts and D. Rokhsar, *Nature (London)* **397**, 327 (1999).

[45] H. Hall and W. F. Vinen, *Proc. Roy. Soc.* **A238**, 204 (1956).

[46] W. F. Vinen, *Proc. Roy. Soc.* **A260**, 218 (1961).

[47] I. Maggio-Aprile, C. Renner, A. Erb, E. Walker, and O. Fischer, *Phys. Rev. Lett.* **75**, 2754 (1995).

[48] F. Chevy, K. W. Madison, and J. Dalibard, *Phys. Rev. Lett.* **85**, 2223 (2000).

[49] V. Schweikhard, I. Coddington, P. Engels, V. P. Mogendorff, and E. A. Cornell, *Phys. Rev. Lett.* **92**, 040404 (2004).

[50] K. W. Madison, F. Chevy, W. Wohlleben, and J. Dalibard, *Phys. Rev. Lett.* **84**, 806 (2000).

[51] K. W. Madison, F. Chevy, W. Wohlleben, and J. Dalibard, *Journal of Modern Optics* **47**, 2715 (2000).

[52] K. W. Madison, F. Chevy, V. Bretin, and J. Dalibard, *Phys. Rev. Lett.* **86**, 4443 (2001).

[53] M. R. Matthews, B. P. Anderson, P. C. Haljan, D. S. Hall, C. E. Wieman, and E. A. Cornell, *Phys. Rev. Lett.* **83**, 2498 (1999).

[54] C. Raman, J. R. Abo-Shaeer, J. M. Vogels, K. Xu, and W. Ketterle, *Phys. Rev. Lett.* **87**, 210402 (2001).

[55] P. Engels, I. Coddington, P. C. Haljan, V. Schweikhard, and E. A. Cornell, *Phys. Rev. Lett.* **90**, 170405 (2003).

[56] T. W. Neely, E. C. Samson, A. S. Bradley, M. J. Davis, and B. P. Anderson, *Phys. Rev. Lett.* **104**, 160401 (2010).

[57] J. A. Seman, E. A. L. Henn, M. Haque, R. F. Shiozaki, E. R. F. Ramos, M. Caracanhas, P. Castilho, C. Castelo Branco, P. E. S. Tavares, F. J. Poveda-Cuevas, G. Roati, K. M. F. Magalhães, and V. S. Bagnato, *Phys. Rev. A* **82**, 033616 (2010).

[58] N. Gemelke, E. Sarajlic, and S. Chu, *arXiv:1007.2677* (2010).

[59] P. G. Kevrekidis, R. Carretero-Gonzalez, D. J. Frantzeskakis, and I. G. Kevrekidis, *Mod. Phys. Lett. B* **18** (2004).

[60] A. L. Fetter, *Rev. Mod. Phys.* **81**, 647 (2009).

[61] N. Cooper, *Adv. Phys.* **57**, 539 (2008).

[62] M. Tsubota, K. Kasamatsu, and M. Kobayashi, *preprint* , arXiv:1004.5458v2 (2010).

[63] G. M. Kavoulakis, A. D. Jackson, and G. Baym, *Phys. Rev. A* **70**, 043603 (2004).

[64] E. P. Gross, *Nuovo Cimento* **20**, 454 (1961).

[65] A. L. Fetter, P. C. Hohenberg, and P. Pincus, *Phys. Rev.* **147**, 140 (1966).

[66] F. Dalfovo and S. Stringari, *Phys. Rev. A* **53**, 2477 (1996).

[67] E. H. Lieb, R. Seiringer, and J. Yngvason, *Phys. Rev. A* **79**, 063626 (2009).

[68] A. L. Fetter, *Phys. Rev. A* **53**, 4245 (1996).

[69] T.-L. Ho, *Phys. Rev. Lett.* **87**, 060403 (2001).

[70] S. K. Adhikari, *Phys. Rev. A* **66**, 043601 (2002).

[71] O. K. Vorov, P. V. Isacker, M. S. Hussein, and K. Bartschat, *Phys. Rev. Lett.* **95**, 230406 (2005).

[72] A. Bourne, N. K. Wilkin, and J. M. F. Gunn, *Phys. Rev. Lett.* **96**, 240401 (2006).

[73] A. D. Jackson and G. M. Kavoulakis, *Phys. Rev. A* **70**, 023601 (2004).

[74] S. Viefers, T. H. Hansson, and S. M. Reimann, *Phys. Rev. A* **62**, 053604 (2000).

[75] T. Papenbrock and G. F. Bertsch, *Phys. Rev. A* **63**, 023616 (2001).

[76] A. D. Jackson, G. M. Kavoulakis, B. Mottelson, and S. M. Reimann, *Phys. Rev. Lett.* **86**, 945 (2001).

[77] M. A. H. Ahsan and N. Kumar, *Phys. Rev. A* **64**, 013608 (2001).

[78] V. Bardek and S. Meljanac, *Phys. Rev. A* **65**, 013602 (2001).

[79] M. A. Cazalilla, *Phys. Rev. A* **67**, 063613 (2003).

[80] O. K. Vorov, M. S. Hussein, and P. V. Isacker, *Phys. Rev. Lett.* **90**, 200402 (2003).

[81] D. Dagnino, N. Barberán, K. Osterloh, A. Riera, and M. Lewenstein, *Phys. Rev. A* **76**, 013625 (2007).

[82] S. Bargi, J. Christensson, G. M. Kavoulakis, and S. M. Reimann, *Phys. Rev. Lett.* **98**, 130403 (2007).

[83] D. Dagnino, N. Barberán, M. Lewenstein, and J. Dalibard, *Nature Phys.* **5**, 431 (2009).

[84] M. C. Tsatsos, *Phys. Rev. A* **83**, 063615 (2011).

[85] R. Onofrio, D. S. Durfee, C. Raman, M. Köhl, C. E. Kuklewicz, and W. Ketterle, *Phys. Rev. Lett* **84**, 810 (2000).

[86] T. P. Simula, S. M. M. Virtanen, and M. M. Salomaa, *Phys. Rev. A* **66**, 035601 (2002).

[87] P. Ring and P. Schuck, *The Nuclear Many-Body Problem*, Springer-Verlag Heidelberg, 1980.

[88] A. L. Fetter and J. D. Walecka, *Quantum theory of many-particle systems*, Dover Publications, 1971.

[89] G. G. Batrouni, R. T. Scalettar, and G. T. Zimanyi, *Phys. Rev. Lett.* **65**, 1765 (1990).

[90] D. S. Petrov, M. Holzmann, and G. V. Shlyapnikov, *Phys. Rev. Lett.* **84**, 2551 (2000).

[91] D. A. W. Hutchinson, C. Gies, S. A. Morgan, M. D. Lee, and B. P. van Zyl, *Las. Phys.* **15**, 1091 (2005).

[92] T. Busch, B.-G. Englert, K. Rzazewski, and M. Wilkens, *Foundations of Physics* **28**, 549 (1998).

[93] F. Dalfovo, S. Giorgini, L. P. Pitaevskii, and S. Stringari, *Rev. Mod. Phys.* **71**, 463 (1999).

[94] A. J. Leggett, *New J. Phys.* **5**, 103 (2003).

[95] L. P. Pitaevskii, *Zh. Eksp. Teor. Fiz.* **40**, 646 (1961), [Sov. Phys. JETP 13, 451 (1961)].

[96] L. S. Cederbaum and A. I. Streltsov, *Phys. Lett. A* **318**, 564 (2003).

[97] O. E. Alon, A. I. Streltsov, and L. S. Cederbaum, *Phy. Lett. A* **362**, 453 (2007).

[98] E. Hylleraas, *Z. Phys.* **48**, 469 (1928).

[99] A. Szabo and N. Ostlund, *Modern Quantum Chemistry*, Dover, Mineola, NY, 1996.

[100] T. Haugset and H. Haugerud, *Phys. Rev. A* **57**, 3809 (1998).

[101] A. I. Streltsov, O. E. Alon, and L. S. Cederbaum, *Phys. Rev. A* **73**, 063626 (2006).

[102] A. L. Fetter, *arXiv:cond-mat/9510037* (1995).

[103] L. S. Cederbaum, A. I. Streltsov, and O. E. Alon, *Phys. Rev. Lett.* **100**, 040402 (2008).

[104] G. Baym and C. J. Pethick, *Phys. Rev. Lett.* **76**, 6 (1996).

[105] H.-D. Meyer, U. Manthe, and L. Cederbaum, *Chem. Phys. Lett.* **165**, 73 (1990).

[106] O. E. Alon, A. I. Streltsov, and L. S. Cederbaum, *Phys. Rev. A* **77**, 033613 (2008).

[107] http://mctdhb.uni hd.de.

[108] A. I. Streltsov, O. E. Alon, and L. S. Cederbaum, *Phys. Rev. Lett.* **99**, 030402 (2007).

[109] A. I. Streltsov, O. E. Alon, and L. S. Cederbaum, *Phys. Rev. Lett.* **100**, 130401 (2008).

[110] K. Sakmann, A. I. Streltsov, O. E. Alon, and L. S. Cederbaum, *Phys. Rev. Lett* **103**, 220601 (2009).

[111] A. I. Streltsov, O. E. Alon, and L. S. Cederbaum, *Phys. Rev. A* **80**, 043616 (2009).

[112] J. Grond, J. Schmiedmayer, and U. Hohenester, *Phys. Rev. A* **79**, 021603(R) (2009).

[113] L. S. Cederbaum and N. Moiseyev, *Israel J. Chem.* **43**, 267 (2003).

[114] C. J. Pethick and L. P. Pitaevskii, *Phys. Rev. A* **62**, 033609 (2000).

[115] P. A. Ruprecht, M. J. Holland, K. Burnett, and M. Edwards, *Phys. Rev. A* **51**, 4704 (1995).

[116] A. G. Morris and D. L. Feder, *Phys. Rev. A* **74**, 033605 (2006).

[117] H. Stoof, *J. Stat. Phys.* **87**, 1353 (1997).

[118] N. Barberán, M. Lewenstein, K. Osterloh, and D. Dagnino, *Phys. Rev. A* **73**, 063623 (2006).

[119] J. L. Roberts, N. R. Claussen, S. L. Cornish, E. A. Donley, E. A. Cornell, and C. E. Wieman, *Phys. Rev. Lett.* **86**, 4211 (2001).

[120] O. Elgarøy and C. J. Pethick, *Phys. Rev. A* **59**, 1711 (1999).

[121] J. Schirmer and L. S. Cederbaum, *Phys. Rev. A* **16**, 1575 (1977).

[122] W. Steeb, A. J. van Tonder, C. M. Villet, and S. J. M. Brits, *Found. Phys. Lett.* **1**, 147 (1988).

[123] J. von Neumann and E. Wigner, *Phys. Z.* **30**, 467 (1929), reprinted in *Quantum Chemistry, Classic Scientific Papers*, edited by H. Hettema (World Scientific, Singapore, 1998).

[124] H. Saito and M. Ueda, *Phys. Rev. A* **65**, 033624 (2002).

[125] S. Wüster, J. J. Hope, and C. M. Savage, *Phys. Rev. A* **71**, 033604 (2005).

[126] C. M. Savage, N. P. Robins, and J. J. Hope, *Phys. Rev. A* **67**, 014304 (2003).

[127] T. K. Das, A. Kundu, S. Canuto, and B. Chakrabarti, *Phys. Lett. A* **373**, 258 (2009).

[128] C. A. R. Sá de Melo, *Phys. Rev. B* **44**, 11911 (1991).

[129] H. Shi and W.-M. Zheng, *Phys. Rev. A* **55**, 2930 (1997).

[130] J. R. Abo-Shaeer, C. Raman, J. M. Vogels, and W. Ketterle, *Science* **292**, 476 (2001).

[131] T. K. Ghosh, *Phys. Rev. A* **69**, 043606 (2004).

[132] E. Lundh, A. Collin, and K.-A. Suominen, *Phys. Rev. Lett.* **92**, 070401 (2004).

[133] N. A. Jamaludin, N. G. Parker, and A. M. Martin, *Phys. Rev. A* **77**, 051603 (2008).

[134] E. J. Mueller, T.-L. Ho, M. Ueda, and G. Baym, *Phys. Rev. A* **74**, 033612 (2006).

List of publications, contributions to conferences, awards

Publications

- *Fragmented Many-Body states of definite angular momentum and stability of attractive 3D Condensates*,
  M. C. Tsatsos, O. E. Alon, A. I. Streltsov, and L. S. Cederbaum, Phys. Rev. A **82**, 033613, (2010).
- *Attractive Bose-Einstein Condensates in three dimensions under rotation: Revisiting the problem of stability of the ground state in harmonic traps*,
  M.C. Tsatsos, Phys. Rev. A **83**, 063615 (2011).
- *Statics and stability of two-dimensional attractive Bose-Einstein condensates.*,
  M. Tsatsos, A. I. Streltsov, O. E. Alon, and L. S. Cederbaum, (in preparation).

Contributions to conferences

- *Angular momentum stabilizes a 3D attractive condensate,*
  Poster presentation, Quo Vadis BEC? Dresden, MPI-KS, August 2010.
- *Fragmentation and angular momentum in 3D attractive condensates*
  Talk, DPG conference in Dresden 2011 – Q 10.8, Mo, Mar 14, 2011.

Awards

- Grant for the Completion of a Doctoral Degree within the "Stipendien- und Betreuungsprogramm" (STIBET) by the German Academic Exchange Service (DAAD) for International Doctoral Candidates, 2011.
- Doctoral Fellowship through the Landesgraduierteförderung - LGFG, (funding program of the State of Baden-Württemberg), Heidelberg University, 2007-2010.
- College Hardship Fund, Imperial College London, 2006.

a) Ich erkläre hiermit an Eides statt, daß ich die vorgelegte Dissertation selbst verfaßt und mich dabei keiner anderen als der von mir ausdrücklich bezeichneten Quellen und Hilfen bedient habe.

b) Ich erkläre hiermit an Eides statt, daß ich an keiner anderen Stelle ein Prüfungsverfahren beantragt beziehungsweise die Dissertation in dieser oder anderer Form bereits anderweitig als Prüfungsarbeit verwendet oder einer anderen Fakultät als Dissertation vorgelegt habe.

Marios Tsatsos